CENTRO INTERNACIONAL DE ESTUDOS
DE DOUTORAMENTO E AVANZADOS
DA USC (CIEDUS)

TESIS DE DOCTORADO

DETERMINING PARAMETERS OF THE OBESTATIN/GPR39 SYSTEM ACTION IN THE PERIPHERAL NERVOUS SYSTEM

Agustín Sánchez Temprano

ESCUELA DE DOCTORADO INTERNACIONAL

PROGRAMA DE DOCTORADO EN ENDOCRINOLOGÍA

SANTIAGO DE COMPOSTELA

2018

USC
UNIVERSIDADE
DE SANTIAGO
DE COMPOSTELA

DECLARACIÓN DEL AUTOR DE LA TESIS

Determining parameters of the Obestatin/GPR39 action in the peripheral nervous system

D. Agustín Sánchez Temprano

Presento mi tesis, siguiendo el procedimiento adecuado al Reglamento, y declaro que:

1) *La tesis abarca los resultados de la elaboración de mi trabajo.*
2) *En su caso, en la tesis se hace referencia a las colaboraciones que tuvo este trabajo.*
3) *La tesis es la versión definitiva presentada para su defensa y coincide con la versión enviada en formato electrónico.*
4) *Confirmo que la tesis no incurre en ningún tipo de plagio de otros autores ni de trabajos presentados por mí para la obtención de otros títulos.*

En Santiago de Compostela., 19 de Octubre de 2018.

Fdo. Agustín Sánchez Temprano

USC
UNIVERSIDADE
DE SANTIAGO
DE COMPOSTELA

AUTORIZACIÓN DEL DIRECTOR / TUTOR DE LA TESIS

Determining parameters of the Obestatin/GPR39 action in the peripheral nervous system

Dña. Yolanda Pazos Randulfe.
D. Jesús Pérez Camiña.
D. José Luís Relova Quinteiro.

INFORMA/N:

Que la presente tesis, corresponde con el trabajo realizado por D. ***Agustín Sánchez Temprano****, bajo mi dirección, y autorizo su presentación, considerando que reúne los requisitos exigidos en el Reglamento de Estudios de Doctorado de la USC, y que como director de ésta no incurre en las causas de abstención establecidas en Ley 40/2015.*

En Santiago de Compostela., 19 de Octubre de 2018.

Fdo.	Fdo.	Fdo.
Dña Yolanda Pazos Randulfe	D. Jesús Pérez Camiña	D. José Luis Relova Quinteiro

USC
UNIVERSIDADE
DE SANTIAGO
DE COMPOSTELA

Yo, D. **Agustín Sánchez Temprano**, con DNI **44848268Q**, presento esta tesis exponiendo, conforme a lo requerido, los siguientes conflictos de intereses:

- Declaro que soy titular de la solicitud de una patente, desarrollada en el contexto de esta tesis de doctorado
  - Solicitante: Universidade de Santiago de Compostela/Servicio Galego de Saúde.
  - Inventores: Sánchez Temprano, A; Pazos Randulfe, Y; Pérez Camiña, J; Gallego Gómez, R y Relova Quinteiro, JL.
  - Numero de solicitud: EP18382680.9.
  - Fecha de solicitud: 21 de septiembre de 2018.

Fdo. Agustín Sánchez Temprano

USC
UNIVERSIDADE
DE SANTIAGO
DE COMPOSTELA

Dedicada a mi padre

y a mi madre

USC
UNIVERSIDADE
DE SANTIAGO
DE COMPOSTELA

USC
UNIVERSIDADE DE SANTIAGO DE COMPOSTELA

INDEX

USC
UNIVERSIDADE
DE SANTIAGO
DE COMPOSTELA

INDEX 11
ABSTRACT 17
ABBREVIATIONS 21
INTRODUCTION 27
Peripheral nervous system 29
Function and anatomy 29
Structure 30
Myelin sheath 32
PNS myelin composition 34
Myelination and regulation 36
Peripheral nerve injury 39
Wallerian degeneration 41
Regeneration 42
Actual strategies in nerve injury treatment 43
Obestatin 44
Obestatin biosynthesis 45
Obestatin expression. 46
Obestatin receptor: GPR39. 47
GPR39 expression 48
Obestatin bioactivity 49
OBJECTIVES 53
MATERIALS AND METHODS 57
Antibodies 59
Cell culture. 61
PC12 neuroprotection model 65
IFRS1 Schwann cell line. 69
PC12-IFRS1 coculture. 71

Animals 77
Data analysis. 83
Formatting and bibliography. 83
RESULTS 85
CHAPTER 1 87
CHAPTER 2 95
CHAPTER 3 103
CHAPTER 4 109
CHAPTER 5 129
DISCUSSION 143
CHAPTER 1 145
CHAPTER 2 149
CHAPTER 3 153
CHAPTER 4 155
CHAPTER 5 159
CONCLUSIONS 163
CHAPTER 1 165
CHAPTER 2 165
CHAPTER 3 165
CHAPTER 4 166
CHAPTER 5 166
RESUMEN 167
ACKNOWLEDGEMENTS 179
BIBLIOGRAPHY 183
ATTACHED DOCUMENTS 208

Figure and table index

Figure I1. Neuroanatomical representation of the input and output of the peripheral nerve in the spinal cord 30
Figure I2. Peripheral nerve fibre structure 31
Figure I3. Diagram of a myelinated axon. 33
Figure I4. Nerve conduction along the axon. 33
Figure I5. Representation of the myelin molecular organization in the PNS. 34
Figure I6. Schwann cell myelination. 37
Figure I7. Nerve injury classification. 40
Figure I8. Nerve regeneration 42
Figure I9. Overview of ghrelin gene structure and relevant peptide variants 46
Figure I10. Obestatin/GPR39 system bioactivity. 50
Table 1. Antibodies. 59
Table 1. Antibodies (continuation). 60
Figure M1. PC12-IFRS1 coculture model 71
Figure M2. Rat sciatic crush model 78
Figure M3. Construction and implantation of sciatic scaffold with catheter. 79
Figure M4. Representation of the footprint and the values used for determination of SFI 80
Figure R1. Expression of obestatin and GPR39 in rat sciatic nerve 89
Figure R2. Expression of obestatin and GPR39 in rat DRGs 90
Figure R3. Expression of obestatin and GPR39 in rat anterior horn of spinal cord 91
Figure R4. Expression of obestatin and GPR39 in sectioned rat sciatic nerve 92
Figure R5. Expression of obestatin and GPR39 in IFRS1 and PC12 cell lines 94
Figure R6. Effect of exogenous obestatin administration on PC12 cells proliferation 98
Figure R7. Effect of obestatin on PC12 viability 98
Figure R8. Effect of obestatin on PC12 cell apoptosis 99
Figure R9. Analysis of proapoptotic and antiapoptotic protein levels in the PC12 nutrient deprivation model 100
Figure R10. Effect of obestatin on PC12 cell survival signalling under nutrient deprivation conditions 101
Figure R11. Effect of obestatin on IFRS1 cells proliferation 105
Figure R12. Evaluation of migration in IFRS1 cell line 106

Figure R13. Evaluation of obestatin ability as chemoattractant and inducer of migration in IFRS1 cell line 107

Figure R14. Immunofluorescence analysis for the identification of markers in the PC12-IFRS1 coculture 111

Figure R15. Immunofluorescence analysis for cell identification in PC12-IFRS1 coculture 112

Figure R16. Immunofluorescence analysis of MBP in PC12-IFRS1 coculture. 113

Figure R17. Immunofluorescence analysis of MBP in PC12-IFRS1 coculture 114

Figure R18. Effect of obestatin on the morphology of PC12 during differentiation..... 116

Figure R19. Effect of obestatin on the morphology of differentiated PC12 cells..... 117

Figure R20. Effect of obestatin on PC12-IFRS1 cell coculture proliferation. 118

Figure R21. Effect of obestatin on IFRS1 and PC12 proliferation. 119

Figure R22. Characterization of the cellular clusters found in a 21 days PC12-IFRS1 coculture. 120

Figure R23. Effect of obestatin on the morphology of cell clusters in PC12-IFRS1 coculture 121

Figure R24. Analysis of MPZ protein levels in PC12-IFRS1 coculture 122

Figure R25. Analysis of MBP isoform 1 protein levels in PC12-IFRS1 coculture 123

Figure R26: Analysis of MAG protein levels in PC12-IFRS1 coculture. 124

Figure R27. Effect of obestatin on lipid biosynthesis. 125

Figure R28. Immunofluorescence analysis of myelination in PC12-IFRS1 coculture..... 126

Figure R29. Analysis of IFRS1 cell density around PC12 neurites 127

Figure R30. Sciatic functional index analysis in a crush injury model..... 132

Figure R31. Immunofluorescence analysis of GAP43 in crush-injured sciatic nerve. 133

Figure R32. Neurofilament expression in distal site of crush injured rat sciatic nerve.. 135

Figure R33. Myelin basic protein expression in distal site of crush injured rat sciatic nerve. 136

Figure R34. Immunoblot analysis of nerve regeneration in crush-injured rat sciatic nerves. 137

Figure R35. Muscle mass loss analysis in a crush-injured sciatic nerve model. 139

Figure R36. Muscle fibre CSA analysis in crush-injured sciatic nerve model..... 141

Figure D1. Model of obestatin mediated neuroprotection 150

Figure D2. Proposed model of obestatin mediated myelination..... 160



ABSTRACT

USC
UNIVERSIDADE
DE SANTIAGO
DE COMPOSTELA

Galego

A lesión do nervio periférico é un problema clínico de alta incidencia, que afecta de forma significativa á calidade de vida do paciente e causa unha enorme carga socioeconómica. Segue sendo unha das tarefas máis desafiantes da neurocirurxía, xa que a recuperación neuromuscular funcional rara vez é satisfactoria. En consecuencia, a mellora das técnicas cirúrxicas e a aplicación clínica de terapias innovadoras foron obxecto de intensos estudos en todo o mundo. Neste escenario, o presente estudo involucra ao sistema obestatina/ GPR39 na mellora da reparación do nervio periférico, mellorando tanto a neuroprotección como a remielinización, e por tanto a rexeneración do nervio danado, contrarrestando a perda severa de función e a atrofia do músculo inervado. En consecuencia, a obestatina postúlase como un axente terapéutico potencial para a rexeneración do sistema nervioso periférico.

Castellano

La lesión del nervio periférico es un problema clínico de alta incidencia, que afecta significativamente la calidad de vida del paciente y causa una enorme carga socioeconómica. Sigue siendo una de las tareas más desafiantes de la neurocirugía, ya que la recuperación neuromuscular funcional rara vez es satisfactoria. En consecuencia, la mejora de las técnicas quirúrgicas y la aplicación clínica de terapias innovadoras han sido objeto de intensos estudios en todo el mundo. En este escenario, el presente estudio involucra al sistema obestatina/GPR39 en la mejora de la reparación del nervio periférico, mejorando tanto la neuroprotección como la remielinización, y por lo tanto la regeneración del nervio dañado, contrarrestando la pérdida severa de función y la atrofia del músculo inervado. En consecuencia, la obestatina se postula como un agente terapéutico potencial para la regeneración del sistema nervioso periférico.

English

Peripheral nerve injury is a high-incidence clinical problem, significantly affecting the patient's life quality and causing an enormous socio-economic burden. It still stands as one of the most challenging tasks in neurosurgery, as functional neuromuscular recovery is rarely satisfactory. Accordingly, the improvement of surgical techniques and the clinical application of innovative therapies have been intensively studied worldwide. In this scenario, the present study involves the obestatin/GPR39 system in the improvement of the peripheral nerve repair, by enhancing both neuroprotection and remyelination, and thus the regeneration of the damaged nerve, counteracting the severe loss of function and the atrophy of the innervated muscle. Consequently, obestatin is postulated as a potential therapeutic agent for peripheral nervous system regeneration.

USC UNIVERSIDADE DE SANTIAGO DE COMPOSTELA

USC
UNIVERSIDADE DE SANTIAGO DE COMPOSTELA

ABBREVIATIONS

USC
UNIVERSIDADE
DE SANTIAGO
DE COMPOSTELA

Abbreviations

Akt	RAC-alpha serine/threonine-protein kinase
BCL2	B-cell lymphoma 2
BDNF	Bone derived neurotrophic factor
BNB	Blood nerve barrier
BrdU	5-bromo-2'-deoxyuridine
BSA	Bovine serum albumin
CCK8	Cell counting kit-8
CNS	Central nervous system
CSA	Cross section area
d	Day(s)
DAPI	4',6-diamidino-2-phenylindole
DM	Differentiation medium
DMEM	Dulbecco's Modified Eagle Medium
DPI	Days post-injury
DRG	Dorsal root ganglia
E	Experimental feet
ECL	Enhanced chemiluminescence
EDL	Extensor digitorum longus
EGF	Epidermal growth factor
EGR2	Early growth response protein 2
ERK	Extracellular signal-regulated kinase
FBS	Foetal bovine serum
GAPDH	Glyceraldehyde-3-phosphate dehydrogenase
GLP1	Glucagon-like peptide 1
GLP1R	Glucagon-like peptide 1 receptor
GM	Gastrocnemius
GPR39	G-protein coupled receptor 39
GSK-3	Glycogen synthase kinase-3
h	Hour(s)
HBSS	Hank balanced salt solution

HE	Haematoxylin-eosin
HHS	Harris haematoxylin system
HRP	Horseradish peroxidase
HS	Horse serum
IHC	Immunohistochemistry
IF	Immunofluorescence
IFRS1	Immortalized Fischer rat Schwann cell 1
IP	Intraperiod line
ISO	International organization for standardization
ITS	Intertoe sectional distance
MAG	Myelin-associated glycoprotein
MAPK	Mitogen activated protein kinase
MBP	Myelin basic protein
MD	Major dense line
min	Minutes
MM	Myelination medium
MPZ	Myelin protein zero
N	Normal feet
NCAM	Neuronal cell adhesion molecule
ND	Nutrient deprivation
NGF	Nerve growth factor
NRG1	Neuregulin 1
NSE	Neuron specific enolase
Oct6	Octamer-binding protein 6
ON	Overnight
PBS	Phosphate saline buffer
Pdx1	Pancreatic and duodenal homebox-1
PI	Propidium iodide
PMP22	Peripheral myelin protein 22
PNS	Peripheral nervous system
PL	Footprint length
RT	Room temperature

RTU	Ready to use
SC(s)	Schwann cell(s)
SCAP	SREBP cleavage activating protein
SDS-PAGE	SDS polyacrylamide gel electrophoresis
SEM	Standard error of the mean
SFI	Sciatic functional index
SMDF	Sensory and motor neuron-derived factor
SOL	Soleus
SREBP	Sterol responsive element binding protein
TA	Tibialis anterior
TH	Tyrosine hydroxylase
TS	Toe sectional distance
WD	Wallerian degeneration
WB	Western blot

USC UNIVERSIDADE DE SANTIAGO DE COMPOSTELA

USC
UNIVERSIDADE
DE SANTIAGO
DE COMPOSTELA

INTRODUCTION

USC
UNIVERSIDADE
DE SANTIAGO
DE COMPOSTELA

Peripheral nervous system

Function and anatomy

The nervous system is the mechanism through which the internal machinery of an organism keeps in touch and reacts to environmental changes. At the most basic level, the nervous system has the function of transmitting, processing and regulating information from sensitive to effector structures (Keijzer, van Duijn, and Lyon 2013).

The central nervous system (CNS), composed of the brain and the spine, is connected to the peripheral tissues by the peripheral nervous system (PNS). The PNS includes pairs of cranial nerves, which mainly control the anatomical and physiological functions of the head, and pairs of spinal nerves, which originate in the spine and control the functions of the rest of the body.

Each nerve contains fibres that can be classified according to their target: somatic, in the case of they innervate the body walls and peripheral tissues, and visceral in which case they innervate the body's viscera. Alternatively, they can also be classified by their function, being named afferent or sensitive fibres, which collect and transmit information to the CNS, and efferent or motor if they are motor or effective fibres (Noback et al. 2012).

The main function of the spinal cord is to convey nerve impulses between PNS and the brain. Sensory information travels up the spinal cord to the brain, and motor information travels from the brain down the spinal cord to the effectors. The second function of the spinal cord is to be an integrated centre for spinal reflexes which are fast, predictable and automatic responses to changes in the environment (Figure I1).

The dorsal (sensory) root has afferent fibres from sensory receptors in the spinal cord, whose neural bodies are grouped together in the dorsal root ganglion. On the other side, the ventral (motor) root consists of efferent fibres that extend from the spine to skeletal muscle (somatic efferent) or involuntary smooth muscle, heart muscle or glands (visceral efferent).

The interneurons present in the grey matter are responsible for the spinal reflexes (Figure I1), connecting the afferent and efferent fibres (Gardner and Bunge 2005; Noback et al. 2012).

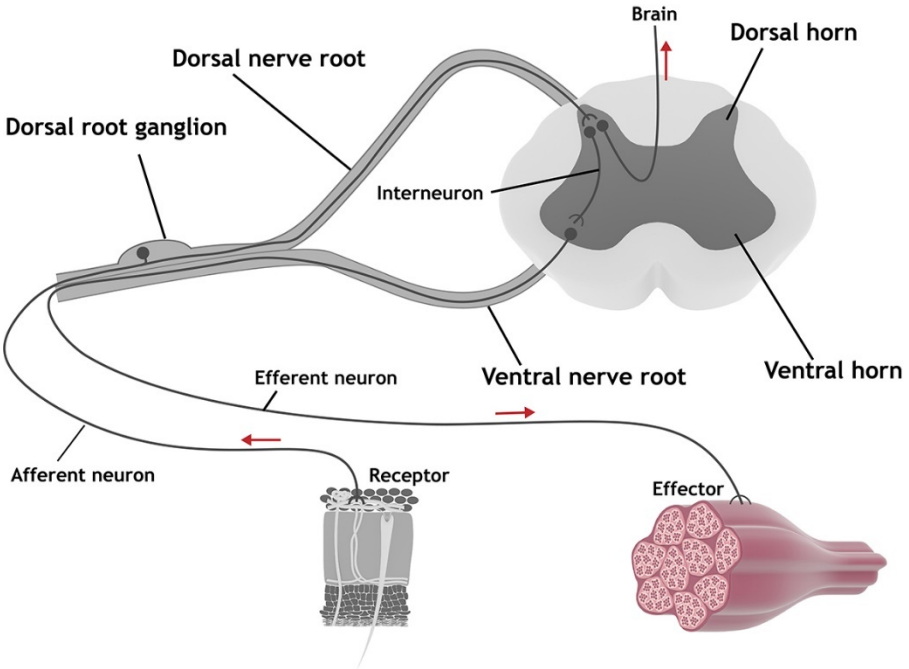

Figure I1. Neuroanatomical representation of the input and output of the peripheral nerve in the spinal cord. *Axial section of spinal cord, showing sensory afferent fibres (dorsal root) and motor efferent fibres (ventral root). Source: author original.*

Structure

The peripheral nerve is composed mainly of axons, Schwann cells (SCs), connective tissue and blood vessels. The minimum functional unit of the peripheral nerve is the nerve fibre, which is composed of an axon and the SCs associated with it (Topp and Boyd 2012).

As shows Figure I2, each nerve fibre is surrounded by the endoneurium, which is formed by loose connective tissue. The axons together with

the endoneurium are gathered in fascicles and encapsulated by the perineurium, a collagen-rich support cells layer that forms the blood-nerve barrier, which helps to protect the axon from the diffusion of toxic substances. Finally, the epineurium is the outermost layer of connective tissue that surrounds the entire nerve (Felten and Shetty 2009).

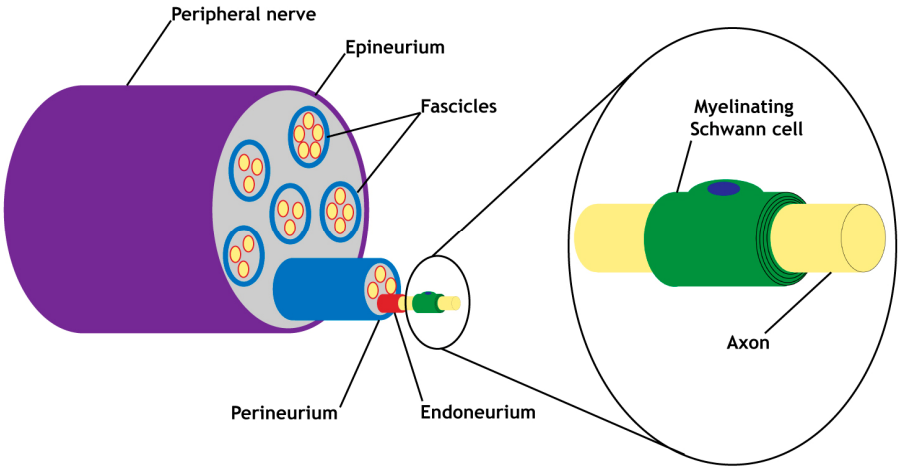

Figure I2. Peripheral nerve fibre structure. *The axons are surrounded by connective tissue and gathered in fascicles. The nerve is made up of several of these fascicles enclosed in connective tissue. Source: author original.*

The nerve fibres can be anatomically divided into myelinated and unmyelinated fibres. In general, thick nerve fibres (> 0.7 µm) are myelinated, while thin fibres (< 0.7 µm) are usually unmyelinated (Garbay et al. 2000).

Whether the axon is myelinated or not, it is surrounded by the cytoplasm of SCs. In the case of myelinated, the SCs form a dense sheath around the axon (myelin sheath) and each segment of the axon is myelinated by a single SC.

Myelin sheath

The rapid nerve conduction has been a crucial evolutionary advantage, as it allows organisms to speed up responses to different environmental changes. The speed of nerve conduction basically depends on the resistance of the nerve fibre to the electric current, and the capacitance of the axon to regenerate a nerve impulse.

Organisms have developed two basic mechanisms to increase the speed of nerve conduction. The first is to increase the diameter of the axons, which decreases the resistance to the nerve signal. The second is to envelope de axon with concentric wrapped insulating plasma membrane sheets, the myelin sheath, which causes a decrease in the capacitance between the outside and the inside of the fibre in certain areas (Hartline and Colman 2007; Seidl 2014).

The membranes that form the myelin sheath have a main proteolipid composition that forms a dense isolation of the axon. The presence of myelin sheath causes changes in the axon membrane or axolemma.

Between each myelin segment, there are non-myelinated areas called the Nodes of Ranvier (Figure I3, red band). It is in the Nodes of Ranvier where the action potentials are produced in myelinated axons so that a large number of voltage-gated Na^+ channels are concentrated in these areas (Rosenbluth, Mierzwa, and Shroff 2013).

Most of the myelin sheath constitutes the internode (Figure I3 yellow band), where the compact myelin is located. The end of the internode is the juxtaparanode (Figure I3, purple band), which has a large number of K^+ channels. These channels play a key role in damping the activity of the retrograde node, enough to allow its reactivation (Rosenbluth, Mierzwa, and Shroff 2013; Zoupi, Savvaki, and Karagogeos 2011).

Flanking the Node of Ranvier there are located the paranodes (Figure I3, green band), which serve as a barrier on the membrane, providing a separation between Na^+ ion channels and K^+ ion channels. This separation of the different ionic channels is essential for the correct functioning of the saltatory conduction in myelinated nerves (Zoupi, Savvaki, and Karagogeos 2011).

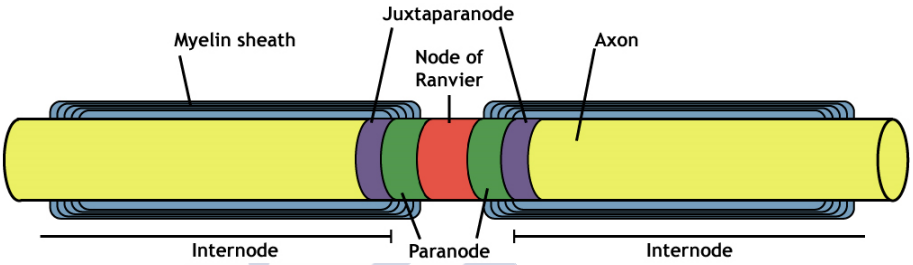

Figure I3. Diagram of a myelinated axon. *The node of Ranvier contains a high concentration of ionic Na+ channels which enables the generation of action potentials, while the juxtaparanode contains a large number of ionic K+ channels. The membrane of both is separated by the paranode. Source: author original.*

All these structures imply that, while nerve conduction in non-myelinated axons occurs in a continuous and slow manner, the presence of myelin in the axons causes a saltatory conduction between nodes of Ranvier, which increases the speed of nerve conduction. (Figure I4).

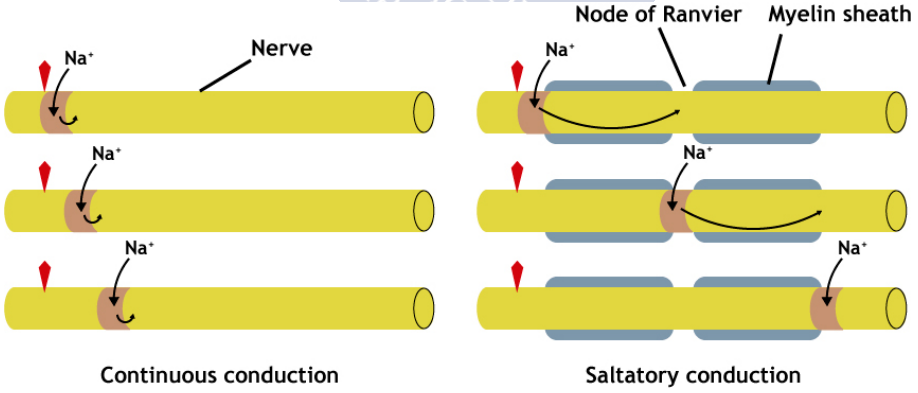

Figure I4. Nerve conduction along the axon. *Spread of action potential along an unmyelinated axon (continuous conduction) and a myelinated axon (saltatory conduction). Source: author original.*

PNS myelin composition

The cell types that produce the myelin sheath and myelin composition differ between the CNS and PNS, however, in both tissues it performs the same insulating function. Compact myelin has a water content of 40% and the dry fraction has a lipid composition of 70-85% and a protein composition of 15-30%. The accepted molecular architecture consists of lipid bilayers bound together with different specific myelin proteins.

Most of the lipid components of myelin are phospholipids, cholesterol and galactolipids. Although there are minor variations, its proportion and composition remain relatively stable in CNS and PNS. In fact, high levels of cholesterol, which is produced by the glial cells, are necessary for the proper production of myelin sheaths. (Saher et al. 2005).

Regarding the protein content of myelin, although some specific myelin proteins are found both in CNS and PNS, there are specific proteins for each one of the tissues. As shows the figure I5, in myelinating cells the outer (extracellular) surfaces of the SC membrane form the interperiod line, while the inner (cytoplasmic) surfaces of the membrane form the major dense line (Quarles, Macklin, and Morell 2006).

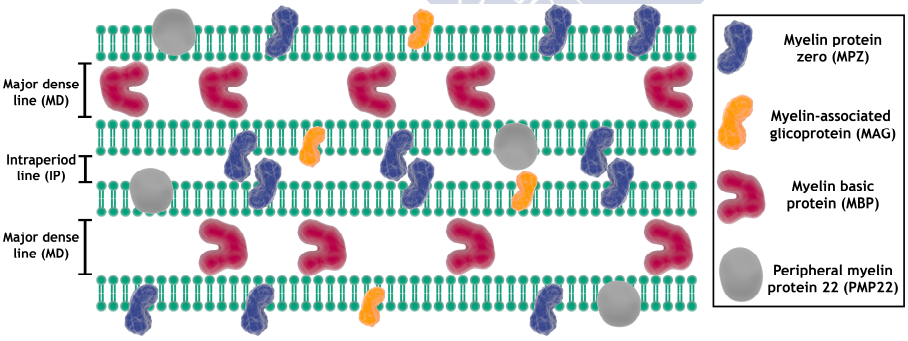

Figure I5. Representation of the myelin molecular organization in the PNS. *The image shows the lipidic membrane structures, as well as the main proteins that form the myelin sheath. Source: author original.*

Myelin protein zero (MPZ) is the most abundant protein in myelin in the SNP, representing between 50 and 70% of the total protein content (Jahn, Tenzer, and Werner 2009). MPZ is a transmembrane protein belonging to the immunoglobulin family, which is formed by an extracellular domain consisting of a simple Ig domain, a hydrophobic transmembrane domain and a cytoplasmic tail with a high positive charge (Han et al. 2013).

Morphological and ultrastructural analyses of knockout mice for MPZ showed that, although it did not appear to affect the initiation of myelinization, it was essential for proper compaction and maintenance of the myelin sheath in the PNS, as well as the maintenance of axonal integrity (Martini et al. 1995; Garbay et al. 2000).

The myelin basic protein (MBP) is a protein with positive charge located in the major dense line (MD; Figure I5), found in both the CNS and PNS, which plays an important role in myelin compaction. Although MBP is present in PNS myelin, it is not required for its formation, as the lack of MBP is compensated for by other proteins such as MPZ. However, without MBP, myelin has an abnormal morphology, such as reduced axon calibre, reduced myelin sheath thickness or aberrant Schwann cell-axon contact (Boggs 2006).

The high positive charge of MBP protein, due to its high amount of arginine and lysine residues, causes a self-assembly of the protein, joining together the negatively charged lipid bilayers (Vassall, Bamm, and Harauz 2015).

The myelin-associated glycoprotein (MAG) is a cell membrane glycoprotein, which is a member of the SIGLEC protein family. MAG is found in both the PNS and CNS and is located in the non-compact regions of the myelin sheath. The expression of MAG is increased in the early stages of myelinization, so it appears to be involved in the initial interactions of the axon with the myelinating cells (Quarles 2007). However, their levels remain relatively high in adult animals, suggesting an important role in the

maintenance of myelin sheaths and myelinated axons. MAG main function is to support the proper connection between the axon and the myelin sheath, contributing to the long-term stabilization of the axon.

Peripheral myelin protein 22 (PMP22) is a transmembrane glycoprotein present mostly in the PNS (Han et al. 2013). PMP22 plays a key role in the formation and maintenance of compact myelin, and its expression is increased when the SCs come into contact with the axon. In addition, its expression also increases during the proliferation of SCs, which suggests that PMP22 may also play a role in cell cycle regulation.

Myelination and regulation

In the PNS the SCs are the cells in charge of the myelinization process, establishing one by one connection with the axon. The myelin sheath is formed due to the spiral wrapping of the SCs around the axon. The spiral wrap results from the rotation of the internal SC loop around the axon. Initially this envelope is very loose, however, over time the myelin becomes compact.

It is well known that only axons larger than a certain calibre are myelinated, whereas axons smaller than a certain calibre are not myelinated. This may be because the addition of myelin does not enhance nerve conduction in smaller axons, but the mechanisms by which the fibres to be myelinated are selected are not well understood (Sherman and Brophy 2005), Some adhesion molecules such as L1 or neuronal cell adhesion molecule (NCAM) are less expressed in myelinated axons, however, this fact has not been able to connect with axon myelinization (Haney et al. 1999; Charles et al. 2002).

One of the first events to occur in the early stages of myelinization is the formation of the axon-glia junctions, which will define the paranodal zone and separate the node of Ranvier and juxtaparanode. At this point, the first components of the nodes of Ranvier, such as ankyrin G and βIV spectrin, are first detected. This is followed by the accumulation of voltage-

gated sodium channels, which is fundamental for proper saltatory nerve conduction. Although myelin ensheathment and node formation occur simultaneously, myelinization is not necessary *per se* for sodium channel clustering (Sherman and Brophy 2005).

After the SC is attached and wrapped around the axon, the SCs change from an immature to a promyelinating phenotype. At this point, the SCs begin to express transcription factors such as octamer transcription factor 6 (Oct6) or early growth response protein 2 (EGR2), which regulate the expression of myelin-specific proteins, and the myelin sheath begins to form and the thickness of the myelin sheath increases (Figure I6). The thickness of the sheath is regulated by different molecules such as neuregulin or bone-derived neurotrophic factor (BDNF). The ratio of the diameter of the axon divided by the diameter of the axon along with the myelin sheath is called the g ratio. This measure is used to evaluate the relative thickness of the myelin sheaths and remains relatively stable in myelinated axons (0.6-0.7). However, in axons that have been remyelinated, the g-ratio is shown reduced (Salzer 2015).

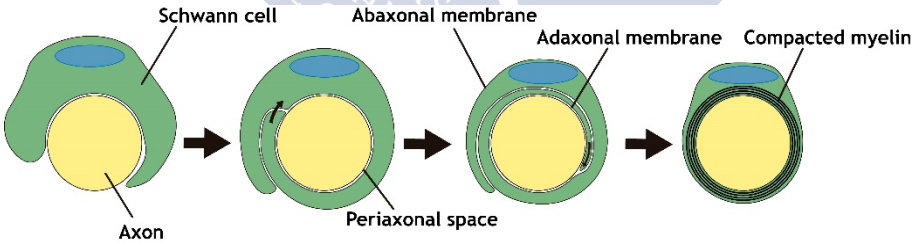

Figure I6. Schwann cell myelination. *The image shows a Schwann cell enveloping and rotating around the axon forming myelin sheath. Source: author original.*

Myelin compaction in the PNS occurs from the inner membranes (abaxonal layers) to the outer ones (adaxonal layers), with a delay of two or three wraps from the leading edge, allowing the myelin sheath to grow below the last layer. Cytoplasmic membrane surfaces, which have a strong negative charge, attract basic proteins such as MBP, while extracellular

compaction of myelin membranes requires the action of adhesion proteins such as MPZ or PMP22 (Nave and Werner 2014).

The cell body and the noncompacted adaxonal myelin from the glial cells maintain cytoplasmic continuity through membrane channels in the paranodal zone, which remains noncompacted permanently. Additionally, in the PNS, there are cytoplasmic channels that remain open during maturehood in the internodal zone called Schmidt-Lanterman incisures (Nave and Werner 2014).

The glial cells and neurons send each other signals which regulate the formation, maintenance and functioning of the nervous system. In that sense, many of the processes that regulate the development of SCs depend on signals associated with axons and myelinization in the PNS is regulated by various intrinsic and extrinsic factors.

One of the main regulators of myelinization is neuregulin (NRG1), a member of the epidermal growth factor (EGF) superfamily. The NRG1 signalling acts through the heterodimer formed by erb2/erb3, expressed by the SCs. Other signalling systems, such as BDNF, also appear to be involved in the formation and maintenance of myelin (Sherman and Brophy 2005).

The components of the extracellular matrix synthesized by the SCs constitute the basal lamina. Different components of the basal lamina, such as laminin or collagen, are also involved in the regulation of the myelinization of SCs (Salzer 2015). The survival, proliferation and cytoskeletal reorganization of SCs are promoted by laminin, while collagen promotes cell adhesion and extension, These are key mechanisms in myelination of the peripheral nerves (Chernousov et al. 2008).

All these signals converge on the activation of different signalling pathways such as PI3K/Akt or mitogen-activated protein kinase (MAPK) pathways which are involved in the regulation of SC development and differentiation (Salzer 2015). The PI3K/Akt signalling pathway plays a key role in proliferation, survival and initiation of myelination of SCs (Ogata et

al. 2006). On the other hand, the MAPK pathway promotes early differentiation of SCs and is a key regulator of promyelinating signals (Salzer 2015).

Peripheral nerve injury

The peripheral nerves can be damaged by various causes, such as excessive pressure, overstretching or a cut. The damage range from temporary discomfort to permanent impairment (Menorca, Fussell, and Elfar 2013).

In 1943, Seddon was the first to implement a classification system for nerve damage, based on the loss of myelin and the damage of the axons and/or surrounding connective tissue (Seddon 1943).

The mildest damage is called neuropraxia, characterized by localized demyelination without affecting the axons or connective tissue. The next level is called axonotmesis which, in addition to localised demyelination, causes damage to the axon integrity, however, the continuity of the connective tissue is maintained. Neurotmesis is the most severe damage, which involves complete discontinuity of the nerve, including the connective tissue.

Later in 1951, Sunderland expanded Seddon's classification into 5 different grades (Sunderland 1951). Grade I corresponds to neuropraxia in the Seddon classification system, while grade V corresponds to neurotmesis. Axonotmesis is divided into grades II, III, and IV based on the amount of connective tissue damage. In grade II there is no damage to the connective tissue, in grade III the endoneurium is damaged, while in grade IV the perineurium is also damaged (Figure I7).

After peripheral nerve damage, morphological and physiological changes occur in the damaged area, as well as in the proximal and distal sites. Almost immediately the sensitive neurons of DRGs, as well as the motor neurons of the ventral horn of the spinal cord, change from a sig-

nalling phenotype to a growing phenotype. Consequently, the protein synthesis of neurotransmitters diminishes, while the synthesis of growth-related proteins increases.

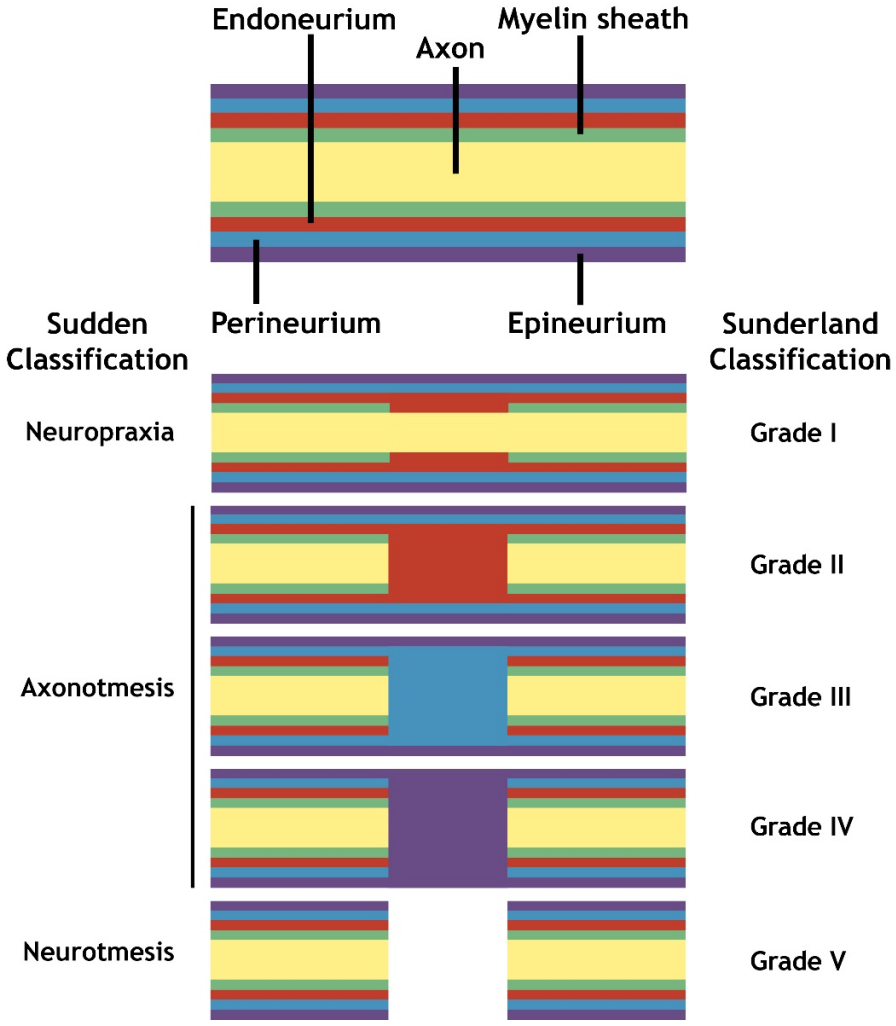

Figure I7. Nerve injury classification. *Schematic representation of the different types of peripheral nerve damage and the main classification systems. Source: author original.*

The axon in the proximal area produces a large number of sprouts that advance towards the distal area inside the basal lamina. The SCs play an essential role in axonal growth, as they are able to direct the axons towards the targets in the distal area, which significantly determines the effectiveness of nerve regeneration (Geuna et al. 2009).

Wallerian degeneration

After nerve damage, the distal area begins a degrading process called Wallerian degeneration (WD; Figure I8). This process begins immediately after the damage and involves the degradation and clearance of peripheral nerves (Geuna et al. 2009).

One of the main events occurring during WD is intrinsic degeneration of the distal axons. WD activates responses in non-neural cells that promote the clearing of the debris in the distal region and the production of an environment suitable for axonal growth (Gaudet, Popovich, and Ramer 2011). The axonal degeneration associated with WD is induced by different mechanisms. One of the main factors is the entry of calcium into the axoplasm, which activates calpain, a key protease in the degradation of the cytoskeleton (Stirling and Stys 2010). The ubiquitin-proteasome system also appears to be involved in axon degradation (Zhai et al. 2003).

An important aspect during WB is the breakdown of the blood-nerve barrier (BNB). The BNB is composed of endothelial cells connected by very tight junctions, whose function is to restrict the flow of molecules into the neural tissue. The BNB breaks down quickly in the area of damage, however, only with the beginning of degeneration, the BNB is involved in the distal site (Gaudet, Popovich, and Ramer 2011).

After a peripheral nerve injury, the SCs in the distal site become differentiated. The SCs decrease the synthesis of proteins associated with myelin and increase the expression of proteins associated with nerve regeneration, such as neuregulin or neurotrophins (Murinson et al. 2005).

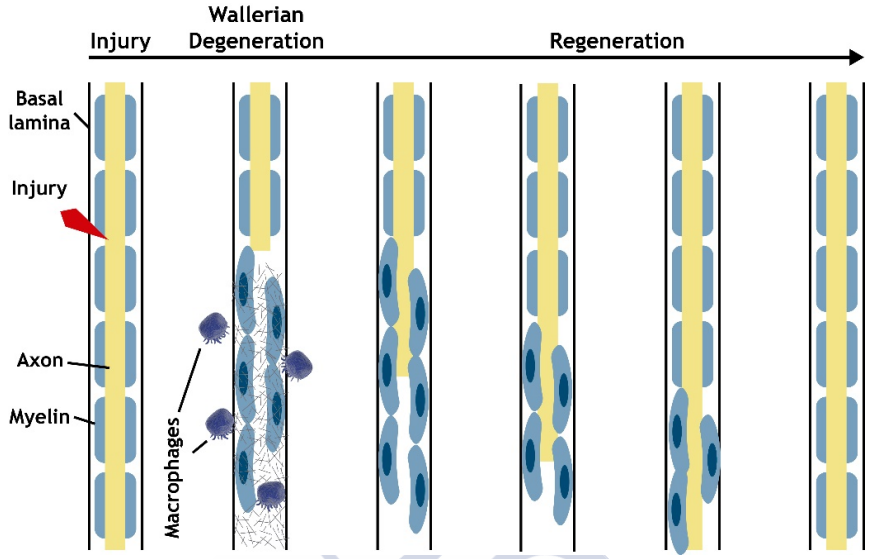

Figure I8. Nerve regeneration. *Schematic representation of Wallerian degeneration, macrophage recruitment and debris clearance and nerve regeneration. Source: author original.*

The SCs begin to clear debris through phagocytosis and recruitment of macrophages. Macrophages are recruited in the last stages of WD, contributing to the removal of cellular debris and myelin (Mueller et al. 2003).

The SCs switch to a proliferating phenotype and they keep confined into the basal lamina, aligned in the denominated Büngner bands. These cells secrete growth factors and generate a suitable substrate for axon growth (Griffin and Thompson 2008).

Regeneration

Axonal regeneration begins once the WD is complete. At the end of the proximal zone, a growth cone is formed that sends filopodia to the distal zone, which verifies the microenvironment. These filopodia are randomly oriented in the beginning, and they enhance their directionality as the expression of actin and myosin increases (Jin et al. 2009). This growth may be attracted to or repelled by contact-mediated or chemical signals called neurotrophism (Menorca, Fussell, and Elfar 2013).

The SCs play a fundamental role in promoting axonal growth, and they are the main source of neurotrophic factors during nerve regeneration (Frostick, Yin, and Kemp 1998). In addition, the SCs increase the synthesis and deposition of extracellular matrix proteins, such as laminin and fibronectin. These proteins favour axonal growth, as the growth cone uses these proteins for adhesion to the basal lamina (Menorca, Fussell, and Elfar 2013).

Although the growing axon reaches the target organs, only if they are properly maintained, a complete nerve regeneration is possible. In the concrete case of motor axons, the neuromuscular junction, composed of the end of the motor neurons, the terminal SC and the end plate of the muscle fibre, must be kept stable.

Actual strategies in nerve injury treatment

Although the PNS has the intrinsic ability to regenerate, the success of the recovery will depend on several factors, such as the age of the patient, the type of damage, the speed of the treatment application or the distance from the damage to the neuron's soma. The most common treatment option is microsurgery with a tensionless epineural suture; however, when end-to-end suturing is not possible, autologous nerve grafts are usually used, which means more intense surgery and the sacrifice of healthy nerves.

Another approach in the case of nerve wounds is the application of nerve growth guidance supports. This provides structural support for axonal growth and nerve regeneration. However, the devices currently used, whether biodegradable or not, are not able to match the results obtained with autologous nerve grafting and are usually used in minor injuries that do not require a large recovery implementation. Recently, the research strategies have moved from passive devices that only serve to guide and isolate the nerve to a more active devices that involve the generation or modification of the microenvironment of the damaged area to enhance the

stimulation of nerve growth. In this aspect, the main research focuses on the generation and modification of biomaterials and the use of extracellular matrix molecules, which promote the attachment, mobility and proliferation of SCs.

Due to the importance of SCs in the development and repair of PNS, they have been the main object of cell therapy research, being transplanted experimentally and showing promising results (Kalbermatten et al. 2008) although other glial cells have also been used and are capable of providing a trophic support to the regenerating nerves (Dombrowski et al. 2006). Nevertheless, these cell therapies have limited expansion capacity and, as in the case of autologous nerve transplants, they require the sacrifice of healthy tissue so current efforts in cell therapy for peripheral nerve regeneration are focused on the use of alternative cell types and stem cells, such as embryonic stem cells, neuronal stem cells, induced pluripotent stem cells and adult mesenchymal stem cells (Faroni et al. 2015).

At present there is no specific pharmacological clinical therapy for the peripheral nerve damage treatment, however, different growth factors, hormones and other small molecules have been proposed as promoters of regeneration, either by increasing proliferation, migration or the production of myelin proteins in SCs (Faroni et al. 2015).

In any case, the greatest probability of success in the PNS damage treatment is presumably due not to a single approach, but to a combination of several of these strategies.

Obestatin

Obestatin is a 23-amino-acid peptide derived from the preproghrelin precursor. This novel peptide was first isolated in 2005 by Zhang et al from rat stomach. The term obestatin is derived from the Latin verb "obedere", which means "to devour" and "statin", which means suppression (Zhang et al. 2005; Trovato et al. 2014).

Initially, obestatin was described as a circulating peptide that has a pulsatile secretion with an ultradian rhythm similar to ghrelin (Zhu et al. 2006). Obestatin was reported as a molecule with an action opposite to the orexigenic action of ghrelin, however, its role in the food intake is still very controversial (Hassouna, Zizzari, and Tolle 2010).

Obestatin biosynthesis

Preproghrelin is a polypeptide encoded by the GHRL gene. After translation, the signal peptide is removed and processed into both ghrelin and obestatin. The post-transcriptional processing of preproghrelin generates different molecules derived from ghrelin based on splicing and post-transcriptional residues modification (Figure I9).

Preproghrelin is composed of a signal peptide and a fragment of 94 amino acids: the proghrelin. In the endoplasmic reticulum, the signal peptide is removed and proghrelin suffers from several proteolytic processes. The proghrelin produces mature ghrelin and c-ghrelin, a 66 amino acid peptide (Jeffery et al. 2005). C-ghrelin can freely circulate and/or be processed resulting in smaller peptides including obestatin (Gualillo et al. 2006).

After excision of the obestatin precursor, a lysine residue is removed from the carboxy-terminal end, while the anterior glycine residue donates an amide group to the carboxyterminal end leucine residue (Garg 2007).

This amidation at the carboxy-terminal end appears to be a key modification necessary for the bioactivity of obestatin (Zhang et al. 2005; Alén et al. 2012).

An obestatin truncated fragment of 13 amino acids has been identified in stomach extracts: obestatin-(11-23). Whether (11-23)-obestatin is formed physiologically and the mechanisms by which it is formed are still largely unknown. Several authors suggest that (11-23)-obestatin may have

a biological activity analogous to obestatin (Scrima et al. 2007; Alén et al. 2012).

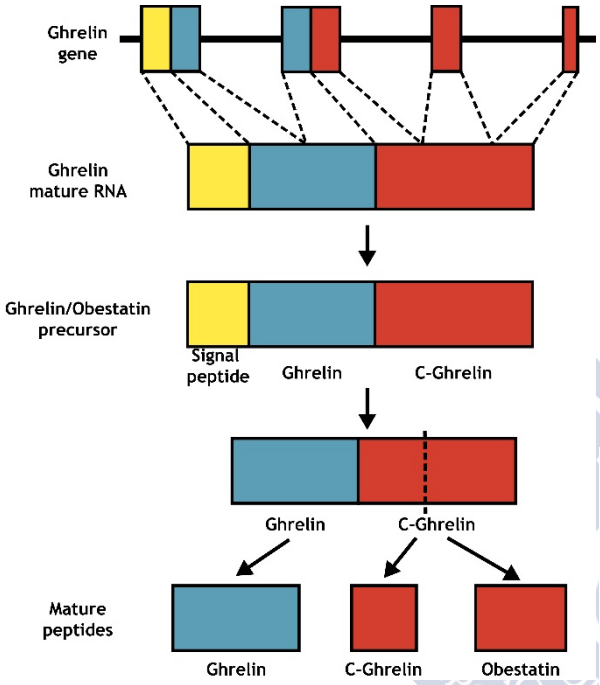

Figure I9. Overview of ghrelin gene structure and relevant peptide variants. *The signal peptide is shown in yellow, the ghrelin in blue, while the c-ghrelin and obestatin appears in red. Source: author original.*

Obestatin expression.

Although in humans the main obestatin-producing cells are found in the stomach and the rest of the gastrointestinal tract, obestatin has also been found in other tissues (Grönberg et al. 2008; Alén et al. 2016). In addition to the stomach, reactive cells for obestatin have also been found at the periphery of the islets of the pancreas, as well as in breast glands. In other tissues such as the pituitary gland, prostate, testicles, placenta, ovaries or thyroid, a weak expression of obestatin can be detected.

Obestatin is expressed in gastric mucosa and pancreas in rats. Leydig and myenteric rat ganglion cells are positive for obestatin too, suggesting

a possible bioactivity of the obestatin in the nervous system (Dun et al. 2006). Obestatin was also found in rat and human skeletal muscle and skeletal muscle cell models, being overexpressed under experimental injury conditions (Gurriarán-Rodríguez et al. 2012).

Obestatin receptor: GPR39.

The orphan G protein-coupled receptor 39 (GPR39) has initially been reported to be the receptor of obestatin (Zhang et al. 2005), however, some authors questioned any stimulatory activity of obestatin on GPR39 suggested that obestatin does not activate GPR39 and that its ligand is yet to be discovered (Chartrel et al. 2007).

Other receptors such as glucagon-like peptide-1 receptor (GLP1R) have been proposed as mediators of the action of obestatin (Granata et al. 2008), however, this fact has been questioned due to the inability of obestatin to displace GLP1 in HEK293T cells overexpressing GLP1R (Unniappan, Speck, and Kieffer 2008).

Zinc ions have been suggested likewise as a specific ligand of the GPR39 receptor, considering it as a key component of the Zn metabotropic signalling (Holst et al. 2007; Besser et al. 2009). Zhang et al again demonstrated the effect of obestatin on body weight, food intake and gastrointestinal mobility in mice, however, it was unable to reproduce the obestatin-GPR39 interaction. (Zhang et al. 2007).

One of the reasons for this low reproducibility could be the irregular quality of peptides provided by different suppliers, which would make it unsuitable in many cases for *in vivo* and *in vitro* experiments (De Spiegeleer et al. 2008).

In addition, obestatin has been shown to have a variety of iodination levels. Peptides with different levels of iodination have distinct metabolizing properties and presumably different biological activities (De Spiegeleer et al. 2012). In this sense, it has been demonstrated that mono-iodo-obestatin is able to bind specifically to the GPR39 receptor in transiently

transfected HEK293T cells with plasmids encoding human and murine GPR39 (Zhang et al. 2008).

There is a great deal of controversy about whether obestatin is the ligand of the GPR39 receptor; however, different studies support this fact. Obestatin is able to induce the expression of transcription factors related to gastrointestinal activity such as c-fos in wild-type mice, while this effect is mitigated when using knockout mice for the GPR39 receptor (Zhang et al. 2008). In addition, the signal triggered by the obestatin is inhibited by GPR39 receptor silencing (Camiña et al. 2007; Gurriarán-Rodríguez et al. 2011, 2012; Alén et al. 2016). Co-immunoprecipitation assays conclusively prove the binding of obestatin as a ligand of the GPR39 receptor (Gurriarán-Rodríguez et al. 2015)

GPR39 expression.

A wide range of tissues expresses GPR39, both in humans and rodents. The expression of GPR39 has been tested in different tissues through the analysis of protein and RNA expression.

The highest levels of GPR39 expression have been found in tissues of the gastrointestinal tract such as the stomach, duodenum, jejunum or ileum (Zhang et al. 2005). A relatively high expression of GPR39 has also been found in white adipose tissue, kidney, pancreatic duct epithelium, pancreatic β-cells, liver, lungs, heart and reproductive tissues (McKee et al. 1997; Depoortere 2012).

An elevated expression of GPR39 has been found in the brain in hippocampus, amygdala and septum cells, but in the hypothalamus, no positivity for GPR39 has been detected (Jackson, Nothacker, and Civelli 2006; Moechars et al. 2006). GPR39 was also discovered in rat and human skeletal muscle *in vivo* and *in vitro* (Gurriarán-Rodríguez et al. 2012; Santos-Zas et al. 2016).

Obestatin bioactivity.

Despite the fact that obestatin was originally described as an opponent of ghrelin activity, and although this fact has been rejected by various publications (Seoane et al. 2006; Nogueiras et al. 2007) this effect is still very controversial nowadays.

Several studies still support the involvement of the obestatin in the regulation of energy homeostasis (Zhang et al. 2013) and intraperitoneal administration of obestatin in rodents has been shown to reduce food intake (Bresciani et al. 2006; Green, Irwin, and Flatt 2007; Zizzari et al. 2007). Obestatin also appears to be involved in thirst inhibition (Samson et al. 2007), anxiety reduction (Carlini, Schiöth, and DeBarioglio 2007), sleep regulation and cortical neuron aggregation (Szentirmai and Krueger 2006). It is also able to decrease apoptosis in adipose tissue, inflammation and insulin resistance (Green, Irwin, and Flatt 2007).

Studies based on GPR39 null mice show that the lack of the receptor accelerates gastric emptying, which increases the signalling of appetite, contributing to increased food intake and body weight (Moechars et al. 2006). These results are controversial, as although in many cases the effect on food intake is corroborated, body weight gain appears to be less reproducible (Tremblay et al. 2007) and some studies suggest that the role of GPR39 may be involved in the regulation of glucose homeostasis more than in body weight gain.

The GPR39 receptor was found in pancreatic β-cells and glucose-induced insulin secretion was reduced in female GPR39 null mice, due to pancreatic and duodenal homebox-1 (PdX1) downregulation (Moechars et al. 2006; Depoortere 2012). In mouse, early onset diet-induced obesity model, blood glucose levels were reduced in GPR39 null mice, which could suggest a role for GPR39 in insulin sensitivity (Verhulst et al. 2011). Obestatin was found to promote the survival of pancreatic β-cells and islet cells in the pancreas, through activation of the ERK1/2 and PI3K/AKT routes. (Granata et al. 2008).

The obestatin/GPR39 system has also been proposed as an important regulator of adipocyte metabolism and adipogenesis. In this sense, preproghrelin and consequently obestatin are overexpressed during adipogenesis *in vitro*. In addition, studies in which obestatin is removed or blocked demonstrated the importance of this peptide during adipogenesis (Gurriarán-Rodríguez et al. 2011). In human adipose tissue, decreased GPR39 expression was found in patients with obesity-associated type 2 diabetes mellitus (Catalán et al. 2007).

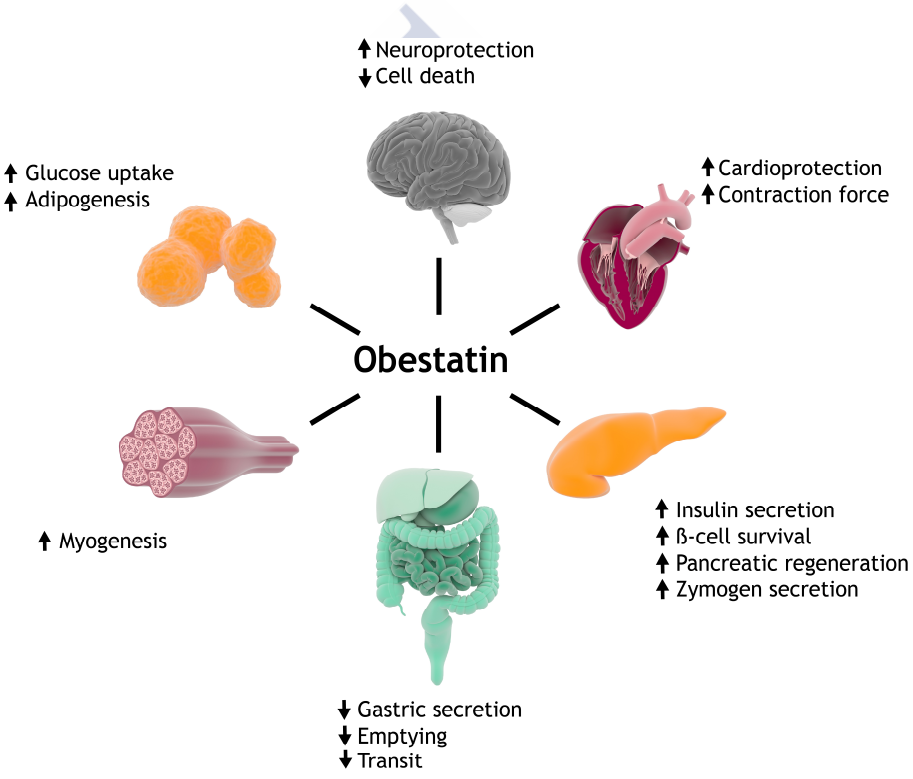

Figure I10. Obestatin/GPR39 system bioactivity. *Summary of proposed physiological actions based on GPR39 overexpression mice, GPR39 knockout mice and in vitro assays published studies. Source: author original.*

Camiña's group has demonstrated that the obestatin/GPR39 system plays a role in myogenesis regulation. Preproghrelin is increased during L6E9 rat myoblast cell differentiation. Overexpression of the obestatin/GPR39 system in skeletal muscle promotes stimulation of expansion and differentiation of satellite cells and hypertrophy of the myofiber, increasing regenerative capacity after muscle damage (Gurriarán-Rodríguez et al. 2012, 2015).

On the other hand, in cardiac muscle, obestatin is capable of increase the secretion of epinephrine from the sympathetic neurons, which leads to an increase in the ex vivo and *in vivo* contraction force (Sazdova et al. 2009).

GPR39 was found upregulated in a hippocampal cell line resistant against cell death stimulators. The overexpression of GPR39 in these cells is able to protect against different proapoptotic signals such as oxidative stress and endoplasmic reticulum stress. These data suggest a possible role for GPR39 as a potential neuroprotective mediator target (Dittmer et al. 2008).

USC UNIVERSIDADE DE SANTIAGO DE COMPOSTELA

USC
UNIVERSIDADE
DE SANTIAGO
DE COMPOSTELA



OBJECTIVES

USC
UNIVERSIDADE
DE SANTIAGO
DE COMPOSTELA

After an injury in the peripheral nervous system the damaged axons begin to grow from the proximal end, while in the damaged area and the distal end the SCs differentiate, proliferate and acquire a repairing phenotype, helping at first in the myelin and cell debris removal, and then myelinating again the axons that are growing.

There is a network of extracellular signals that determine the activity of SCs during nerve regeneration, however, the current state of knowledge leaves many questions unanswered. Considering the biological qualities described for obestatin, we believe it is necessary to study the effect of obestatin on the SNP, especially aimed at the treatment of pathologies associated with peripheral nerve regeneration.

The main objective of this doctoral thesis is to establish the relationship between the obestatin/GPR39 system with processes related to peripheral nerve neuroprotection and repair, to explore fundamental parameters that can contribute to the recovery of nerve and neuromuscular function.

This issue will be accomplished with the following points:

1. To determine the expression of the system obestatin/GPR39 in peripheral nerve tissue and cellular models.

2. To analyse the possible neuroprotective effect of obestatin and its mechanisms of action.

3. To study the effects of obestatin on Schwann cells and the processes involved in regeneration.

4. To elucidate the mitogenic, morphological and physiological effects of obestatin in an *in vitro* myelinization model.

5. To determine the effect of local administration of obestatin on a rat sciatic nerve crush model.

USC
UNIVERSIDADE
DE SANTIAGO
DE COMPOSTELA

USC
UNIVERSIDADE DE SANTIAGO DE COMPOSTELA

MATERIALS AND METHODS

USC
UNIVERSIDADE
DE SANTIAGO
DE COMPOSTELA

Antibodies

Table 1. Antibodies.

Antibody	Use	Dilution	Supplier	Reference
Anti-phospho-AKT (ser473)	WB	1:1,000	Cell Signalling Tech.	9271S
Anti-Akt	WB	1:1,000	Cell Signalling Tech.	9272S
Anti-BCL2	WB	RTU	Dako	IS614
Anti-EGR2	WB	1:100	Santa Cruz Biotech.	sc-293195
Anti-GAP43	IF	1:250	Novus Biologicals	NB300-143
Anti-GAPDH	WB	1:2,000	Abcam	ab9485
Anti-GPCR GPR39	IHC	1:500	Abcam	ab39227
Anti-phospho-GSK3α/β (S21/9)	WB	1:1,000	Cell Signalling Tech.	9331S
Anti-GSK- GSK3α/β	WB	1:1,000	Santa Cruz Biotech.	sc-56913
Anti-Neurofilament	IHC IF	RTU	Dako	IR607
Anti-NGF	WB	1:250	Santa Cruz Biotech.	sc-365944
Anti-NSE	IF	RTU	Dako	IS612
Anti-MAG	WB	1:1,000	R&D	AF538
Anti-MBP	WB (cc)	1:500	Abcam	ab62631
Anti-MBP	IHC	1:100	Dako	A0623
	IF	1:100		
	WB (t)	1:200		
Anti-(Ki67 antigen) MIB-5	IHC	1:50	Dako	M7248
Anti-MPZ	WB	1:1,000	Abcam	ab31851
Anti-Obestatin	IHC	1:100	Abcam	ab41704
Anti-Oct6	WB	1:200	Santa Cruz Biotech.	sc-390056
Anti-phospho-p44/42 MAPK (ERK1/2) (T202/Y204)	WB	1:1,000	Cell Signalling	9101S
Anti-P44/42 MAPK (ERK1/2)	WB	1:1,000	Cell signalling	9102S
Anti-TH	IF	1:500	Abcam	ab101853

Relation of the antibodies used in the different analyses performed in this work. Abreviations: IF: Immunofluorescence IHC: immunohistochemistry; WB: western blot; cc: cell culture lysate; t: tissue lysate; RTU: ready to use.

Table 1. Antibodies (continuation).

Antibody	Use	Dilution	Supplier	Reference
Anti-Goat alexa fluor 488	IF	1:1,000	Invitrogen	A11055
Anti-Mouse alexa fluor 594	IF	1:1,000	Invitrogen	A21125
Anti-rabbit alexa fluor 594	IF	1:1,000	Invitrogen	A11012
Peroxidase-AffiniPure Goat Anti-Rabbit IgG (H+L)	WB	1:10,000	Jackson	111-035-003
Peroxidase-AffiniPure Goat Anti-Mouse IgG (H+L)	WB	1:10,000	Jackson	115-035-003
Peroxidase-AffiniPure Rabbit Anti-Goat IgG (H+L)	WB	1:10,000	Jackson	705-035-003

Relation of the antibodies used in the different analyses performed in this work. Abreviations: IF: Immunofluorescence IHC: immunohistochemistry; WB: western blot; cc: cell culture lysate; t: tissue lysate; RTU: ready to use.

Cell culture.

Rat tail collagen type I extraction and plate coating.

Rat tails were collected from Sprague-Dawley rats and stored at -80ºC until use. The skin was removed exposing tail tendons, which were extracted using fine tweezers, washed with phosphate saline buffer (PBS; Sigma-Aldrich, St. Louis, MO, US) and 70% (v/v) ethanol (Montplet, Barcelona, ES). Tendons were dissolved in 250 mL of 0.1% (v/v) acetic acid per g of tendons at 4 ºC under stirring. Tendons/acetic acid mixture was then centrifuged (3,200 x g, 4 ºC, 90 min), the supernatant (collagen extract) was collected and chloroform (10% of collagen volume; JT Baker, Avantor, PA, US) was added to sterilize the collagen extract and the mixture was allowed to settle overnight (ON) at 4 ºC. The upper collagen solution was aseptically removed and stored at 4 ºC.

The protein content of the collagen solution was quantified using the QuantiPro™ BCA Assay Kit (Sigma-Aldrich, St. Louis, MO, US), and the concentration was adjusted to 0.5 g/L for the stock solution. The stock solution was diluted to a 0.1 g/L working solution in sterile water suitable for cell culture (Sigma-Aldrich, St. Louis, MO, US). Plate coating was performed treating the plates with collagen working solution for 1 h at room temperature (RT) or ON at 4 ºC. Then, the solution was removed and the plate was allowed to dry up for 1 h under laminar flow and UV light.

PC12 cell culture.

PC-12 cells (CRL-1721, ATCC, Rockville, MD, US) are derived from a pheochromocytoma of the rat adrenal medulla and represent a widely used model in neuronal differentiation. They can acquire a sympathetic neuronal phenotype in response to nerve growth factor (NGF) administration (Greene and Tischler 1976). PC-12 were maintained in RPMI 1640 (Lonza, Basel, CH), and supplemented with 10% (v/v) foetal bovine serum (FBS; Hyclone, GE Healthcare Life Sciences, South Logan, UT, US), 5% (v/v)

heat inactivated horse serum (HS; Gibco, NY, USA) and 1% glutamine/penicillin/streptomycin (Sigma-Aldrich, St. Louis, MO, US). Cells were seeded on rat tail collagen I coated plates (Corning, NY, US) and incubated in an atmosphere containing 5% CO_2 at 37 ºC.

IFRS1 cell culture.

IFRS1 (Immortalized Fischer rat Schwann cell 1) cell line was kindly donated by Dr Kazunori Sango (Tokyo Metropolitan Institute of Medical Medicine, Tokyo, JP). IFRS1 is a spontaneously immortalized Schwann cell line derived from long-term cultures of adult rat dorsal root ganglia (DRG) and peripheral nerves. Cells were maintained in Dulbecco's Modified Eagle Medium (DMEM; Lonza, Basel, CH), supplemented with 5% (v/v) FBS, 20 ng/mL recombinant human heregulin-βIII (Merck, Darmstadt, DE), 5 µM forskolin (Abcam, Cambridge, UK), 100 U/mL penicillin and 100 mg/mL streptomycin (Sigma-Aldrich, St. Louis, MO, US).

Immunohistochemistry and immunocytochemistry.

IFRS1 and PC12 cells were cultured as described above at a density of 5,000 cells/cm^2 on coverslips and rat tail collagen type I coated coverslips, respectively. Cells were fixed by immersion in 96 % (v/v) ethanol.

Histological sections of rat dorsal root ganglia (DRG), anterior horn of the spinal cord and sciatic nerves were kindly donated by Dra. Rosalía Gallego Gómez (University of Santiago de Compostela, Santiago de Compostela, Spain). Histological sections of sectioned rat sciatic nerves were obtained from previous studies of Dr Jose Luis Relova Quinteiro (University of Santiago de Compostela, Santiago de Compostela, Spain). The histological sections were dewaxed at 60 ºC for 30-60 min following by immersion in xylene (PanReac, Castellar del Valles, ES), and rehydrated with decreasing concentrations of ethanol.

Samples were washed with washing buffer (50 mM Tris-HCl, 150 mM NaCl, 0.05% (w/v) Tween 20, pH 7.6) twice for 5 min and blocked with peroxidase-blocking reagent (Dako, Agilent, CA, USA) for 10 min.

Samples were incubated with anti-GPR39 and anti-obestatin in Dako antibody diluent (Dako, Agilent, CA, US) overnight at 4 ºC, and EnVision™ FLEX/HRP (Dako, Agilent, CA, US) was used as the detection system.

3,3'-diaminobenzidine DAB-tetrahydrochloride (Dako, Agilent, CA, US) was used as chromogen, and nuclei were counterstain with Harris haematoxylin solution (HHS; PanReac, Castellar del Valles, ES) for 1 min. Slides and coverslips were dehydrated and mounted with Entellan® mounting medium (Merk, Darmstadt, DE).

USC UNIVERSIDADE DE SANTIAGO DE COMPOSTELA

USC
UNIVERSIDADE
DE SANTIAGO
DE COMPOSTELA

PC12 neuroprotection model

PC12 proliferation

For the analysis of proliferation, PC12 cells were seeded on a rat tail collagen type I-coated 96-well plates at a cell density of 5,000 cells/cm2 and cultured in DMEM supplemented with 5 % (v/v) FBS. Cells were maintained for 24 h in culture to allow them to attach to the plate.

The medium was completely removed and replaced with serum-free DMEM for additional 16-18 h. Then, cells were treated or not with different doses of rat obestatin (50, 100, 200 nM; BCN peptides, Barcelona, ES) and 5% (v/v) FBS, used as a positive control. The cells were restimulated after 24 h, and proliferation assay was finished at 48 h.

To evaluate cell proliferation, 10 µL of Cell Counting Kit-8 (CCK8) solution (Dojindo, Kumamoto, JP) was added 4 h before the assay endpoint and the plates were incubated at 37 ºC. Absorbance at 450 nm was measured in an Epoch 2 microplate reader (Biotek Instruments, Winooski, VT, US). The mean blank value was subtracted from all values of samples. All samples were normalized to the mean control values raised to an arbitrary value of 100.

Nutrient deprivation model in PC12 cells.

Cells were seeded at an approximate cell density of 30,000 cells/cm^2 on 6-well plates, 96-well plates and/or on immunofluorescence slides (Biomerieux, Marcy l'Etoile, FR) and allowed to settle and grow in DMEM supplemented with 5% (v/v) FBS for 24 h.

After serum deprivation for 16 h, DMEM was replaced with Hank's balanced salt solution (HBSS; Lonza, Basel, CH) and treated or not with 200 nM rat obestatin for 6 h. DMEM supplemented with 5% (v/v) FBS was used as positive control.

Viability analysis of nutrient-deprived PC12 cells

The viability of nutrient-deprived PC12 cells treated or not with rat obestatin was evaluated in cells seeded on rat tail collagen a type-I coated 96-well plate following the nutrient deprivation protocol explained previously. Three different doses of rat obestatin were used (50, 100 and 200 nM). Viability was measured using the CCK8 kit as described above. The mean blank value was subtracted from all values of samples. All samples were normalized to the mean control values raised to an arbitrary value of 100.

Immunofluorescence detection of propidium iodide.

Nutrient deprived PC12 cells in the presence or absence of 200 nM rat obestatin were washed with PBS and fixed with methanol for 10 minutes at RT. Samples were equilibrated with 0.03 M sodium citrate pH 7.0 (5 min, RT), and cells were incubated with a 500 nM solution of propidium iodide (PI; Invitrogen, Thermo Fisher Scientific, Waltham, MA, US) for 5 min.

Samples were rinsed with PBS and after buffer excess was drained, an anti-fade reagent with 4′,6-diamidino-2-phenylindole (DAPI) counterstain (Invitrogen, Thermo Fisher Scientific, Waltham, MA, US) was used to mount and counterstain nuclei. Digital images were acquired with a Leica TCS SP8 confocal microscope (Leica, Wetzlar, DE). Images were evaluated and colocalization was quantified by using Fiji image processing software (National Institutes of Health, Bethesda, MD, US) and M2 Manders coefficient (Manders, Verbeek, and Aten 1993).

Metabolic signalling under nutrient deprivation of PC12 cells

PC12 cells were carefully washed with ice-cold PBS and lysed using RIPA; 50 mM Tris-HCl, 150 mM NaCl, 1 mM EDTA, 1% (v/v) NP40, 0.25% (w/v) Na-deoxycholate, protease inhibitor cocktail (1:100, Sigma-Aldrich, St. Louis, MO, US), phosphatase inhibitor cocktail (1:100, Sigma-Aldrich, St. Louis, MO, US), pH 7.2.

The QuantiPro™ BCA Assay Kit was used to determine lysates protein concentration. The same amount of protein for each sample was loaded on 10% sodium dodecyl sulphate–polyacrylamide gel electrophoresis (SDS-PAGE), and transferred onto 0.45 µm pore nitrocellulose membrane (GE Healthcare, Chicago, IL, US).

Blots were then washed using washing buffer (50 mM Tris-HCl, 150 mM NaCl, 0.05% Tween 20, pH 7.6), blocked with 5% (w/v) bovine serum albumin (BSA; Sigma-Aldrich, St. Louis, MO, US) in washing buffer (1 h, RT), and then incubated with the corresponding antibodies (Table 1) ON at 4ºC. Blots were incubated with the corresponding secondary antibodies (1h, RT; Table 1).

Unbound conjugate was washed off and protein bands were visualized using enhanced chemiluminescence substrate (ECL; Pierce, Thermo Fisher Scientific, Waltham, MA, US) and exposed to Mamoray® film (Agfa, Mortsell, BE) or Hyperfilm ™ MP (GE Healthcare, Chicago, IL, US).

The blots shown are representative of six experiments. After scanning, the relative signal intensity of each band of sub-saturation exposure images was quantified using Fiji software (Schindelin et al. 2012).

USC
UNIVERSIDADE
DE SANTIAGO
DE COMPOSTELA

IFRS1 Schwann cell line.

IFRS1 proliferation.

For the IFRS1 cell line, cell proliferation was analysed by measuring bromodeoxyuridine (BrdU) incorporation, using a BrdU cell proliferation enzyme-linked immunosorbent assay kit (Roche Diagnostics, Basel, CH) according to the manufacturer's protocol. In brief, the cells were cultured in a 96-well plate at a cell density of 15,000 cells/cm^2 in DMEM supplemented with 5% (v/v) FBS. The last 8 wells did not content cells and were used as a blank.

The cells were serum-deprived for 16 h and then stimulated with different doses of rat obestatin (25, 50, 100, 200 nM) for 24 h using 5% (v/v) FBS as a positive control. BrdU labelling solution (10 µL) was added to each well 3 h before stimulation time was completed. Cells were fixed with Fixdenat solution (200 µL, 30 min, RT) and incubated with anti-BrdU-peroxidase (POD) antibody solution (100 µL, 90 min, RT). The samples were washed and then 100 µL of substrate solution was added to each well. BrdU incorporation was quantified at 370 nm with an Epoch 2 microplate reader. Mean blank value was subtracted from all sample values. All samples were normalized to mean control values raised to an arbitrary value of 100.

IFRS1 wound healing and migration assay.

For the wound healing assay, IFRS1 cells (22,000 cells/cm^2) were seeded as described above in a 2-chamber silicon insert (Ibidi, Martinsried, DE) in triplicate, and allowed to grow to a full confluence. After serum-deprived for 16 h, the insert was removed with sterile tweezers, showing a cell-free gap between chambers, and then treated or not with 200 nM rat obestatin (32 h, 37 ºC).

Phase contrast images were taken before stimulation, and at 8, 24 and 32 h after stimulation with an AxioVert A1 inverted microscope (Zeiss, Oberkochen, DE). The wound area was measured by tracing along the gap

border using the Fiji analysis software and the wound closure was calculated as follows:

$$Wound\ closure\ (\%) = \left(\frac{Wound\ Area_0 - Wound\ Area_i}{Wound\ Area_0}\right) \times 100$$

To evaluate the migration of IFRS1 cells, an inverted transwell assay was performed as previously described (Muinelo-Romay et al. 2011; Alén et al. 2016) with some modifications. Rat obestatin (200 nM) was added as the chemoattractant and cells were allowed to migrate into growth factor-reduced Matrigel® (Gibco, NY, US) for 24 h. The cells were stained with 4 μM calcein-acetoxymethyl ester (Invitrogen, Thermo Fisher Scientific, Waltham, MA, US) and visualized with a Leica TCS SP2 confocal microscope (Leica Microsystems AG, Wetzlar, DE).

Optical 5 μm sections were taken, moving up from the underside of the membrane into the Matrigel®. The fluorescence of each section was quantified with Fiji Analysis software and a 3D reconstruction was done using the Volume Viewer software package. Fluorescence intensities of each section were normalized to the fluorescence intensity of the initial section. Four independent experiments have been carried out and pictures from three random fields were taken for each sample.

PC12-IFRS1 coculture.

PC12 cells were seeded on rat tail type I collagen-coated 12-well plates at an approximate density of 3 x 10^2 cells/cm^2 and maintained in DMEM supplemented with 5% FBS, 100 U/mL penicillin and 100 mg/mL streptomycin for 24-48 h. The attached PC12 cells were maintained for 7 d in PC12 differentiation medium (DM) consisting in DMEM supplemented with N2 supplement (Millipore, Merck, Darmstadt, DE), 50 µg/mL of ascorbic acid (Sigma-Aldrich, St. Louis, MO, US), 50 ng/mL of recombinant rat β nerve growth factor (R&D Systems, Inc., Minneapolis, MN, US).

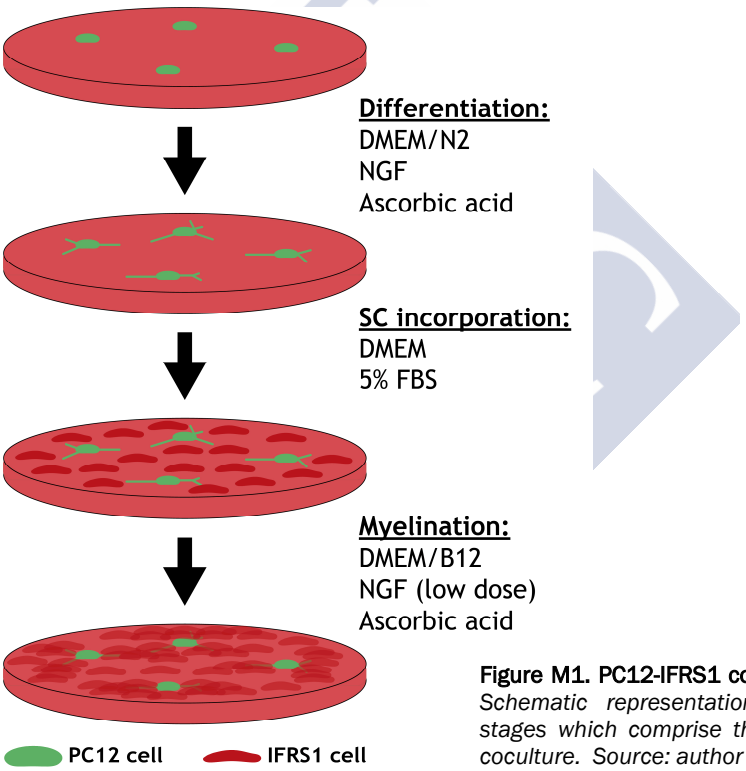

Figure M1. PC12-IFRS1 coculture model. *Schematic representation of different stages which comprise the PC12-IFRS1 coculture. Source: author original.*

Then, IFRS1 cells were added to NGF-primed PC12 cells suspended in DMEM 5% using a density of 1.5 x 10^4 cells/cm^2. Coculture was maintained in DMEM 5% for 48 h. PC12-IFRS1 coculture was fed three times a week in myelination medium [MM; consisting in DMEM supplemented with B27 supplement (Gibco, NY, US), 50 µg/mL of ascorbic acid, 10 ng/mL of recombinant rat β nerve growth factor, and 25 ng/mL of soluble neuregulin-1 type III] and were maintained for up 21 d as described previously (Sango et al. 2012).

Mouse/rat obestatin was added along with MM every 72 h to a final concentration of 200 nM. PC12/IFRS1 cocultures were maintained for 7, 14 and 21 d to examine the effect of obestatin on myelination.

Characterization of PC12-IFRS1 coculture.

PC12 and IFRS1 cells were seeded on separately on rat tail type collagen-coated slides until they were attached. Cells were fixed in 4% (w/v) paraformaldehyde in PBS (30 min, RT) and blocked with 5% (v/v) normal goat serum (Invitrogen, Thermo Fisher Scientific, Waltham, MA, US) in PBS (10 min, RT). After washing, cells were incubated with anti-NSE, anti-NF, anti-TH and anti-S100 (ON, 4ºC; Table 1) without agitation. After washed, cells were incubated with corresponding Alexa 488 secondary antibody (1h, RT; Table 1). Antifade reagent with DAPI counterstain was used to mount and counterstain nuclei.

A 21 d PC12-IFRS1 coculture was maintained as described previously, and immunofluorescence was performed as described above with anti-TH as PC12 cell marker, and anti-S100 or anti-MBP to stain IFRS1 cells. Digital images of random fields were acquired with a Zeiss AxioVert A1 inverted microscope.

Morphological analysis of PC12 cells during differentiation and post-differentiation.

PC12 cells were seeded on rat tail type I collagen-coated 12-well plates at an approximate density of 3 x 10^2 cells/cm^2 and maintained in

DMEM supplemented with 5% FBS, 100 U/ml penicillin and 100 mg/mL streptomycin for 24 h. The attached PC12 cells were maintained for 7 d in DM in the presence or absence of different doses of obestatin (50, 100 and 200 nM) to evaluate the effect of obestatin on PC12 differentiation. To check the effect on post differentiation 7 d DM-primed PC12 cells were maintained in DMEM 5% in the presence or absence of different doses of obestatin (50, 100 and 200 nM) for 48 h.

The plates were washed with distilled water and images of random fields were taken per well using an AxioVert A1 inverted microscope and cell differentiation and neurite characteristics were analysed with NIH ImageJ software.

Proliferation in PC12-IFRS1 coculture.

After 21 d, MM was removed from each well and washed with distilled water, preventing from hitting the cell monolayer directly. After water removal, the plate was inverted on filter paper. Then 400 µL of 0.5% crystal violet staining solution was added and incubated (20 min, RT) on a bench rocker with minimum frequency to avoid cell lifting from the plate. The plates were washed with distilled water and two images of random fields were taken per well using an AxioVert A1 inverted microscope.

The plates were inverted on filter paper and allowed to air dry (2 h, RT) Then 500 µL of methanol (Thermo Fisher Scientific, Waltham, MA, US) was added to each well and incubated on a bench rocker (20 min, RT). The content of each well was collected and optical density at 570 nm was measured using an Epoch2 microplate reader. All data were normalized to mean control values raised to an arbitrary value of 100. The mean and standard error of the mean were calculated for six independent experiments.

To discriminate between IFRS1 and NGF primed-PC12 proliferation separately, each cell line was cultivated in MM for 7 d and treated or not with 200 nM obestatin. Cells were seeded at the same cell density used

in the coculture general protocol. For the IFRS1, proliferation was estimated by crystal violet staining as described above, while NGF primed-PC12 cell number was counted directly in 10 random fields per assay.

Morphology and cell density analysis in PC12-IFRS1 coculture.

The PC12-IFRS1 coculture treated or not with 200 nM rat obestatin was cultured for 21 d and phase contrast images of random fields were collected using a Zeiss AxioVert A1 inverted microscope. Number, size and cellular density of formed cell clusters were analysed by using Fiji image processing package in inverted 8-bit images. The number of clusters was quantified in random fields from six independent experiments. In each image, the area of each cluster was measured independently ($n \geq 13$). To measure cluster's cell density, 800 x 100 px transects were made in each cluster and their profile was plotted ($n \geq 13$).

A baseline correction was applied, using GraphPad Prism software, defining the baseline as the average of the first 200 and last 200 values of the transect, and performing the calculation as the difference between original value and baseline.

Lipid quantification in PC12-IFRS1 coculture.

The oil red O stain (Sigma-Aldrich, St. Louis, MO, US) stock solution (3 mg/mL) was prepared in 100% isopropanol. Working solution was made by mixing 3 parts of stock solution with 2 parts of sterile distilled water and filtered through a 0.22-micron syringe filter prior to use.

After 21 d of PC12-IFRS1 coculture treated or not with rat obestatin (200 nM), samples were fixed with 4% paraformaldehyde in PBS (RT, 30 min). Paraformaldehyde was removed and the plates were washed with distilled water twice. After discarding water, 60% isopropanol (JT Baker, Avantor, PA, US) was added to cover the bottom of each well and allowed to settle for 5 min.

Isopropanol was discarded and 1 mL of working solution was pipetted along the side of each well so that the cells were completely covered. Samples were stained (RT, 10 min) and the wells were carefully washed with distilled water to remove unbound dye.

For quantification, 200 µL of isopropanol was added to each well and vigorously stirred in an orbital shaker for at least 10 min. For the eluates, absorbance was measured at 520 nm using an Epoch2 microplate reader.

Immunofluorescence analysis of myelination in PC12-IFRS1 coculture.

After 7, 14 and 21 d of coculture treated or not with rat obestatin (200 nM), cells were fixed in 4% (w/v) paraformaldehyde in PBS (30 min, RT). Samples were blocked with 5 % (v/v) normal goat serum (Invitrogen, Thermo Fisher Scientific, Waltham, MA, US) (10 min). After washing, cells were incubated with anti-MBP antibody and anti-TH antibody (ON, 4 ºC; Table 1) without agitation to prevent detaching of the cells. Samples were then washed and incubated with Alexa 488 and Alexa 594 secondary antibodies (1 h, RT; Table 1). Anti-fade reagent with DAPI counterstain was used to mount and counterstain nuclei.

Digital images were acquired with a Zeiss AxioVert A1 inverted microscope. The "Coloc 2" plugin of NIH ImageJ software was used to analyse co-localization. Manders M2 overlap coefficient was used to determine the co-localization of MBP over the PC12 cell marker.

To measure IFRS1 cell density around PC12 neurites, 400 x 10 px transects were made in each cluster and their profile was plotted for both TH (green) and MBP (red) ($n \geq 10$). A baseline correction was applied, using GraphPad Prism software, defining the baseline as the average of the first 50 and last 50 values of the transect, and performing the calculation as the difference between original value and baseline.

Immunoblot analysis of myelination in PC12-IFRS1 coculture.

After 7, 14 and 21 d of coculture treated or not with rat obestatin (200 nM), the cells were washed using ice-cold PBS and lysed in ice-cold RIPA buffer. After 15 min of incubation on ice, cells were detached, and the soluble cell lysates were pre-cleared by centrifugation (18,000 x g, 15 min, 4 ºC).

The QuantiproTM BCA assay kit was used to determine supernatants protein concentration. The same amount of protein for each sample was loaded on SDS-PAGE as described above. Protein bands were visualized using ECL substrate and exposed to Mamoray® film or Hyperfilm™ MP. The blots shown are representative of six experiments. After scanning, the relative signal intensity of each band of sub-saturation exposure images was quantified using Fiji software.

USC UNIVERSIDADE DE SANTIAGO DE COMPOSTELA

Animals

In vivo experiments were carried out in *Rattus norvergicus* rats, obtained from the Central Animal Facility of the University of Santiago de Compostela. Male Sprague-Dawley rats, weighing 250 g on arrival, were housed 4 per cage at a constant temperature of 22 ± 2º C and at a 12 h light/dark cycle. The rats were kept for 5 d for acclimation, with free access to water, and a standard rat chow with a composition of 5.5 % fat, 23 % protein and 70 % carbohydrate (SAFE-Panlab, ES).

All protocols and experiments were carried out in accordance with the recommendations of the guide for the care and use of laboratory animals of the Animal Committee at the University of Santiago de Compostela by personnel accredited by the Xunta de Galicia for the handling of experimentation animals (Certificates number B322 and C357; see attached documents). Experiments were performed in agreement with the rules of laboratory animal care and the international law on animal experimentation, and all efforts were made to minimize animal suffering (Bioethical experimental procedure committee code: 15010/17/005 granted to Dr Jesús Pérez Camiña; see attached documents). Assays were performed under appropriate conditions (REGA: ES150780275701).

Surgical procedures.

Surgical procedures were carried out aseptically and all surgical material was cleaned and sterilized 24 h before surgical intervention. The rats were anaesthetized with a ketamine/xylazine cocktail: 42.5 % ketamine (Ketolar 50 mg/mL, Parke-Davis, Morris Plañis, NJ, US) and 20 % xylazine (Rompun 2 mg/mL, Bayer, Leverkusen, DE) in saline buffer (Braun Medical, Hessen, DE). General anaesthesia was administered intraperitoneally at a dose of 200 µL per 100 g of body weight.

Elaboration of sciatic scaffolds with catheter port.

Scaffolds with a subcutaneous catheter have been developed by connecting a section of 200 mm of 0.64 mm Helixmark® silicone tube (Helix

Medical, Freudenberg Group, Weinheim, DE) in a pre-drilled section of 10 mm long 1.58 mm Helixmark® silicone tube (Helix Medical, Freudenberg Group, Weinheim, DE). Scaffolds were tested with saline discarding those that show leaks. After drying the scaffolds, they were sterilized by autoclaving at 121 ºC for 20 min in individually sealed bags and stored at RT until use.

Sciatic nerve crush and catheter port implant.

The sciatic nerve crush procedure was performed on the right hind limb whereas the left side served as control. The site of the incision area was shaved and cleaned with povidone iodine. A 2-3 cm incision was made on the skin, along the proximal half of the line between the trochanter major and the knee joint. The sciatic nerve was exposed through gluteal muscle splitting incision, through which the overlying lateralis and biceps femoris muscles were separated without cutting the muscle fibres using a pair of straight forceps.

The visible sciatic nerve was crushed 1 cm proximal to the division of the sciatic nerve into tibial and common peroneal nerves. The crush was made using a Dumont N7 negative action curved tweezers (Dumont, Montignez, CH), taking care to do it within the same section, located 0.5 cm from the end of the tweezer and exerting a constant pressure for 10 s (Figure M2A).

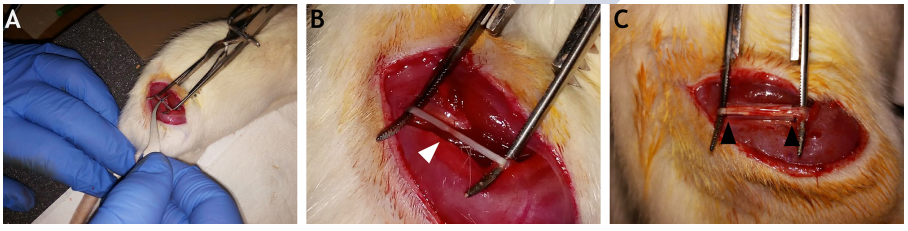

Figure M2. Rat sciatic crush model. *(A) Longitudinal incision on the posterolateral right hind limb, sciatic nerve exposure and sciatic crush 1 cm proximal to sciatic nerve division of tibial and common peroneal nerves. (B) Visible crush injury (white arrowhead) and inspection to check if epineurium is intact. (C) Scaffold made from 1.58 mm Helixmark® silicone tube (black arrowheads).*

After the crush was achieved, the sciatic nerve was checked to be certain that the epineurium was intact and the nerve was completely crushed, observing a clear area where the injury was made (Figure M2B). The damaged area was encapsulated with the catheter port and closed with cyanoacrylate glue (Figure M2C).

The inlet end of the catheter port was inserted subcutaneously to the neck of the rat, extracted through a small incision and secured with a 4-0 silk suture (Ethicon, Livingston, UK) with a drop of cyanoacrylate glue (Figure M3).

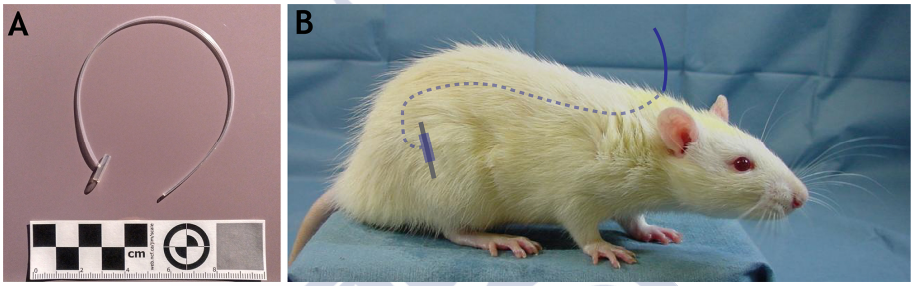

Figure M3. Construction and implantation of sciatic scaffold with catheter. *(A) Scaffold and catheter macrophotography. (B) Subcutaneous implantation scheme of scaffold and catheter (Adapted from NBRP-Rat resource).*

Before closing the wound, a solution of rat obestatin (500 nM/kg of animal) or saline was passed through the system with a syringe to check for correct position and to verify that there were no leaks.

Catheter inlet end was sealed with a drop of cyanoacrylate glue and the incision was closed with a 4-0 silk suture. Treatment and saline were administered every 48 h through the inlet end and sealed again with cyanoacrylate glue.

Motor nerve functional studies.

A motor nerve functional recovery assay was performed after surgery. A walking track (115 x 750 mm) with a darkened chamber at the end (270 x 260 mm) was developed for this assay. White filter paper strips were placed on the bottom of the track. The rat's hind limbs were inked with

stamp pad ink (Pelikan, Lleida, ES) and rats were allowed to walk through the track, leaving the footprint on the paper (Figure M4). The footprints were obtained on day 3, 6 and 12 after surgery and saline or obestatin treatment (500 nM/kg of animal). Contralateral leg footprint measurements served as a sham group.

The measurements were taken from 8 animals in each group. The strips containing the footprints were allowed to dry and digitalized with a high-resolution scanner (300 dpi). At least two consecutive tracks of each animal were measured using Fiji software (NIH, Bethesda, MD, US), considering the average. The parameters measured for both normal (N) and experimental (E) feet were: a) the longitudinal distance between the tip of the longest toe and the heel (PL); b) the cross-sectional distance between the first and the fifth toes (TS); and c) the cross-sectional distance between the second and the fourth toes (ITS).

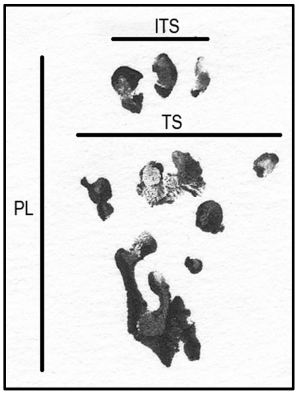

Figure M4. Representation of the footprint and the values used for determination of SFI: *distance between the tip of the longest toe and the heel (PL), cross-sectional distance between the first and the fifth toes (TS) and cross-sectional distance between the second and the fourth toes (ITS).*

The sciatic functional index (SFI) was calculated using the formula proposed previously (Bain, Mackinnon, and Hunter 1989) as follows:

$$SFI = -38.3 \times \frac{EPL - NPL}{NPL} + 109.5 \times \frac{ETS - NTS}{NTS} + 13.3 \times \frac{EITS - NITS}{NITS} - 8.8$$

Tissue extraction and sample processing.

Animals were sacrificed by cervical dislocation after sedation administration described above. The sterilized surgical material was used for the tissue extraction. Sciatic nerve and tibialis anterior (TA) were carefully removed from each animal minimizing contamination with surrounding tissue or rat hair. Contralateral sciatic nerve and tibialis anterior served as a sham group.

For histological analysis, sciatic nerves samples were fixed in 4% (w/v) paraformaldehyde in PBS at room temperature overnight. After fixation, samples were dehydrated and embedded in paraffin blocks. For this study, 3-micron sections were cut from each block and placed on pre-cleaned slides (Thermo Fisher Scientific, Waltham, MA, US).

The sectioned tissue slides were covered with a thin layer of paraffin, stoked at 60 ºC for 1 h and stored protected from light at RT to preserve the antigenicity of sections. Rat muscles samples for histology were immediately frozen with dry ice and stored at -80 ºC until use.

Histological analysis of sciatic nerve regeneration

Slides were maintained at least 60 min at 60 ºC, previously to being dewaxed and rehydrated. Antigen retrieval was performed by heating in a microwave oven at 750 W in 10 mM sodium citrate buffer pH 6.0 (Dako, Agilent, CA, US) for 20 min.

For immunofluorescence analysis of growth associated protein 43 (GAP-43), samples were blocked for 10 min with 5% (v/v) normal goat serum in PBS and incubated with the corresponding primary antibody (Table 1) in Dako antibody diluent (Dako, Agilent, CA, US; ON, 4ºC). After washing the slides were incubated with the corresponding secondary antibody (1h, RT; Table 1) and mounted by using anti-fade reagent with DAPI counterstain.

The immunohistochemical protocol was automatically performed using an AutostainerLink 48 instrument (Dako, Agilent, CA, US). Slides were

blocked with a peroxidase-blocking agent (Dako, Agilent, CA, US) for 5 minutes. Then, the samples were incubated with the corresponding antibodies (Table 1) in Dako antibody diluent for 30 min, and EnVisionTM FLEX/HRP (Dako, Agilent, CA, US) was used as the detection system.

DAB-tetrahydrochloride was used as chromogen, and nuclei were counterstain with HHS for 9 min. At least, triplicate slides were used for each experimental point.

Immunoblot analysis of sciatic nerve regeneration and myelination markers.

For immunoblot analysis, the sciatic nerves were immediately frozen in dry ice and stored at -80 ºC until use. Tissues were homogenized using a TissueLyser II tissue homogenizer (Qiagen, Hilden, DE), in 200 µL of RIPA lysis buffer at 30 Hz for 3 min. The lysates were clarified by centrifugation (18,000 x g, 15 min, 4 ºC), and the protein concentration was quantified using the RC-DC™ protein assay (Biorad, Hercules, CA, US).

An equal amount of protein of each sample was loaded on 10% SDS-PAGE, as described above. Protein bands were visualized using ECL substrate and exposed to Mamoray® film (or Hyperfilm™ MP). The blots shown are representative of six experiments. After scanning, the relative signal intensity of each band of sub-saturation exposure images was quantified using Fiji software.

Skeletal muscle atrophy analysis.

Just after the muscle was removed, it was weighed to assess the loss of muscle mass in the saline-treated and obestatin-treated rats. The data were presented as loss of mass compared to the sham group.

The isolated skeletal muscle was mounted using tragacanth gum (Santa Cruz Biotech Inc., Dallas, TX, US) and quickly frozen in liquid nitrogen-cooled isopentane (Panreac, Barcelona, ES).

Muscle sections of 5 µm were mounted on Histobond Adhesion Microslides (Marienfeld, Lauda-Königshofen, DE). The slides were stained with Dako® Haematoxylin-Eosin (HE) Stain System. Images of the stained sections were taken with an AxioVert A1 inverted microscope and 10 fields of each sample were randomly chosen for measurements.

The area of each myofiber in each field was measured. Those myofibers that do not have a clear cross-section have been excluded from the measurement.

Data analysis.

All the data were reported as the mean ± standard error of the mean (SEM). ROUT test with a Q=5% was performed to statistically detect the presence of outliers. Kolmogorov-Smirnov test with Dallal-Wikilnson-Lilief P value was performed to evaluate the normality of each data set. Unpaired Student t-test was used to compare means for two data sets with a normal distribution. Mann-Whitney test was used to compare medians for two data sets with non-normal distribution. A one-way ANOVA with a Fisher LSD multiple comparison post-hoc test was used to determine any significant differences between three or more datasets with normal residuals distribution. Values of $P<0.05$ were considered to be statistically significant and are marked with an asterisk (*). Asterisk (**, ***, ****) denotes $P<0.01$, $P<0.001$ and $P<0.0001$, respectively.

Formatting and bibliography.

The acronyms of the countries have been designated by the use of ISO 3166-1 alpha-2 code published by the International Organization for Standardization (ISO).

The Chicago Manual of Style (seventeenth edition) was used as a bibliographic format for the in-text citations (author-date format) and the complete reference list, respecting the title format of each journal.

Vectorial images and illustration used to design figures were obtained from the Library of Science and Medical Illustrations, under a creative commons (CC BY-NC-SA 4.0) license (Gumroad, San Francisco, CA, US).

The manuscript was analysed with Plagiarism Checker X® (Plagiarism Checker X, New York, NY, US) anti-plagiarism software (see attached documents).

USC UNIVERSIDADE DE SANTIAGO DE COMPOSTELA



RESULTS

USC
UNIVERSIDADE
DE SANTIAGO
DE COMPOSTELA

CHAPTER 1

Obestatin/GPR39 system expression in rat peripheral nervous system

USC
UNIVERSIDADE DE SANTIAGO DE COMPOSTELA

USC
UNIVERSIDADE
DE SANTIAGO
DE COMPOSTELA

The Obestatin/GPR39 system is expressed in the adult CNS, PNS and *in vitro* cellular models.

The obestatin/GPR39 system is present in many different tissues, including stomach (Alén et al. 2016), muscle (Gurriarán-Rodríguez et al. 2012), pancreas and spinal cord (Popovics and Stewart 2011) and it was proposed as an autocrine regenerative system in muscle (Gurriarán-Rodríguez et al. 2012, 2015).

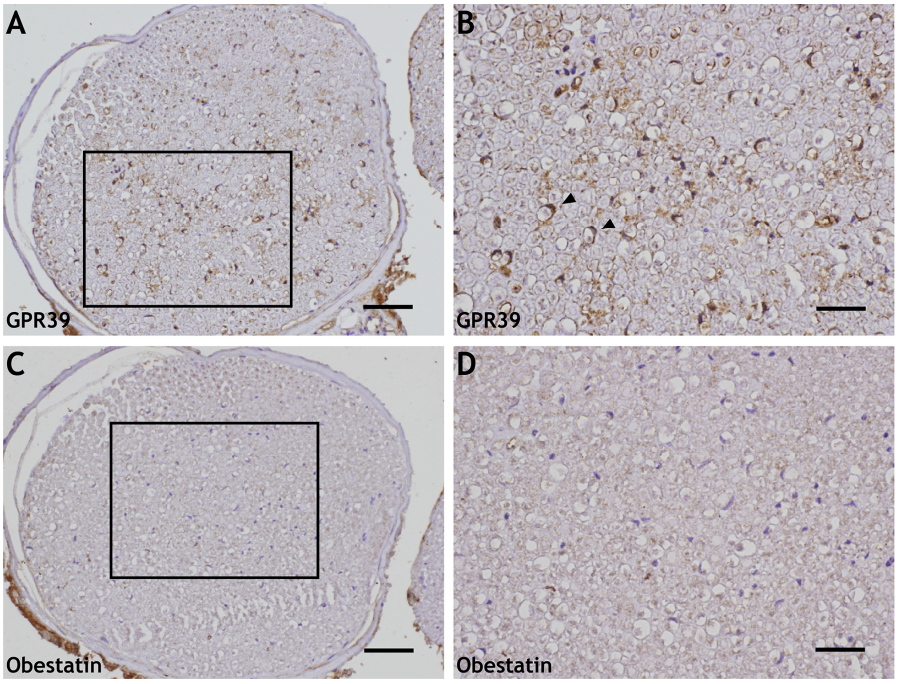

Figure R1. Expression of obestatin and GPR39 in rat sciatic nerve. *(A) Immunohistochemical detection of GPR39 in a cross-section of rat sciatic nerve. (B) At higher magnification, intense GPR39 staining was observed in the SCs (black arrowheads). (C) Immunohistochemical detection of obestatin in a cross section of a rat sciatic nerve. (D) Obestatin immunoreactivity was weakly observed in the sciatic nerve. The scale bars correspond to 100 µm for A and C or 50 µm for B and D.*

Based on this regenerative capacity discovered in muscle we explored its potential role in nerve regeneration. We analysed the expression of

obestatin and GPR39 in PNS, so we selected histological sections of intact and injured sciatic nerve, DRGs and medulla anterior horn from rat, as well as a cellular model of the nervous system.

In adult rat, sciatic nerve intense GPR39 staining was located in the SCs that wrap along the axons (Figure R1A-B, black arrowheads), however, obestatin was faintly expressed in the sciatic nerve with a diffuse location (Figure R1C-D). Obestatin expression was also observed in the SCs.

The expression of the obestatin/GPR39 system in sensory neurons was evaluated in adult rat DRGs (Figure R2A-C). In these neurons, an intense expression of GRP39 was observed mainly in the cytoplasm of these

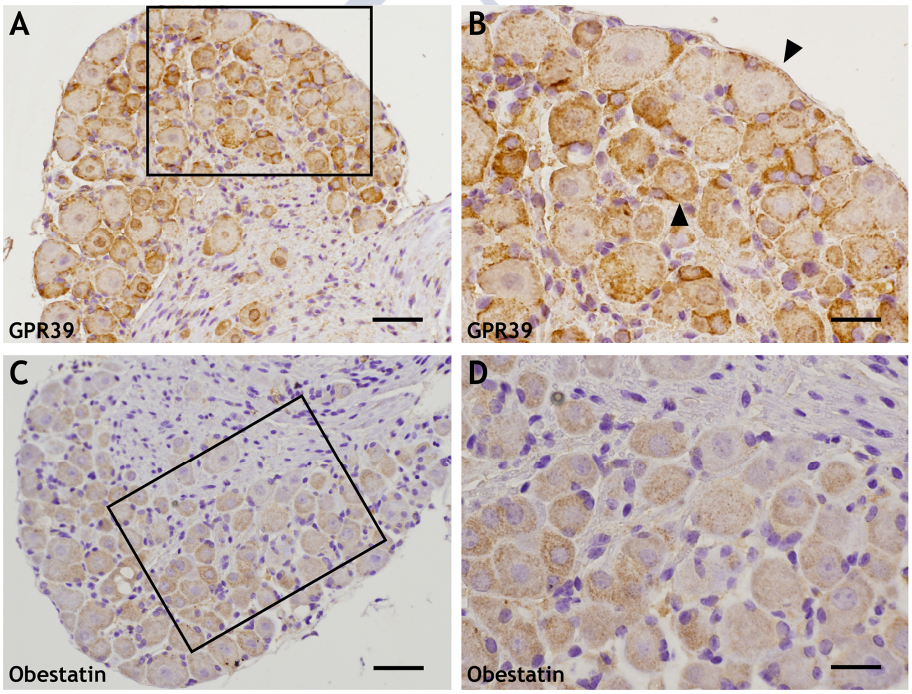

Figure R2. Expression of obestatin and GPR39 in rat DRGs. *(A) Immunohistochemical detection of GPR39 in a cross-section of DRGs. (B) At higher magnification, intense GPR39 staining was detected in the cytoplasm, but specially in the ectoplasm and the membrane of sensitive neurons (B, black arrowheads). (C) Immunohistochemical detection of obestatin in a cross section of a DRG. (D) Obestatin immunoreactivity was weakly observed in the cytoplasm of sensitive neurons. The scale bars correspond to 100 µm (A, C) or 50 µm (B, D).*

cells. Besides, GPR39 staining was even more intense in the ectoplasm and the plasma membrane (Figure R2A, black arrowheads). The sensitive neurons exhibited a uniform granulated cytoplasmic obestatin expression pattern (Figure R2D).

In adult rat anterior horn of spinal cord, GPR39 staining was observed in the motor neurons (Figure R3A-B, black arrowhead) and glia (Figure R3A-B); however, obestatin expression was only detected in the motor neurons (Figure R3C-D, black arrowheads).

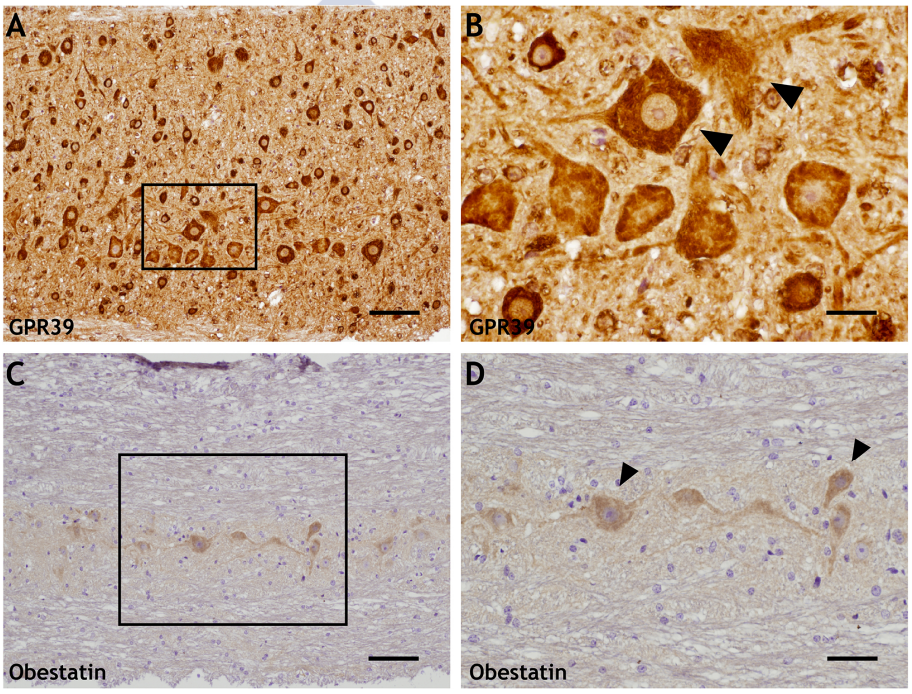

Figure R3. Expression of obestatin and GPR39 in rat anterior horn of spinal cord. *(A) Immunohistochemical detection of GPR39 in a cross-section of anterior horn of spinal cord. (B) At higher magnification, intense GPR39 staining was detected in both motor neurons (B, black arrowheads) and glia. (C) Immunohistochemical detection of obestatin in a cross-section of rat anterior horn of spinal cord. (D) Obestatin immunoreactivity was diffusely observed in cytoplasm of motor neurons. The scale bars correspond to 100 µm (A, C), 50 µm (D) or 25 µm (B).*

To study the expression of the obestatin/GPR39 system in a pathological situation in a peripheral nerve, we selected a regenerated, previously injured, rat sciatic nerve (Figure R4A). This model allowed us to analyse the expression of the system in both the proximal and distal site of the regenerating nerve.

The morphology of the proximal end resembled healthy tissue and showed an intense positivity for GPR39 (Figure R4B-C). This intense staining was also observed at the distal end (Figure R4F-G), although with a different expression pattern compared to the proximal site. GPR39 expression seemed to be associated with the Büngner bands (Figure R4G; black arrowheads). By contrast, obestatin was weakly expressed at the proximal end (Figure R4D-E), whereas higher staining was detected at the distal end (Figure R4H-I).

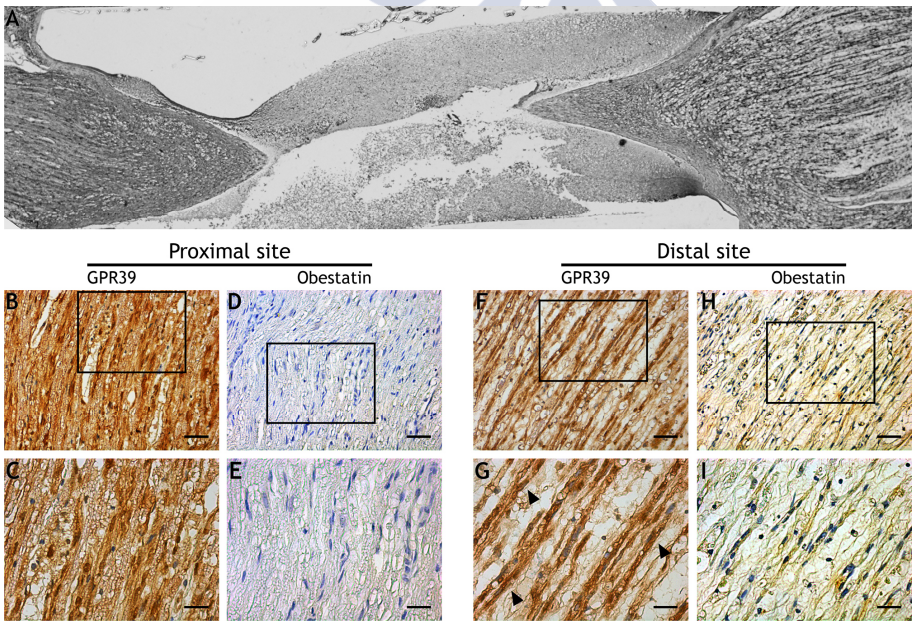

Figure R4. Expression of obestatin and GPR39 in sectioned rat sciatic nerve. *Immunohistochemical detection of GPR39 (B, C, F, G) and obestatin (D, E, H, I) at proximal site (B-E) and distal site (F-I). At the distal end GPR39 expression seemed to be associated to Büngner bands (G black arrowheads), and obestatin immunoreactivity was higher than in proximal site. The scale bars correspond to 50 μm (B, D, F, H) or 25 μm (C, E, G, I).*

To study the underlying mechanisms of the obestatin/GPR39 system in the PNS, we selected two *in vitro* models: a) a cell line derived from a rat pheochromocytoma of the rat adrenal medulla widely used in neurological studies, the PC12 cell line, which after nerve growth factor treatment present a neuronal phenotype (Greene and Tischler 1976); and b) a spontaneously immortalized Schwann cell line, the IFRS1 cell line (Sango et al. 2011).

The use of PC12 makes it possible to evaluate *in vitro*, in a very controlled way, essential processes in the regeneration of the nervous system such as cell death, neuroprotection, neurosecretion or differentiation, while IFRS1 cells allow to study in the same way key processes of SCs that exert an influence on regeneration after damage such as proliferation, migration or myelinization. However, these models can only be useful in the study of the effect of obestatin if they present an expression of the obestatin/GPR39 system or at least the receptor.

In this sense, the expression of the obestatin/GPR39 system was analysed by immunocytochemistry in PC12 and IFRS1 cell lines. Intense GPR39 staining was observed in both IFRS1 and PC12 cell lines. This expression was located in the perinuclear region (Figure R5A, white arrowhead), the plasma membrane (Figure R5A, black arrowheads) and/or the ectoplasm (Figure R5B, black arrowheads). Nevertheless, obestatin expression was detected diffusely and uniformly in the cytoplasm of both PC12 and IFRS1 cell lines (Figure R5C and R5D).

Having into account the expression of the obestatin/GPR39 system found in PC12 cells and IFRS1 cells, we prompted to study the significance of this expression in these two stable cell lines, and the usefulness of these models was validated for the study of the effect of obestatin on the peripheral nervous system.

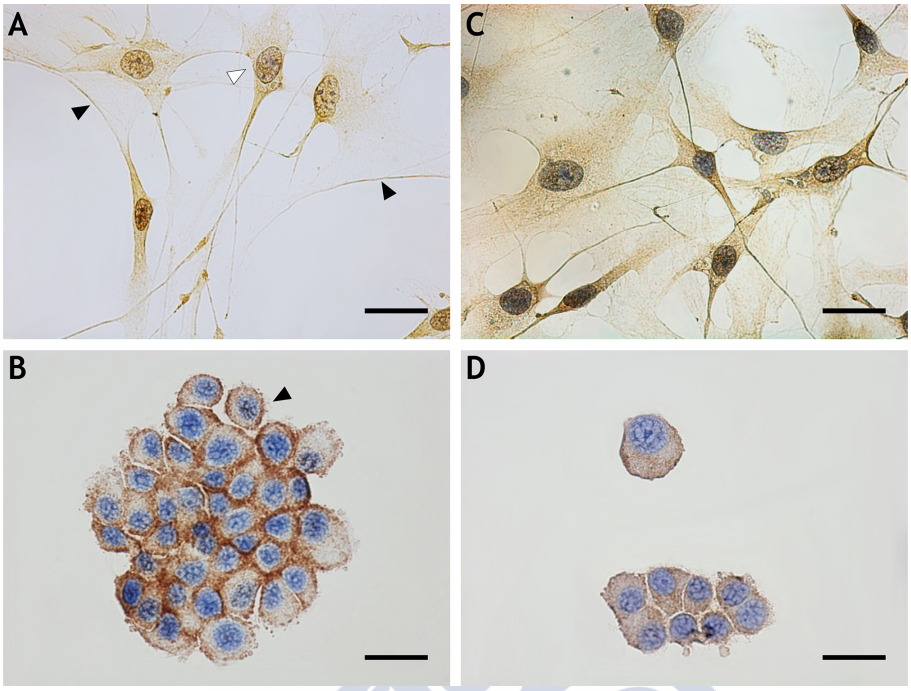

Figure R5. Expression of obestatin and GPR39 in IFRS1 and PC12 cell lines. *GPR39 immunoreactivity was intense in both IFRS1 (A) and PC12 (B) cell lines, located at perinuclear region (A, white arrowhead) plasma membrane (A, black arrowhead) and ectoplasm (B, black arrowhead). Obestatin presented a diffuse and cytoplasmic expression in IFRS1 (C) and PC12 (D) cell lines. The scale bars correspond to 20 µm.*

CHAPTER 2

Neuroprotective effect of obestatin

USC
UNIVERSIDADE
DE SANTIAGO
DE COMPOSTELA

After a PNS injury, a high percentage of sensitive and motor neurons are at risk of suffering damage leading to cell death. Surgical repair of nerve tissue can have a certain neuroprotective effect, but its use is only partially effective and has to be applied early (Hart, Terenghi, and Wiberg 2008). Neuroprotective therapeutic strategies have focused on tissue engineering and pharmacotherapy with adjuvants, however, little has been studied in the PNS. The active mechanism of neuronal death induced by damage to the peripheral nerve allows several potential therapeutic sites. The initial removal of trophic factors in neurons is one of the main causes of cell death and can be partially counteracted with the exogenous addition of trophic factors, but other types of molecules can also be used to control the cell cycle or activate signalling pathways that favour regeneration (Hart, Terenghi, and Wiberg 2008).

Considering the functions already described for obestatin (Gurriarán-Rodríguez et al. 2012, 2015; Santos-Zas et al. 2017), it seems a promising candidate to exert a neuroprotective effect on motor and sensory neurons. Consequently, we analyse in PC12 cell line whether obestatin enhances processes that favour neuroprotection, and we examine the effect of obestatin on nutrient deprivation-induced cell death and the signalling pathways through which obestatin may act.

Obestatin increases PC12 cells proliferation.

Obestatin has been described to stimulate the proliferation of many cell lines (Camiña et al. 2007; Gurriarán-Rodríguez et al. 2012; Alén et al. 2016). As a first approach in the study, we analysed the effect of obestatin exogenous administration on the proliferation of the PC12 cells. To this end, a water-soluble tetrazolium salt assay (CCK8) was used to evaluate the obestatin effect in PC12 proliferation.

Obestatin treatment (50, 100 and 200 nM) caused an increase in the proliferation of PC12 cells (116.9±1.9%, 123.4±10.9% and 136.9±9.7; respectively) at 48 h in a dose-dependent manner (Figure R6). FBS (5%) was used as a positive control of the proliferation.

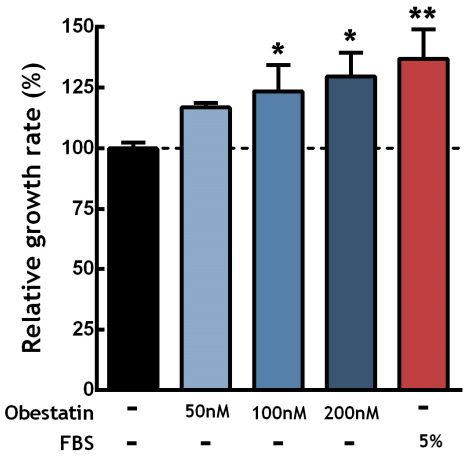

Figure R6. Effect of exogenous obestatin administration on PC12 cells proliferation. *CCK8 assay was used to determine PC12 cells proliferation. Obestatin significantly enhances proliferation at 48 h. The data were expressed as a percentage of the basal proliferation of untreated cells (Mean ± SEM, n=8). The asterisk (*, **) denotes P<0.05 and P<0.01 when comparing treated with the untreated control group, respectively (ANOVA with Fisher LSD post-hoc test).*

Obestatin mitigates the loss of viability in PC12 nutrient deprivation model.

The PC12 cells are commonly used as a model to analyse neuronal stress-responses, neurotoxicity and neurosecretions (Westerink and Ewing 2008; Heusinkveld and Westerink 2017). In this sense, a nutrient deprivation model was selected to study obestatin neuroprotective effect in undifferentiated PC12 cells, a method previously used to analyse apoptosis

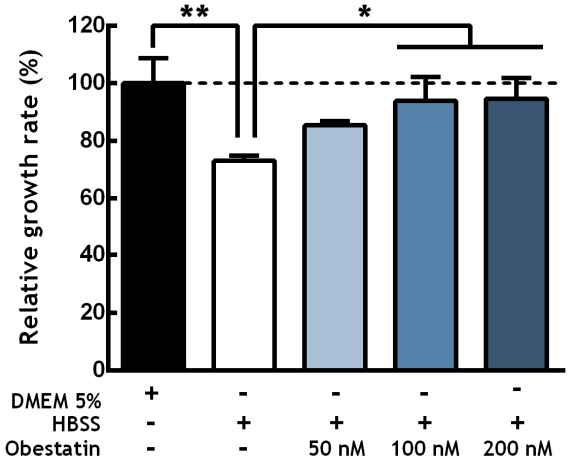

Figure R7. Effect of obestatin on PC12 viability: *CCK8 assay was used to determine PC12 cells viability under nutrient deprivation model. Obestatin significantly mitigated loss of cell viability at 6 h. The data were expressed as a percentage of the control (Mean ± SEM; n=6). The asterisk (*, **) denotes P<0,05 and P<0,01 when comparing treated with control group (ANOVA with Fisher LSD post-hoc test).*

and neuroprotection *in vitro* (Pang et al. 2014). Thus, a CCK8 cell viability assay was performed to study the obestatin effect. DMEM supplemented with 5% FBS was used as the control group.

Nutrient deprivation caused a significant decrease in PC12 cell viability (73.04±4.36 %) after 6 h (Figure R7). Obestatin treatment (100, and 200 nM) recovered cell viability in a dose-dependent manner reaching control levels at the 100 and 200 nM doses (Figure R7).

Obestatin attenuates the apoptosis induced by nutrient deprivation in PC12 cells.

Nutrient deprivation in PC12 cells for 6 h caused an increase in PI uptake calculated as the co-localization of PI and DAPI staining in confocal images by using the M2 Manders colocalization coefficient. Obestatin treatment (200 nM) significantly attenuated the PI uptake induced by the nutrient deprivation (Figure R8A-B).

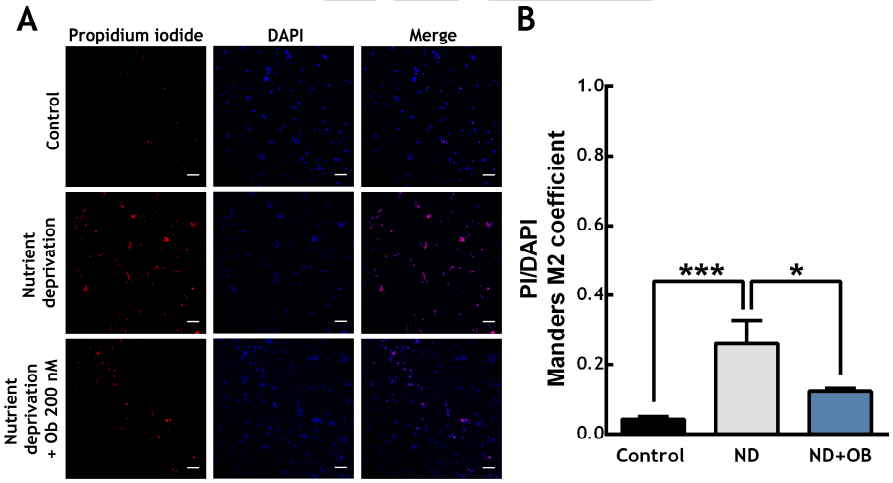

Figure R8. Effect of obestatin on PC12 cell apoptosis. *(A) Confocal images showing colocalization for propidium iodide (red) and DAPI (blue) at the nucleus. The scale bars correspond to 100 µm. (B) Calculation of Manders M2 colocalization coefficient in PC12 cells under nutrient deprivation in treated or not with 200 nM rat obestatin. The data were expressed as mean ± SEM of six independent experiments. The asterisk (*, ***) denotes P<0.05 and P<0.001 compared with nutrient deprivated group (ANOVA with Fisher LSD post-hoc test).*

To confirm this point, an immunoblot analysis of the antiapoptotic BCL2 protein and the proapoptotic Caspase 3 protein levels was carried out (Figure R9). According to the results showed above, BCL2 levels diminished with nutrient deprivation, and this effect was counteracted by obestatin treatment (Figure R9C). On the other hand, the levels of active caspase 3 were increased with nutrient deprivation, an effect that was reverted with obestatin treatment (Figure R9A).

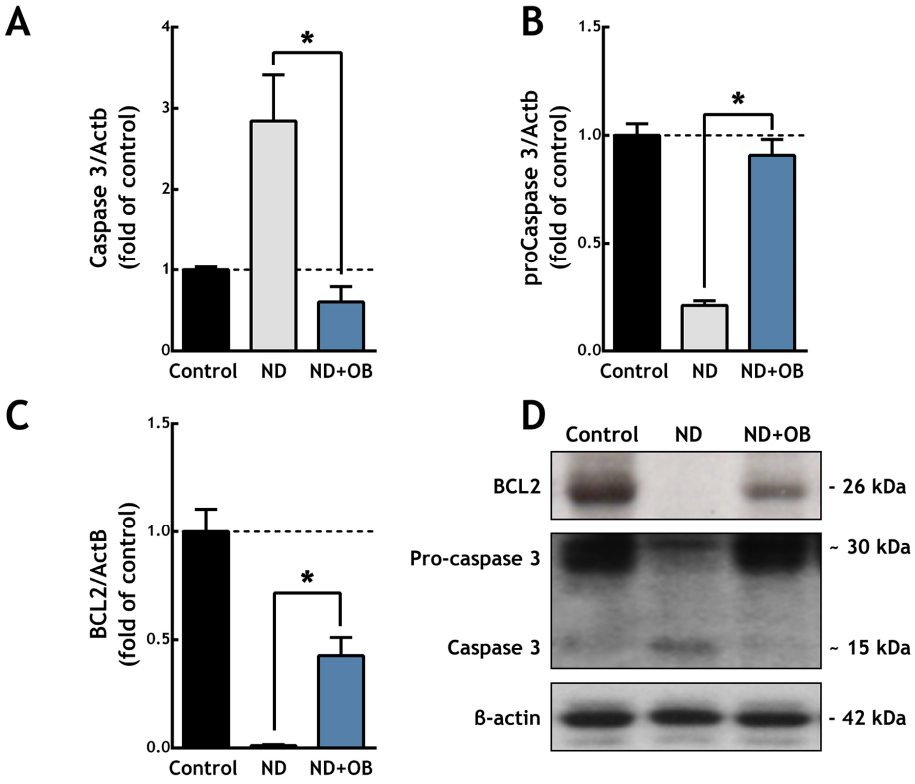

Figure R9. Analysis of proapoptotic and antiapoptotic protein levels in the PC12 nutrient deprivation model. *Immunoblot analysis of (A) active caspase 3, (B)pro-caspase 3 and (C) anti-apoptotic BCL2 protein levels in response to nutrient deprivation (ND) and with 200 nM obestatin treatment (ND+OB). The data were expressed as fold change over the control (Mean ± SEM) of four independent experiments. The asterisk (*) denotes P<0.05, when comparing treated with ND group (Mann-Whitney test). (D) Representative WB images of PC12 under nutrient deprivation for 6 h.*

In concordance with the caspase 3 response, there was an entirely opposite effect on pro-caspase 3 (Figure 9B). Taken together, these results suggested that obestatin caused neuroprotection against the stress induced by 6 h nutrient deprivation in the undifferentiated PC12 cells.

Obestatin activates Akt, ERK1/2 and GSK3α/β phosphorylation in nutrient-deprived undifferentiated PC12 cells.

The PI3K/Akt and ERK1/2 signalling pathways are linked to survival/neuroprotective effects in neuronal cells (Chung et al. 2008; Ahn 2014). These proteins are also the main targets in the signalling pathway previously described for the obestatin/GPR39 system (Camiña et al. 2007; Alvarez et al. 2009; Alén et al. 2012; Gurriarán-Rodríguez et al. 2012).

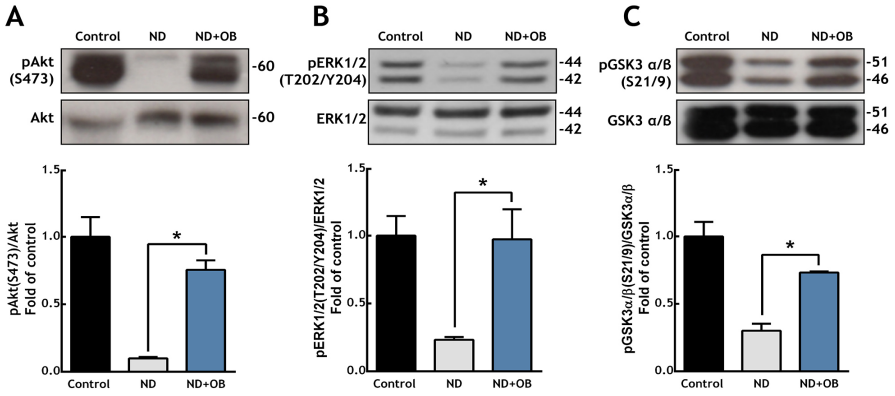

Figure R10. Effect of obestatin on PC12 cell survival signalling under nutrient deprivation conditions. *PC12 cells subjected to nutrient deprivation (ND) showed a decrease in (A) Akt, (B) ERK1/2 and (C) GSK3α/β phosphorylation, and this effect is partially counteracted by the treatment with obestatin. Protein phosphorylation was expressed relative to the targeted total protein level from the same sample. The protein expression was expressed as fold change over the control as mean ± SEM of four independent experiments. The asterisk (*) denotes P<0.05 when comparing with ND group (Mann-Whitney test).*

Besides, the Akt/GSK-3β signalling pathway has been well studied as a survival-promoting signalling mechanism in neurons (Yuan and Yankner 2000). With these pieces of information, we investigated the involvement

of these kinases in the neuroprotective effects of obestatin in nutrient-deprived undifferentiated PC12 cells. To this end, the PC12 cells were subjected to nutrient deprivation (ND) for 6 h and treated (ND+OB) or not (ND) with 200 nM obestatin. Nutrient deprivation caused a decrease in the phosphorylation levels of Akt, ERK1/2 and GSK3α/β in these cells. Obestatin treatment partially restored Akt and ERK1/2 phosphorylation levels (~75% increase related to ND, Figure R10A; and ~74% increase related to ND, Figure R10B; respectively).

Concomitant with this augment in Akt and ERK1/2 phosphorylation, obestatin treatment resulted in a ~43% increase in GSK3α/β phosphorylation related to ND (Figure R10C).

USC UNIVERSIDADE DE SANTIAGO DE COMPOSTELA

CHAPTER 3

Obestatin effect on Schwann cells

USC
UNIVERSIDADE
DE SANTIAGO
DE COMPOSTELA

In response to a PNS injury, the SCs dedifferentiate and acquire a repairing phenotype (Kim, Mindos, and Parkinson 2013), aiding in the clearance of myelin and cellular debris, and then form regeneration tracks, aligned in cellular columns called Büngner bands. Once axonal regeneration progresses, the SCs are re-associated with the axons to differentiate back into myelinating cells (Jessen and Mirsky 2016). After nerve injury, the repairing SCs begin to migrate to the damaged area and, during this migration, they proliferate supporting axonal regeneration. These two processes are key targets in the search of new therapies. The obestatin/GPR39 system has been described to be involved in the migration and proliferation of several systems (Gurriarán-Rodríguez et al. 2012, 2015; Santos-Zas et al. 2017). To study the effect of this system in Schwann cells we used IFRS1 cell line as an *in vitro* model.

Obestatin increases proliferation in IFRS1 cell line.

The involvement of the endogenous obestatin/GPR39 system in the proliferation of the cell lines that bear this system prompted us to study the effect of obestatin treatment in this cell line. Then, a 5-bromo-2'-deoxyuridine (BrdU) incorporation-based ELISA assay was used to evaluate the proliferative effect of obestatin on IFRS1 cells.

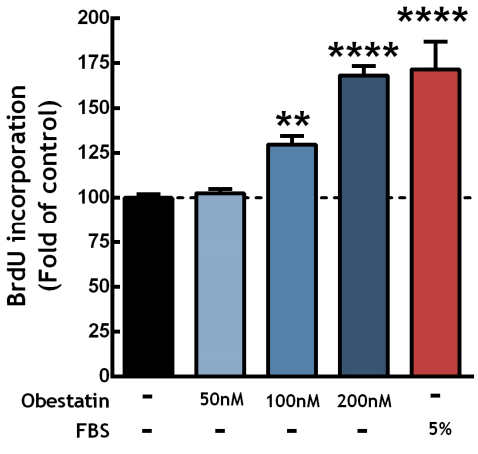

Figure R11. Effect of obestatin on IFRS1 cells proliferation. *BrdU incorporation assay was used to determine IFRS1 cells proliferation treated or not with obestatin (50,100,200 nM). 5% FBS was used as positive control. The data were expressed as a percentage of the basal proliferation of untreated cells (Mean ± SEM; n=8)). The asterisk (**, ****) denotes P<0.01 and P<0.0001 when comparing treated with the untreated control group. (ANOVA with Fisher LSD post-hoc test).*

Obestatin treatment caused an increase in proliferation at 24 h in a dose-dependent manner with its maximum at 200 nM (168.1 ± 5.2 %; Figure R11). Obestatin effect was comparable to that of the positive control (5% FBS; 171.5 ±15.5 %; Figure R11).

Obestatin acts as a chemoattractant in promoting motility of IFRS1 cell line.

The migration of SCs is critical for the development of the PNS and is essential for regeneration and remyelination after nerve injury (Wang, Teng, and Huang 2012). Obestatin has also been described as a peptide that promotes migration in different cell lines. To examine the migratory capabilities of the IFRS1 cells driven by obestatin, a wound-healing assay was performed. This assay showed that the obestatin-treated cells exhibited a significant increase in their migration capability when compared with the control (Figure R12).

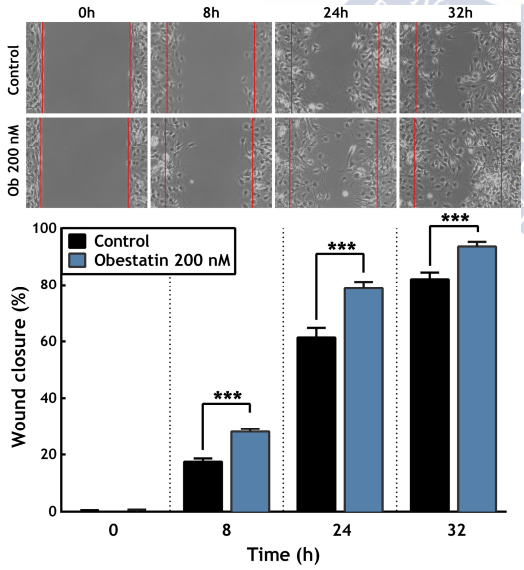

Figure R12. Evaluation of migration in IFRS1 cell line. *The IFRS1 cells were treated or not with 200 nM obestatin. Images were taken at 0, 8, 24 and 32 h after insert removal with a 10x objective magnification. Data were expressed as the mean ± SEM (n=10). The asterisk (***) denotes P<0.001 when comparing the treated with the untreated control group (unpaired Student t-test).*

Additionally, we analysed whether obestatin was driving cell invasion using a 3-dimensional (3D) culture assay. For this purpose, the inverted version of the classical Boyden chamber invasion assay was used (Alén et al. 2016). As shown in Figure R13A, the IFRS1 cells were able to migrate through the membrane, mimicking basement membrane invasion and invade into the Matrigel® as an extracellular matrix when obestatin was applied on top of the Matrigel® as a chemoattractant (200 nM).

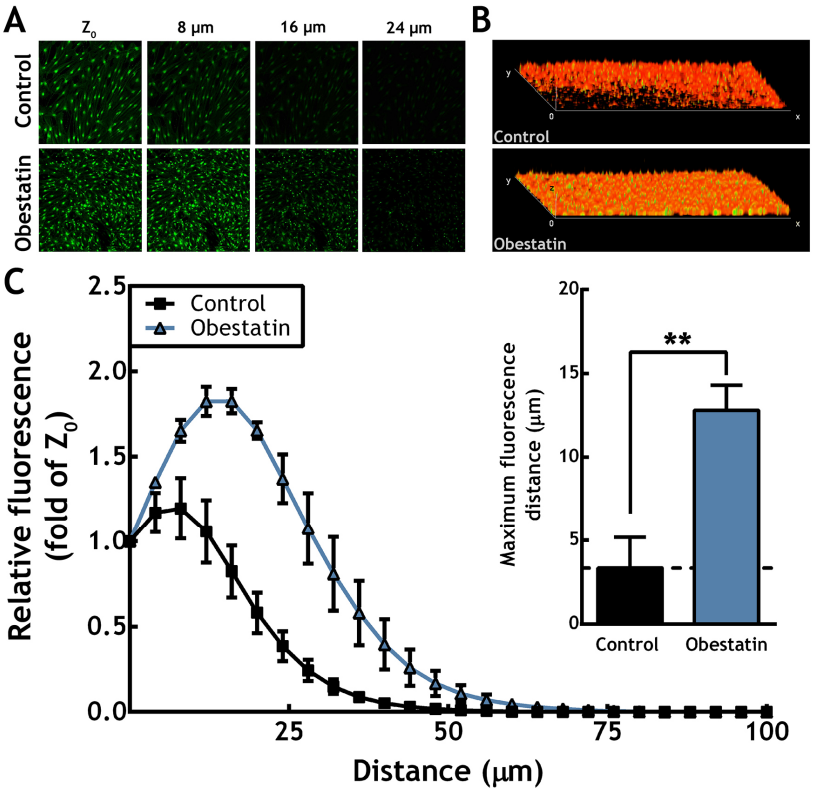

Figure R13. Evaluation of obestatin ability as chemoattractant and inducer of migration in IFRS1 cell line. *(A) Sequential confocal microscopy sections every 4 µm from membrane to the top of Matrigel® in an inverted migration assay. Obestatin (200nM was used as chemoattractant. (B) 3D reconstruction of microscopy sections by using fluorescence image stack of each dataset. (C) Fluorescence intensity quantification of each section from the membrane. The data was presented as fold to initial section (Z0) for each dataset, and was shown as mean ± SEM (n=6). The asterisk (**) denotes p<0.01 when compared to untreated control group (Mann-Whitney test).*

Data was presented with respect to the fluorescence intensity of the initial section (Z_0) of each data set, and the section with maximum fluorescence intensity was identified for each dataset (Figure R13C). We also performed a 3D reconstruction, by using fluorescence images of all sections of a representative dataset for both untreated and treated cells (Figure R13C). The extent of cell migration was quantified by measuring the fluorescence intensity at each confocal section every 4 μm from the bottom membrane, and the differences between the untreated and treated cells were statistically significant ($P < 0.001$; Figure R13B-C) and the peak of maximum fluorescence advanced 10 μm further in the obestatin-treated cells with respect to the control group.

USC UNIVERSIDADE DE SANTIAGO DE COMPOSTELA

CHAPTER 4

Obestatin effects on an *in vitro* myelination model

USC
UNIVERSIDADE DE SANTIAGO DE COMPOSTELA

USC
UNIVERSIDADE
DE SANTIAGO
DE COMPOSTELA

Cocultures of neuronal and glial cells were widely used as a model for the study of the myelination process *in vitro.* In 2012, Sango's group developed an *in vitro* myelination model consisting of a PC12-IFRS1 cell lines coculture (Sango et al. 2012). This coculture system is a valuable tool to study peripheral nerve myelination, degeneration and regeneration, as it allows a first approximation to the study of many of the processes that happen during the PNS regeneration in a very controlled way and reducing animal sacrifices.

Characterization of PC12-IFRS1 coculture.

In order to perform a correct characterization of the coculture system, it is necessary to clearly identify each cell type present in it, for which a battery of antibodies was selected and analysed by IF. NF (neurofilaments), NSE (Neuron specific enolase) and TH (tyrosine hydroxylase) were selected for the identification of PC12 cells while S100 was chosen for the identification of IFRS1 (Figure R14).

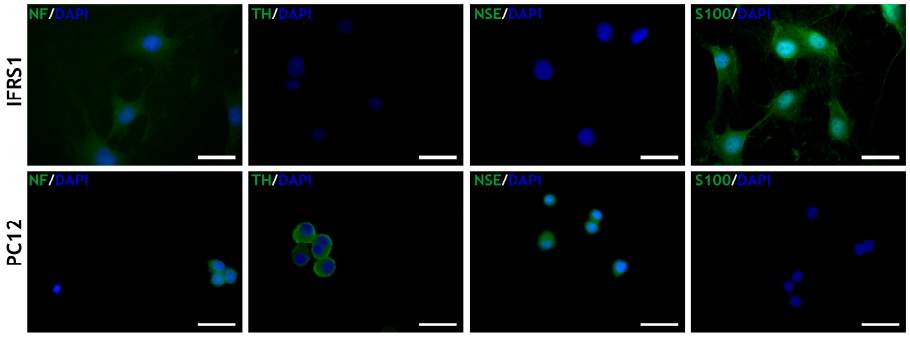

Figure R14. Immunofluorescence analysis for the identification of markers in the PC12-IFRS1 coculture. Representative images of IF staining of NF, NSE, TH and S100 for both PC12 and IFRS1 cells. The scale bars represent 20 µm.

A weak NF staining was detected in PC12 cells; however, this signal is also observed in IFRS1 so it can be discarded as a PC12 marker. Both NSE and TH were clearly detected in PC12 cells, with strong specificity, that were absent in IFRS1 cells, with the strongest, most defined and specific TH signal. S100 is a commonly used marker for SCs, and in IFRS1

cells a clear and specific signal was detected. Based on this data we selected TH as a PC12 marker, while S100 was chosen for IFRS1 cells.

These markers were also evaluated in the coculture system to discard cross-reactions. In the coculture system, staining with TH (Figure R15, green) is observed in the cell body and neurites of PC12 cells, while IFRS1 cells are specifically marked with S100 (Figure R15, red).

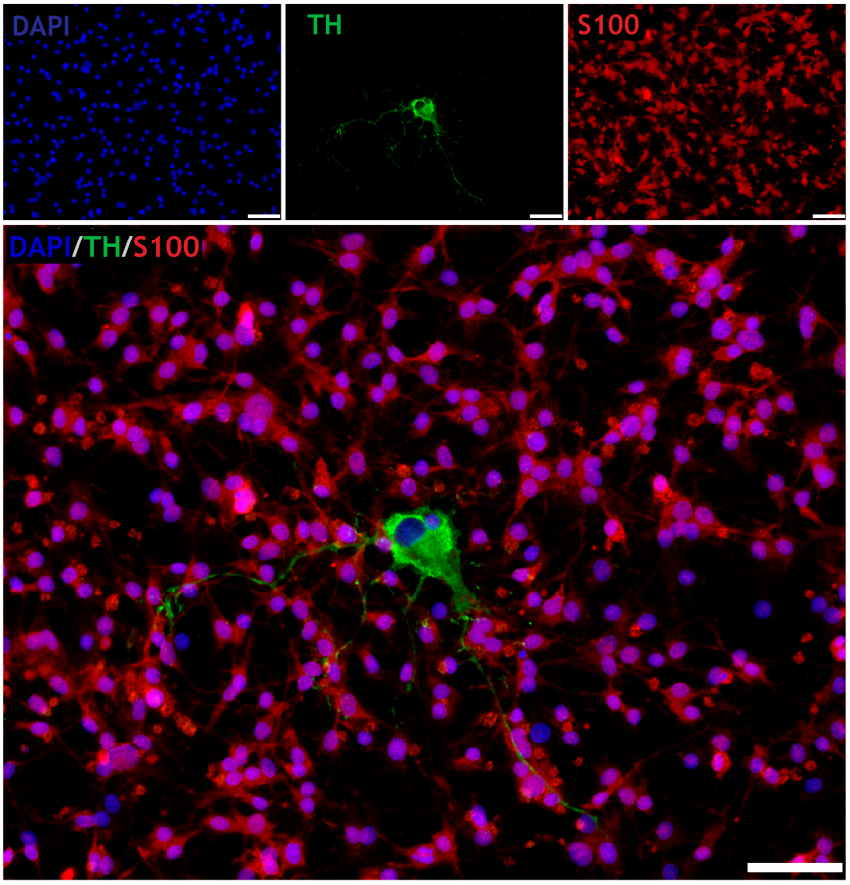

Figure R15. Immunofluorescence analysis for cell identification in PC12-IFRS1 coculture. Representative images of IF staining with TH (green) and S100 (red) for PC12 and IFRS1 cells respectively and DAPI (blue) for the nucleus. The scale bars represent 50 µm.

Once both cell types were characterized and identified, the PC12-IFRS1 coculture system was evaluated as a myelinization model, for which the expression of MBP was analysed by IF, one of the main components of myelin in both the CNS and PNS.

MBP staining was weakly observed in the coculture, except in some areas where there is a differential increase, many of them in IFRS1 cells in contact with the cell body of PC12 cells or their neurites (Figure R16),

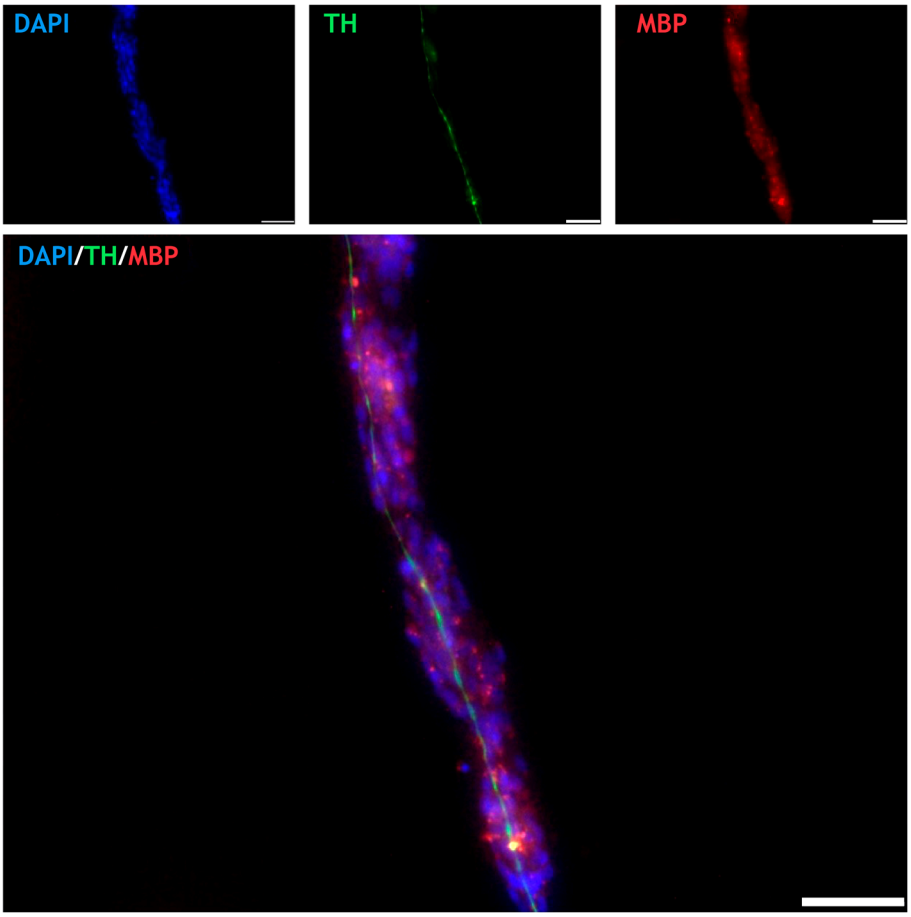

Figure R16. Immunofluorescence analysis of MBP in PC12-IFRS1 coculture. Representative images of IF staining with TH (green) and MBP (red) for PC12-IFRS1 cells respectively and DAPI (blue) for the nucleus. The scale bars represent 50 µm.

although in some cases high levels of MBP were found associated with cells close to PC12 cells but not in direct contact with them (Figure R17), suggesting that the interaction with PC12 cells stimulates the expression of MBP in IFRS1 cells.

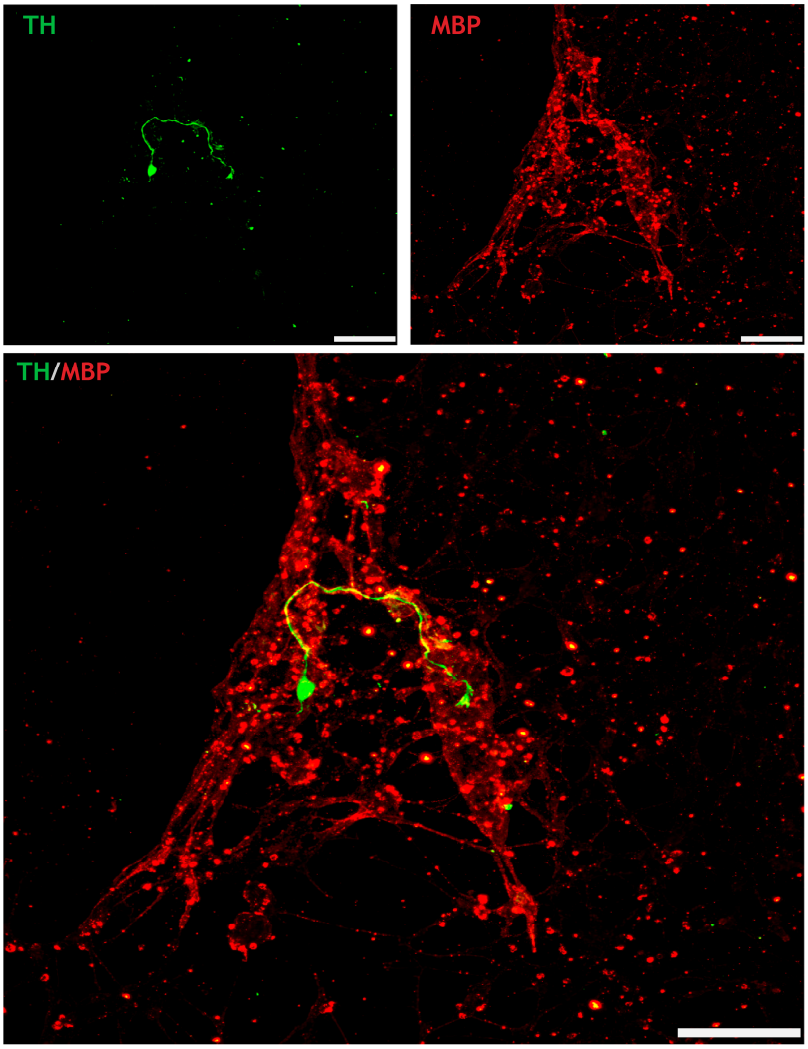

Figure R17. Immunofluorescence analysis of MBP in PC12-IFRS1 coculture. Representative images of IF staining with TH (green) and MBP (red) for PC12-IFRS1 cells respectively and DAPI (blue) for the nucleus. The scale bars represent 50 µm.

Effect of obestatin on differentiating and differentiated PC12 cells.

As a first approach, we evaluated the effect of obestatin on PC12 cells during differentiation and after differentiation, by quantifying the presence or absence of neurites and their length. All cytoplasmic extensions that exceed the maximum diameter of the cell body were considered neurites, and a cell was considered differentiated when it had at least one neurite. The neurite with the greatest length present in each cell was defined as the main neurite.

During differentiation, the addition of obestatin caused a clear decrease in the differentiation of PC12 cells in a dose-dependent manner, decreasing approximately 34% for 50nM and 100 nM obestatin and 60 % for 200nM of obestatin (Figure R18A). According to the decrease in differentiation, the number of neurites per cell decreased by approximately 2 neurites per cell (Figure R18B), and the mean length of the principal neurite was also slightly decreased (Figure R18D); however, it did not seem to affect the mean length of neurites (Figure R18C). An analysis of the length distribution of neurites showed that although obestatin caused a tendency to decrease the length of neurite (Figure R18E), it nevertheless maintained the same pattern as in the control group. Finally, we analysed polarity by using the polarity index (Figure R18F), defined as the percentage of the length of the main neurite versus the total length of neurites in the cell. During differentiation, obestatin increased the polarity index in PC12 cells by approximately 20%.

In differentiated PC12 cells, obestatin reduced the percentage of differentiation at high doses (Figure R19A), decreasing by 45% for obestatin 100nM and by approximately 60% for obestatin 200nM. In this sense, obestatin decreased the number of neurites per cell by approximately 1 at high doses (Figure R19B), but the differences are not significant at low doses.

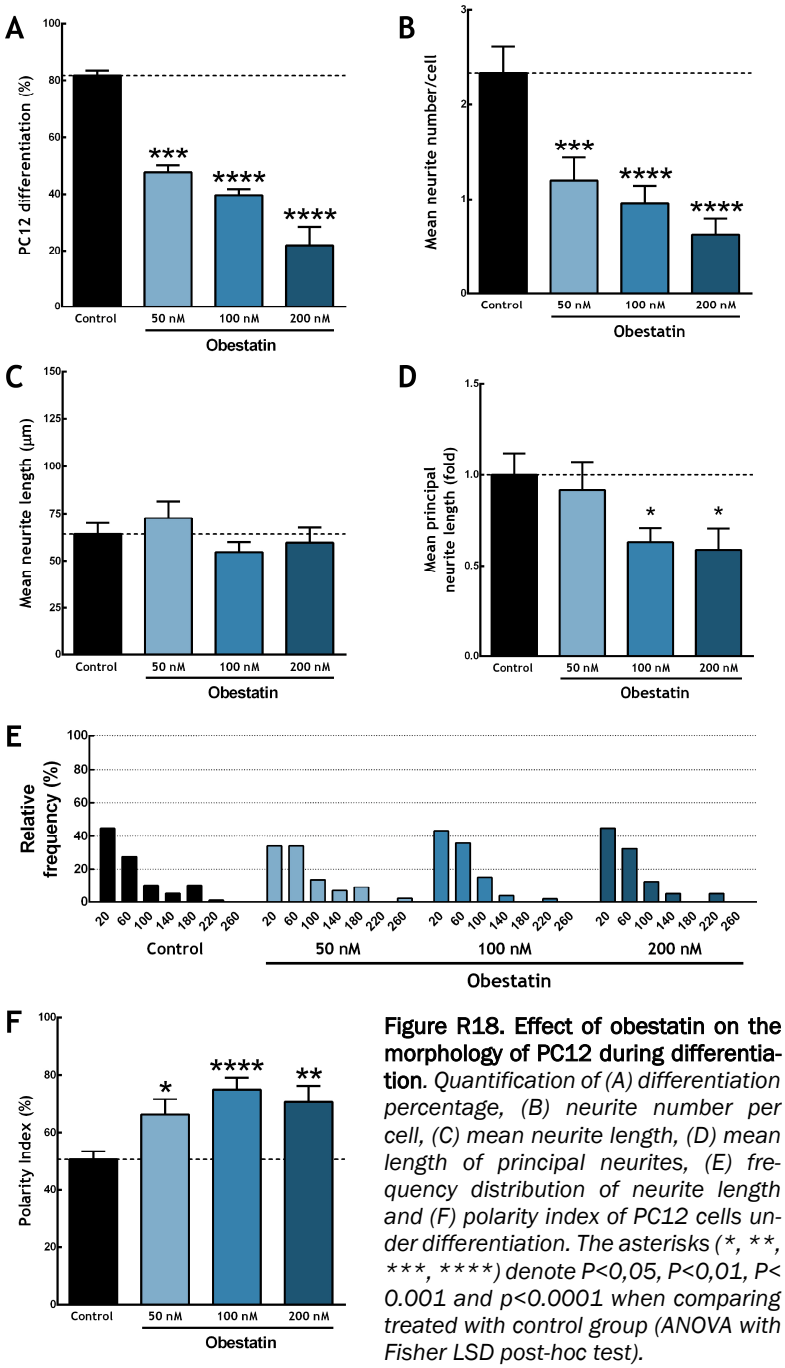

Figure R18. Effect of obestatin on the morphology of PC12 during differentiation. *Quantification of (A) differentiation percentage, (B) neurite number per cell, (C) mean neurite length, (D) mean length of principal neurites, (E) frequency distribution of neurite length and (F) polarity index of PC12 cells under differentiation. The asterisks (*, **, ***, ****) denote P<0,05, P<0,01, P< 0.001 and p<0.0001 when comparing treated with control group (ANOVA with Fisher LSD post-hoc test).*

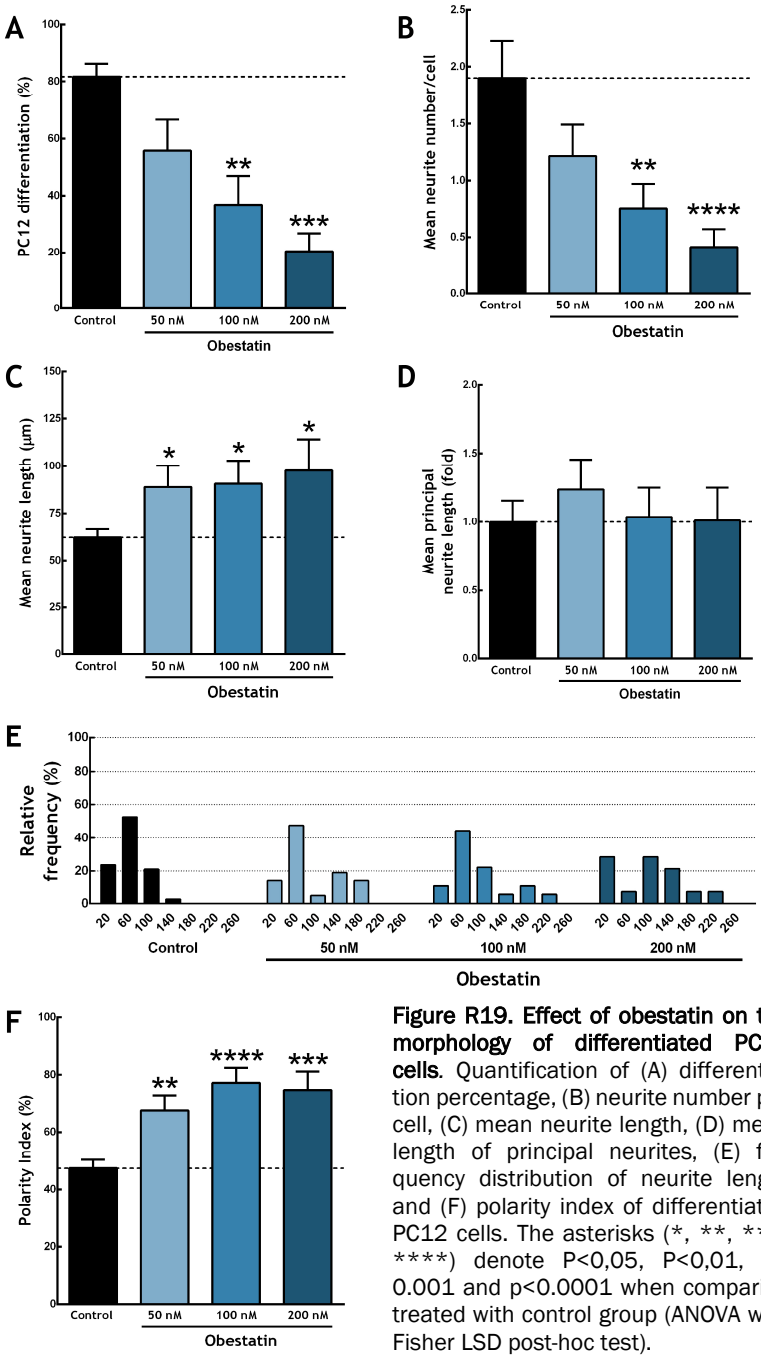

Figure R19. Effect of obestatin on the morphology of differentiated PC12 cells. Quantification of (A) differentiation percentage, (B) neurite number per cell, (C) mean neurite length, (D) mean length of principal neurites, (E) frequency distribution of neurite length and (F) polarity index of differentiated PC12 cells. The asterisks (*, **, ***, ****) denote P<0,05, P<0,01, P< 0.001 and p<0.0001 when comparing treated with control group (ANOVA with Fisher LSD post-hoc test).

The addition of obestatin increased the mean length of neurites by approximately 30% for 50 nM obestatin and 35% for 100 nM and 200 nM obestatin (Figure R19C); however, the mean length of the neurites was not affected (Figure R19D).

The analysis of the relative frequency of neurite length reveals a change in pattern with the addition of obestatin, which seems to promote a population of neurites with longer neurites (Figure R19E). As with the PC12 differentiation, the addition of obestatin increased the polarity index by 20% for 50nM obestatin, and by 30% for the 100nM and 200nM doses (Figure R19F).

Obestatin enhances SC proliferation in PC12-IFRS1 coculture.

One of the first events that occur during nerve regeneration after an injury is the change of SCs from a myelinating phenotype to a proliferative phenotype. It has been proved that the proliferation of SCs is essential for their migration and for axon re-growth (Chen et al. 2005).

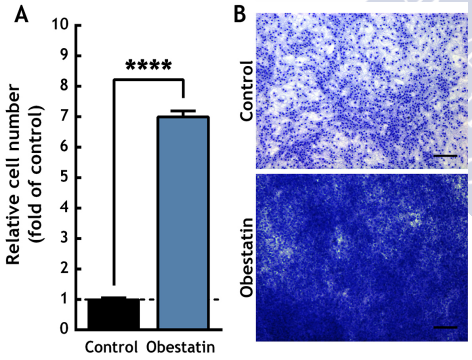

Figure R20. Effect of obestatin on PC12-IFRS1 cell coculture proliferation. *(A) Violet crystal incorporation was used to determine PC12-IFRS1 coculture proliferation. The data were expressed as fold of control (Mean ± SEM; n=6). The asterisk (****) denotes P<0.0001 when comparing treated with the untreated control group. (unpaired Student t test. (B) Representative images of violet crystal stain of PC12-IFRS1 coculture after 21 days of obestatin treatment. The scale bars correspond to 100 µm.*

In this sense, a violet crystal incorporation assay was used to determine PC12-IFRS1 coculture proliferation. After 21 d of coculture, obestatin significantly enhances cell proliferation (~7 fold over control) under myelinating conditions (Figure R20A) and the crystal violet incorporation was clearly appreciable (Figure R20B).

However, these results did not allow us to know which cell was proliferating. To discriminate between IFRS1 and NGF-primed PC12 cell proliferation, both cell types were cultured for 7 d in MM, treated or not with 200 nM obestatin, and the proliferation was analysed separately.

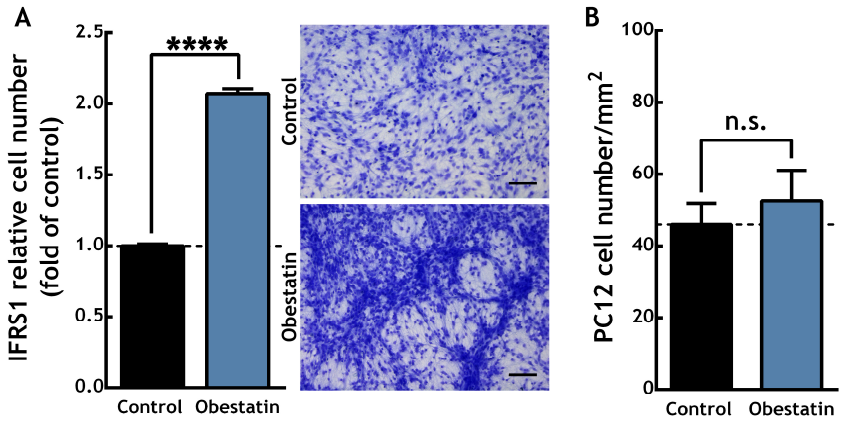

Figure R21. Effect of obestatin on IFRS1 and PC12 proliferation. *(A) Violet crystal incorporation was used to determine IFRS1 proliferation under myelinating conditions. The data were expressed as a fold of control (Mean ± SEM; n=6). The asterisk (****) denotes P<0.0001 when comparing treated with the untreated control group (unpaired Student t test). Representative images of violet crystal incorporation in PC12-IFRS1 coculture. The scale bars correspond to 100 µm. (B) Direct PC12 cell counting after 7 days of obestatin treatment under myelinating conditions. The data were expressed as mean ± SEM (n=6). n.s. denotes no significant difference (unpaired Student t test).*

IFRS1 cells treated with obestatin under myelinating conditions showed an increment in proliferation when compared with the control group (Figure R21A). On the other hand, direct counting of PC12 cells after obestatin under myelinating conditions reveals that there was no significant increase in the number of cells after 7 d (Figure R21B).

Obestatin increments density, number and size of cell clusters in PC12-IFRS1 coculture.

During the PC12-IFRS1 coculture, cell clusters were formed, whose size and number seemed to increase over time. As a first step, Ki67 was

tested as a marker of proliferating cells. A clear increase in the expression of Ki67 was found in the cell clusters (Figure R22, white arrowhead).

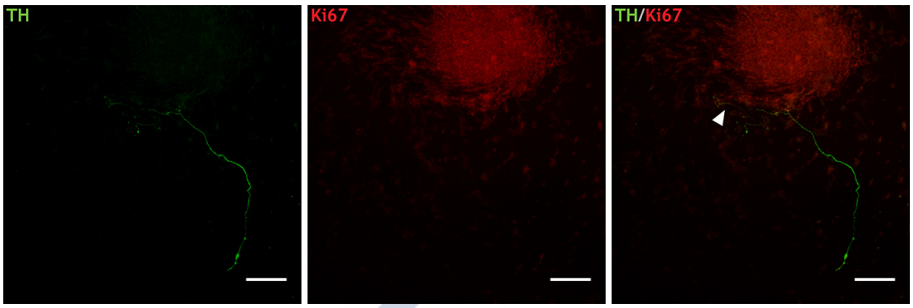

Figure R22. Characterization of the cellular clusters found in a 21 days PC12-IFRS1 co-culture. *Representative confocal images of Ki67 Immunofluorescence staining in PC12-IFRS1 coculture clusters (white arrowhead). The scale bars correspond to 100 µm.*

In many cases, the clusters were found in contact with a PC12 cell, however, no proof of a direct relationship between this fact and the increment of proliferation was found.

Starting from this premise, we tested whether obestatin caused any effect on the morphology of these clusters, for which a morphological analysis was performed at 21 d of coculture, with or without 200 nM obestatin treatment. We examined phase contrast images from 10 independent experiments, analysing cell density, surface area and number of clusters. Transect measurements across the clusters indicated a clear increase in cell density in those samples treated with obestatin, whose maximum cell density was doubled compared to the untreated control group (Figure R23A-B).

In addition to this increase in cell density, the clusters showed a significant increase in cluster number in obestatin treated coculture (44.97 clusters/mm^2) compared with the untreated control group (11.11 clusters/mm^2; Figure R23C), as well as a significant increase in the surface area in obestatin treated cocultures (37% increment over control; Figure R23B-C).

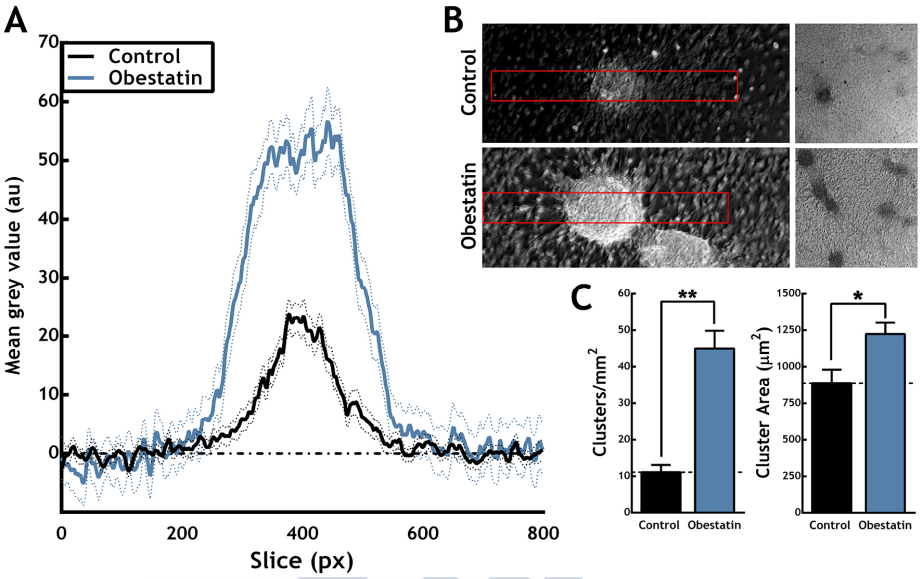

Figure R23. Effect of obestatin on the morphology of cell clusters in PC12-IFRS1 coculture. *(A) Cell density representation, measured in transects taken through cell clusters. The data were expressed as mean ± SEM [control (n=23); obestatin (n=32)]. (B) Phase contrast images of 21 days coculture with or without obestatin. The red boxes represent transects analysed for the cell density calculation. (C) Measurements of the number and surface area of clusters. The data were expressed as mean ± SEM (n=10). The asterisks (*, **) denotes P<0.05 and P<0.01 respectively when comparing treated with the untreated control group (Mann Whitney test and unpaired Student t-test, respectively).*

Obestatin increments myelin-associated proteins levels in PC12-IFRS1 coculture.

Myelin protein zero (MPZ), myelin basic protein (MBP) and myelin-associated glycoproteins (MAG) are key components of different structures of the myelin sheath of PNS and they are expressed by the SCs. We analysed these myelination markers in PC12-IFRS1 coculture after treatment or not with obestatin (200nM) for 7, 14 and 21 d.

MPZ is the most abundant protein in the PNS, acting as a membrane adhesion protein (Han et al. 2013). Obestatin treatment caused a significant increase in MPZ protein levels at day 7 (~2 fold over control), 14 (~3 fold over control) and 21 (~2 fold over control) when compared with the untreated control group (Figure R24).

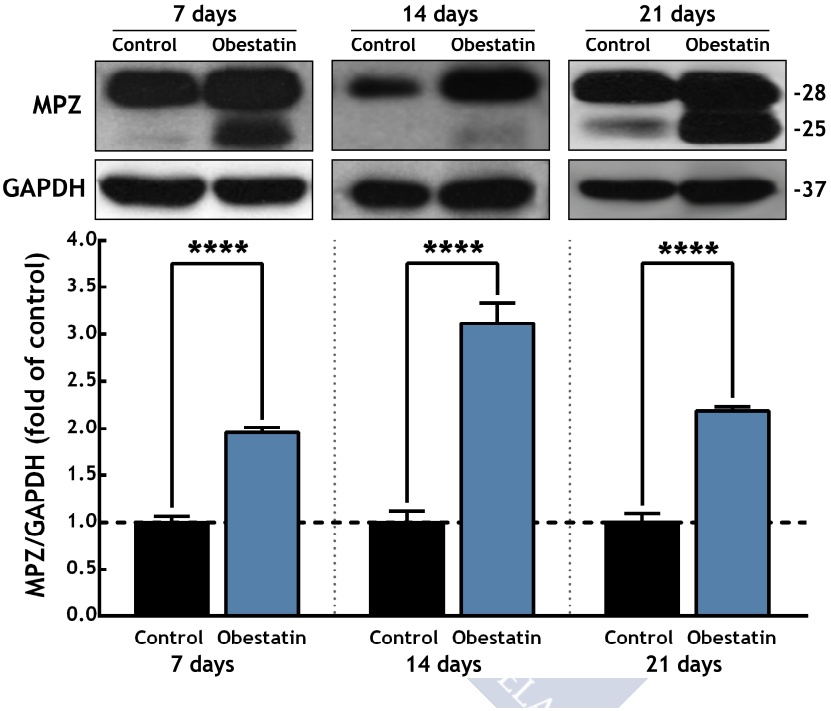

Figure R24. Analysis of MPZ protein levels in PC12-IFRS1 coculture. *Relative protein expression of MPZ after 7, 14 and 21 d of coculture, treated or not with 200 nM obestatin. The data were expressed as fold of control (mean ± SEM; n=6). The asterisks (****) denote P<0.0001 (unpaired Student t test).*

MBP belongs to a group of proteins with a basic isoelectric point, whose function consists mainly in the compaction of myelin (Han et al. 2013). In the PC12-IFRS1 coculture, MBP isoform 1 was detected, showing a significant increase after obestatin treatment at 7 d (~2 fold over control), 14 d (~2.5 fold over control) and 21 d (~1.5 fold over control) when compared with the untreated control group (Figure 25).

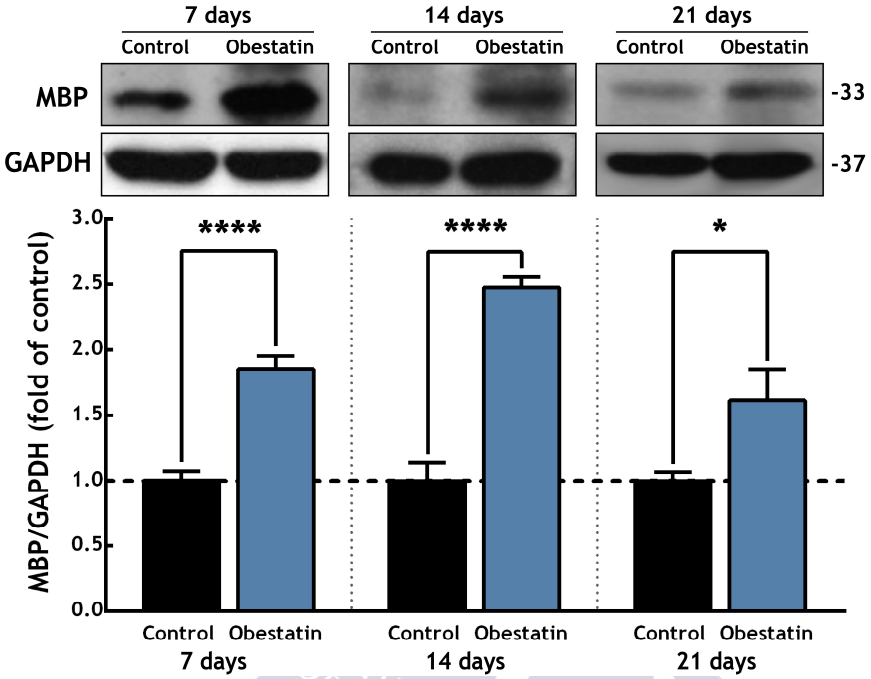

Figure R25. Analysis of MBP isoform 1 protein levels in PC12-IFRS1 coculture. *Relative protein expression of MBP at 7, 14 and 21 d of coculture, treated or not with 200 nM obestatin. The data were expressed as fold of control (mean ± SEM; n=6). The asterisk (*, ****) denotes p<0.05 and p<0.0001 (unpaired Student t test).*

MAG is expressed in both the CNS and the PNS and is located in areas with uncompacted myelin and in the periaxonal space (Han et al. 2013). Its function has been related to the beginning of myelination and the maintenance of the myelin sheath (Schnaar and Lopez 2009). L-MAG (~100kDa) and S-MAG (~96kDa) were detected in the PC12-IFRS1 coculture, and both have significantly higher expression after obestatin treatment (200nM) at 7 d (~1.5 fold over control), 14 d (~1.75 fold over control) and 21 d (~2 fold over control) compared to the control group (Figure R26).

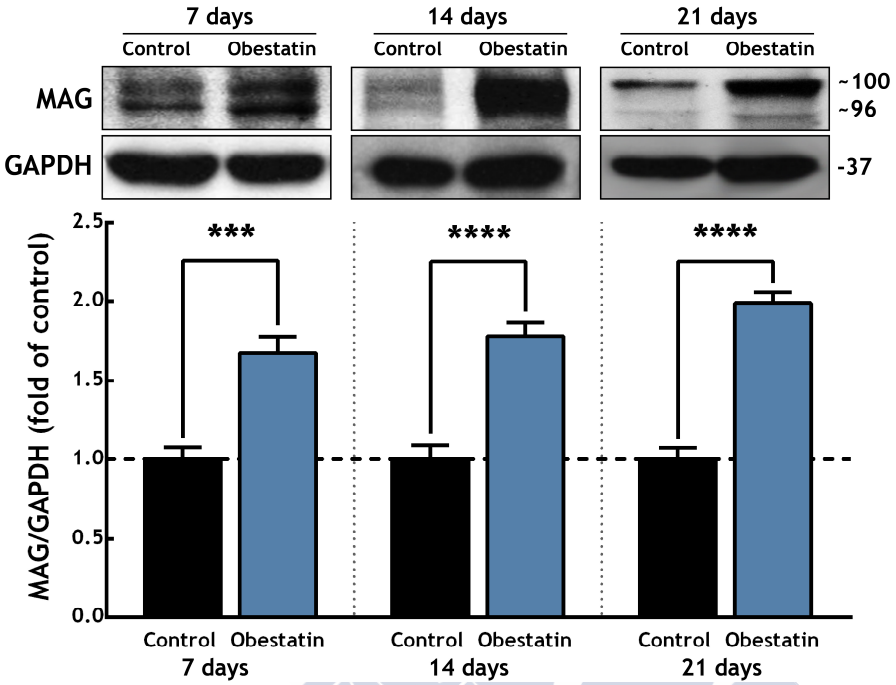

Figure R26: Analysis of MAG protein levels in PC12-IFRS1 coculture. *Relative protein expression of MAG at 7, 14 and 21 d of coculture, treated or not with 200 nM obestatin. The data were expressed as fold of control (mean ± SEM; n=6). The asterisk (***, ****) denotes p<0.001 and p<0.0001 respectively (unpaired Student t test).*

Obestatin activates the SCAP-SREBP related lipid biosynthesis machinery.

During the myelination process, the coordination of myelin-associated protein synthesis and lipid biosynthesis is a crucial aspect (Saher and Stumpf 2015). SCAP (SREBP cleavage activating protein) plays a key role in this aspect as it is required for the proteolytic excision and activation of SREBP (sterol responsive element binding protein), which is one of the main promoters of sterol biosynthesis (Svaren and Meijer 2008).

In this sense, to assess the effect of obestatin on the lipid biosynthesis, an oil-red incorporation assay was performed to try to estimate the lipid biosynthesis in the PC12-IFRS1 coculture system. Obestatin enhanced oil red incorporation in the PC12-IFRS1 coculture, which translated into an increase in the amount of lipids in the system (Figure 27A).

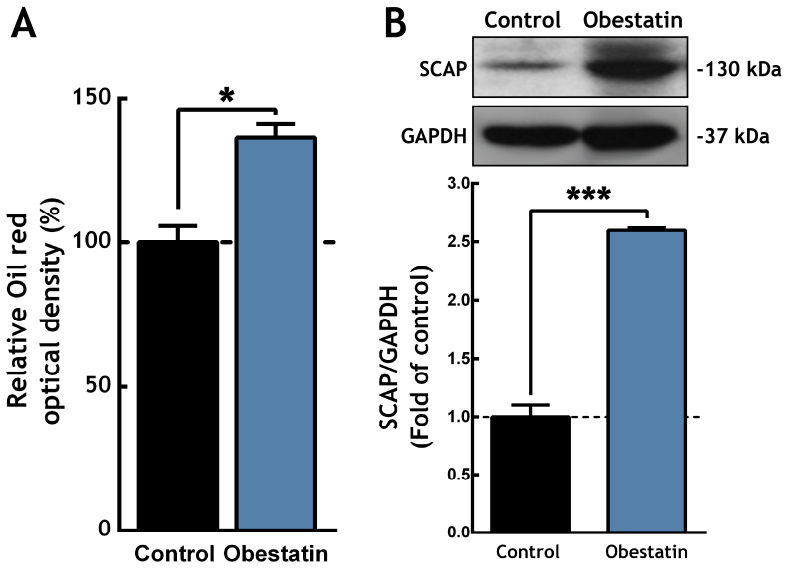

Figure R27. Effect of obestatin on lipid biosynthesis. *(A) Oil red incorporation quantification at 21 d in the PC12-IFRS1 coculture. The data were expressed as percentage of control (mean ± SEM; n=6). (B) Relative protein expression of SCAP at day 21 of coculture, treated or not with 200 nM obestatin. The data were expressed as fold of control (mean ± SEM; n=6). The asterisk (*, ***) denotes p<0.05 and p<0.001, respectively (unpaired Student t test).*

In addition, SCAP expression was tested as it is a key component of the sterol biosynthesis required for myelination (Verheijen et al. 2009). Obestatin treatment led to an increase in SCAP protein levels after 21 d of the PC12-IFRS1 coculture (Figure R27B).

Obestatin increase myelination in PC12-IFRS1 coculture model.

To explore whether obestatin affects not only the expression of proteins related to myelin biosynthesis but also the morphological changes that occur during myelination, a PC12-IFRS1 coculture was tracked at 7, 14 and 21 d. Immunofluorescence staining was performed using TH (Figure R28, green) as PC12 cell marker and MBP as myelin marker (Figure R28, red).

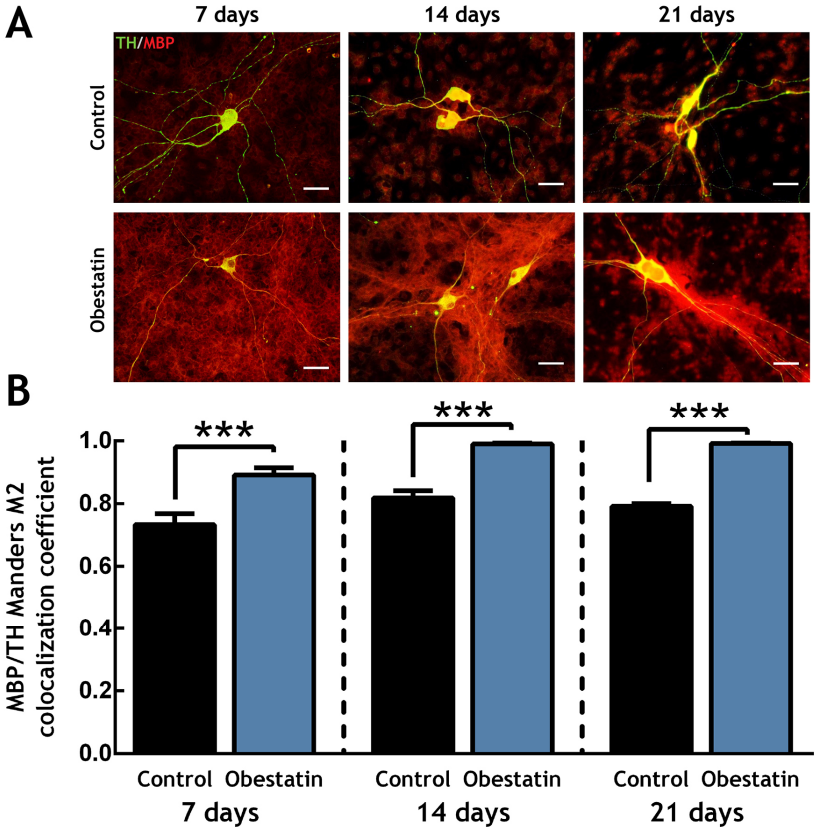

Figure R28. Immunofluorescence analysis of myelination in PC12-IFRS1 coculture. *(A) Representative immunofluorescence images of PC12-IFRS1 coculture at 7, 14 and 21 d stained with TH (green) and MBP (red). The scale bars correspond to 50 µm. (B) Calculation of Manders M2 colocalization coefficient. The data were expressed as mean ± SEM of six independent experiments. The asterisk (***) denotes P<0.001 compared with control group (Mann-Whitney test).*

According to the proliferation results, obestatin treatment (200nM) caused an increase in the number of IFRS1 cells from day 7 to the end of the coculture process (Figure R28A).

Besides, the images showed that the IFRS1 cells appear to be grouped around the neurites and the cell bodies of the PC12 cells. For the quantification of TH and MBP immunofluorescence signal colocalization, we used the Manders M2 colocalization coefficient. These results led us to confirm that the treatment with obestatin significantly increased the colocalization coefficient (~20% fold over control in all cases), resulting in a higher overlap of the PC12 cells by the IFRS1 cells (Figure R28B).

Following this approach, the transects taken perpendicularly along PC12 neurites were analysed, measuring the fluorescence intensity for TH and for MBP in each transect section (Figure R29).

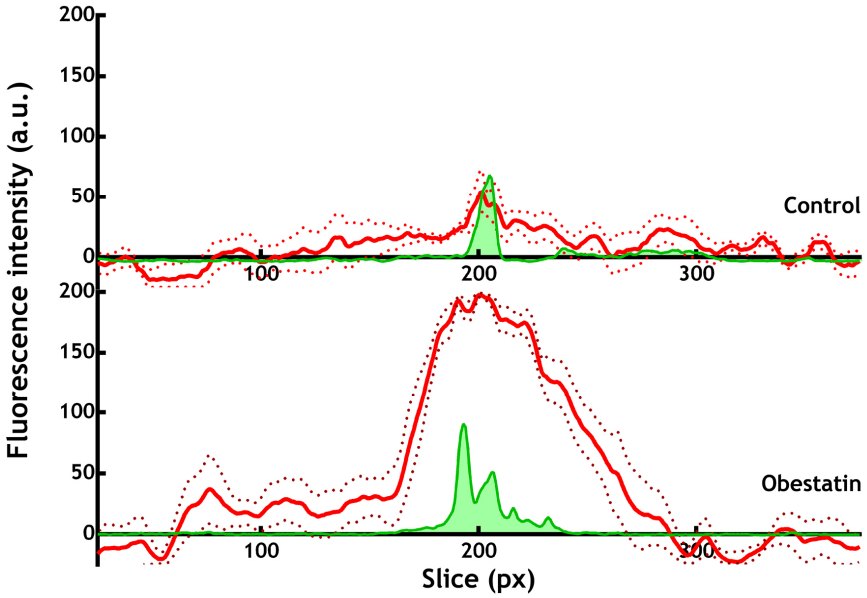

Figure R29. Analysis of IFRS1 cell density around PC12 neurites. *Representation of the cell density of MBP⁺ cells (red line) around PC12 neurites (green area. Cell density of MBP⁺ cells was expressed as mean ± SEM (n=10).*

The data showed an increment of the MBP^+ cell density around PC12 neurites in the obestatin treated group (~4 fold of maximum relative immunofluorescence signal over control) compared to the untreated control group, in which a more uniform cell density was observed along the transect (Figure R29).

USC UNIVERSIDADE DE SANTIAGO DE COMPOSTELA

CHAPTER 5

Obestatin effect on an *in vivo* nerve crush injury model

USC
UNIVERSIDADE DE SANTIAGO DE COMPOSTELA

USC
UNIVERSIDADE
DE SANTIAGO
DE COMPOSTELA

One of the main goals in the treatment of damaged peripheral nerves is the recovery of the motor function. In this sense, the sciatic nerve damage model has been widely used to study nerve recovery and it is a fundamental tool in the discovery of new therapeutic targets and biological and artificial grafts. One of the most common models of peripheral nerve damage and regeneration is the sciatic nerve crush (axonotmesis). This model allows the precise study of the axon regrowth and its interaction with the glia and the basal laminae, partly because it interrupts axonal continuity but preserves the basal lamina and the SCs (Bauder and Ferguson 2012).

Obestatin increments the sciatic functional index (SFI) in a sciatic crush injury model.

To address whether the exogenous administration of obestatin was able to enhance PNS regeneration, rat obestatin (500nM/Kg of body weight) was administered into a crush-injured sciatic nerve of ~250 g Sprague-Dawley rats (n=8/group; see Materials and methods). Right after the nerve crush damage was done and the catheter port was installed, the treatment began and was re-administered every 48 h for a total of 12 d.

Functional assays were performed by calculating the SFI as previously described (Bain, Mackinnon, and Hunter 1989). SFI has been a commonly used parameter to quantify nerve regeneration, by using morphometric measurements of the rat footprint (Figure R30A). Although it has suffered several modifications, it is still one of the main tools for analysing nerve functionality. Figure R30B shows the morphometric changes in the footprints of the two groups at the indicated days. A clear improvement in the footprint morphometry of the obestatin treated group can be observed in relation to the control group treated with saline (R30B). After 3 days postinjury (DPI), the SFI drops drastically to - 85.04 ± 2.34 %, while a significant recovery was observed in the obestatin group (69.85 ± 4.25 %). These differences were intensified at later stages. At 6 DPI, the saline group barely increased the SFI (- 82.34 ± 1.80 %), while the obestatin group was able to increase the SFI to - 58.00 ± 9.27 % (R30C).

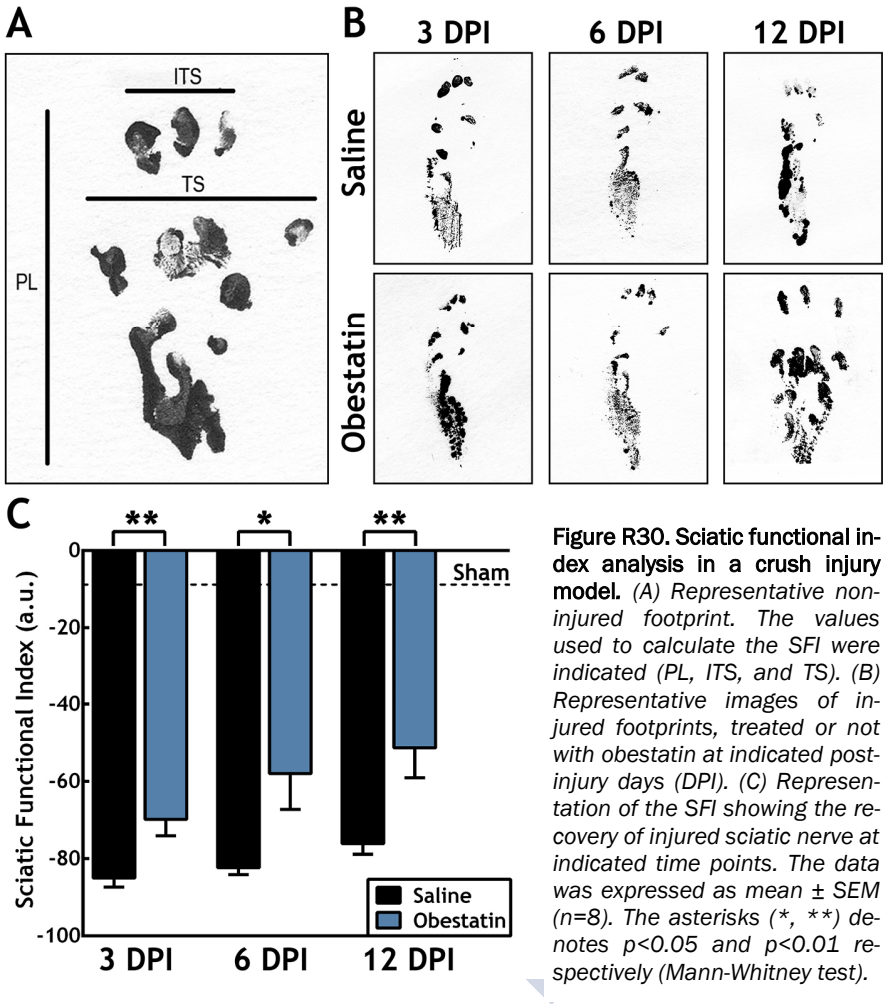

Figure R30. Sciatic functional index analysis in a crush injury model. *(A) Representative non-injured footprint. The values used to calculate the SFI were indicated (PL, ITS, and TS). (B) Representative images of injured footprints, treated or not with obestatin at indicated post-injury days (DPI). (C) Representation of the SFI showing the recovery of injured sciatic nerve at indicated time points. The data was expressed as mean ± SEM (n=8). The asterisks (*, **) denotes p<0.05 and p<0.01 respectively (Mann-Whitney test).*

Finally, with the conclusion of the assay, on the twelfth day, the difference between both groups reached its maximum. The SFI of the saline-treated group was 76.14 ± 2.77 %, while in the obestatin-treated group it reached 51.34 ± 7.72 % (R30C).

Obestatin increases axon enervation and nerve regeneration.

The expression of GAP43, just like other growth associated proteins, is upregulated after peripheral nerve injury, as well as in certain encephalic lesions (Perrone-Bizzozero and Tanner 2007).

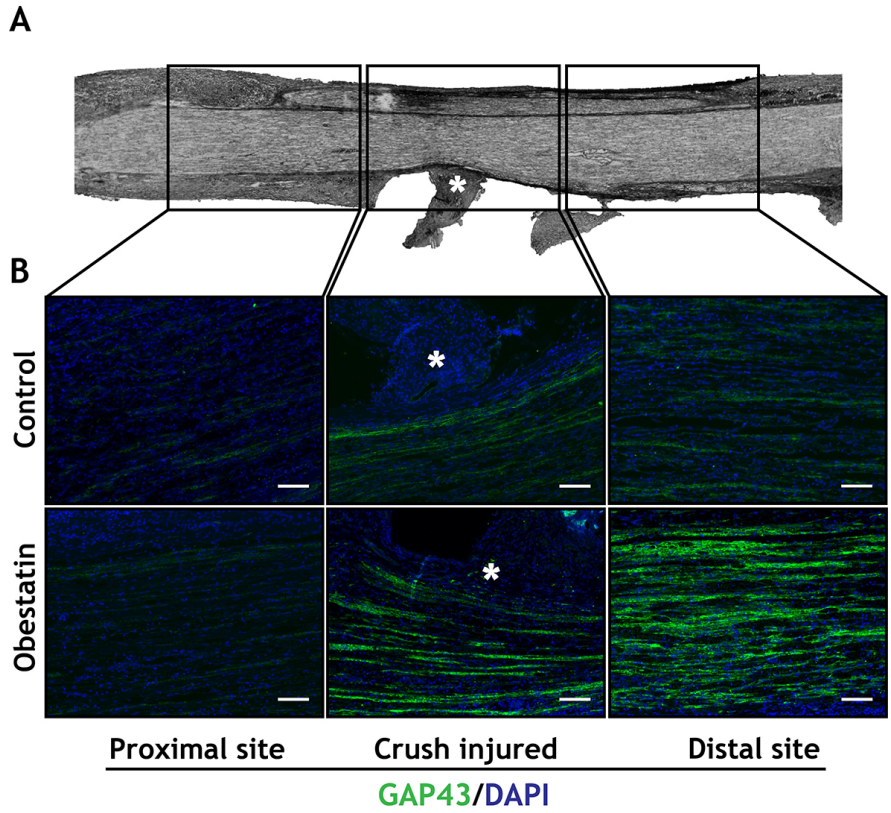

Figure R31. Immunofluorescence analysis of GAP43 in crush-injured sciatic nerve. *(A) Representative image of a crush-injured sciatic nerve. (B) GAP43 (green) was stained in a proximal section, an injured section and a distal section of the crush-injured sciatic nerve treated or not with 200nM obestatin. DAPI (blue) was used to counterstain nuclei. The asterisk indicates the crush spot. The scale bars correspond to 100 µm.*

In vivo studies showed that shortly after rat sciatic nerve injury, GAP43 appears to be synthesized in the DRG cells and transported to the growth cone. The presence of GAP43 on the damaged nerve increases to a peak at 21 d after damage and disappears 9 weeks after damage (Woolf et al.

1990; Holahan 2017). GAP43 seems to play a fundamental role in the creation of new sprouts and the beginning of axonal re-growth (Allegra Mascaro et al. 2013; Holahan 2017).

Therefore, the expression of GAP43 was analysed in a crush injured nerve model treated or not with obestatin. After the identification of the damaged area, marked by the forceps on the perineurium (Figure R31A-B, white asterisks), the expression of GAP43 was studied in three critical areas in the regeneration process: the area before the damage (proximal site), the damaged area (crush injured), and the area after the damage (distal site).

GAP43 expression increased from the proximal to the distal site. This staining was more intense in the obestatin treated animals. Remarkably, GAP43 maximum expression differed from saline to obestatin treated animals: while the highest immunoreactivity was located in the injured area for the saline group, in the obestatin treated animals it was observed at the distal site. (Figure R31B). In addition, the maximum expression of GAP43 in the saline-treated group was located in the injured area, while in the obestatin treated group the maximum expression was more advanced in the distal site.

Obestatin increases axon restoration and myelin compaction in a sciatic nerve crush injury model.

When an injury is caused to a nerve, a degenerative process is produced towards the distal region. In the early stages, digestion chambers are generated, which can be appreciated in paraffin-embedded sections, and the myelin and the axons are degraded. The digestion chambers progressively disappear as the nerve regeneration progresses, and the axons grow. (Zochodne 2012; Tricaud and Park 2017).

To determine the integrity and the regeneration status of the crush injured sciatic nerve after 12 d of treatment with obestatin, the expression of neurofilaments (NF) and MBP were analysed in the distal segment from

injury. This area was selected according to the results obtained in the analysis of GAP43 expression in the obestatin-treated animals, which is closely related to axonal growth (Figure R31).

Neurofilaments are intermediate filaments found in the cytoplasm of neurons. These protein polymers are part of the neural cytoskeleton and their main function is to provide structural support to the axon and regulate its diameter. During nerve degeneration, there is a decrease and disorganization of neurofilaments stain due to a decrease in axons.

After a nerve injury, the nerve presents a low immunoreactivity for NF with discontinuous staining (Figure R32A-C). Obestatin-treated nerves exhibit a higher NF immunoreactivity with a much more organised pattern (Figure R32B-D) than the saline group (Figure R32A-C). Additionally, the NF^+ axon density was augmented in the obestatin-treated samples, compared to those in which only the saline was used (Figure R32E).

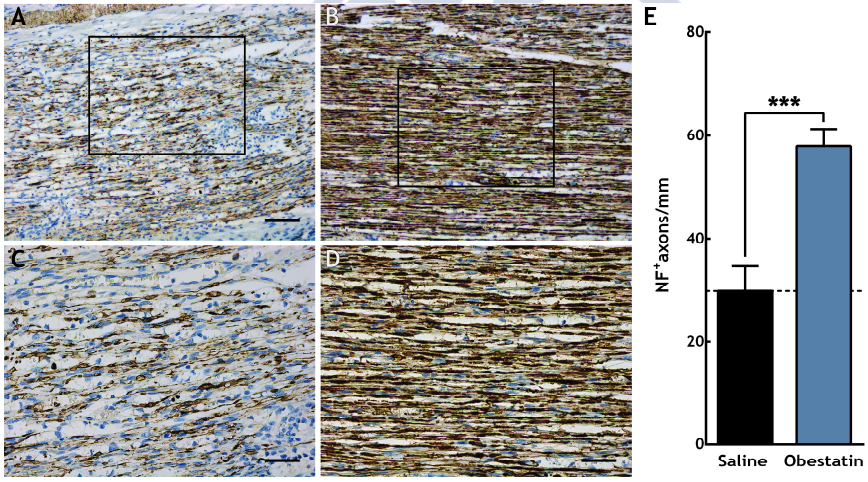

Figure R32. Neurofilament expression in distal site of crush injured rat sciatic nerve. *Representative images of distal site of crushed sciatic nerve treated with saline (A, C) or obestatin (B, D) during 12 days. The scale bar correspond to 100 µm (A,B) or 50 µm (C, D). (E) Measurement of the number of NF^+ axons per mm of sections of sciatic nerve, treated or not with obestatin. The data were shown as mean ± SEM (n=6). The asterisks (***) denotes P<0.001 (unpaired t-test).*

Regarding MBP, it is one of the main structural proteins present in the CNS and PNS myelin sheath and is involved in the compaction of the myelin membranes. In our system, the expression of MBP also appears to be increased in the distal area of the injured sciatic nerves treated with obestatin (Figure R33B-D) with respect to those treated with saline (Figure R33A-C).

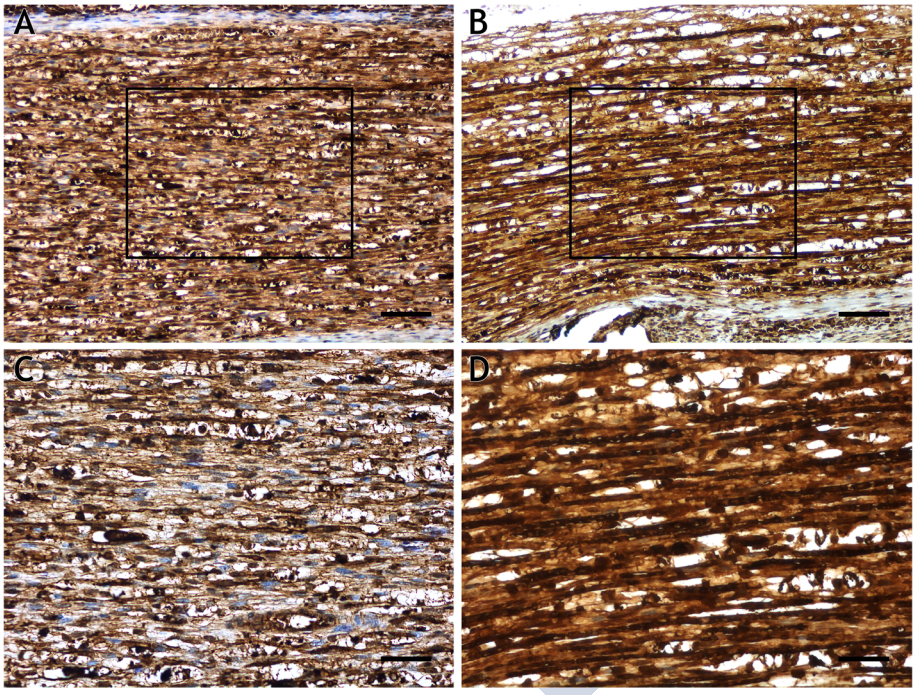

Figure R33. Myelin basic protein expression in distal site of crush injured rat sciatic nerve. *Representative images of distal site of crushed sciatic nerve treated with saline (A, C) or obestatin (B, D) during 12 days The scale bar correspond to 100 µm (A,B) or 50 µm (C, D).*

In addition, an anatomorphological difference between the obestatin and the saline treatment could be appreciated. Obestatin-treated nerves showed an increase in the longitudinal tubular structures that present a very high positivity for MBP (Figure R33B-D) when compared with the saline-treated sciatic nerves (Figure R33A-C).

Additionally, images of the obestatin-treated nerves showed a decrease in the presence of degeneration chambers, suggesting a more advanced stage of regeneration (Figure R33C-D).

Obestatin increases myelination-associated proteins in rat crushed sciatic nerves.

To find out if obestatin had an effect on myelin-related protein synthesis, sciatic nerve damage sections (~1 cm) of the obestatin-treated or untreated animals during 12 d were analysed by immunoblot (Figure 34). Contralateral sciatic nerves were used as a sham group.

MBP and MPZ were examined, as they are the main proteins related to myelin synthesis and compaction (Garbay et al. 2000; Han et al. 2013; Bakhti, Aggarwal, and Simons 2014). Four different isoforms (21.5, 18.5,

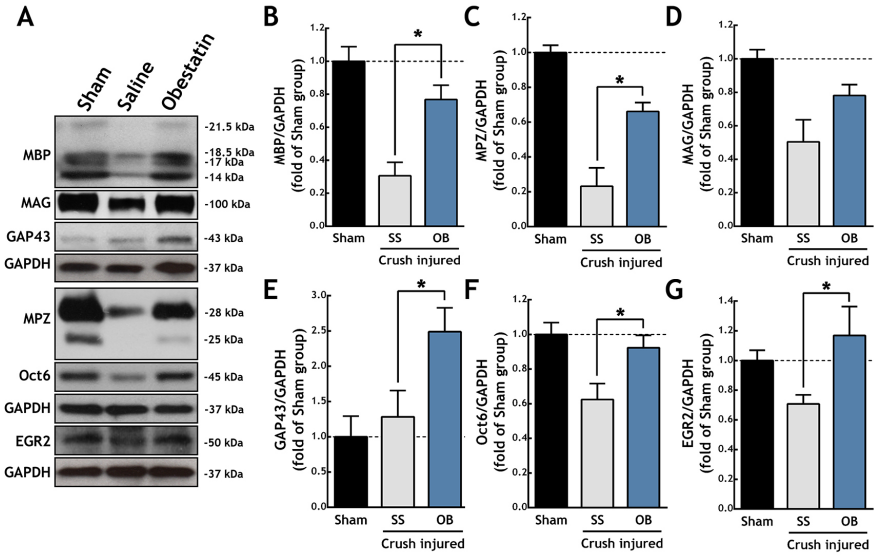

Figure R34. Immunoblot analysis of nerve regeneration in crush-injured rat sciatic nerves. *Relative protein expression of (B) MBP, (C) MPZ, (D) MAG, (E) GAP43, (F) Oct6 and (G) EGR2 in crush-injured nerves 12 days after injury treated or not with obestatin. The data were expressed as fold of control (mean ± SEM; n=4). The asterisks (*) denotes p<0.05 (Mann-Whitney test).*

17 and 14 kDa) were identified for MBP. MBP protein levels were drastically reduced (0.31 ±0.08 fold) in the crush injured nerves treated with saline, while the exposure to obestatin caused a significant increase in the protein levels of all MBP isoforms in these injured nerves (0.76 ± 0.09-fold; Figure R34B).

As with MBP, in the damaged nerves, the levels of MPZ protein decrease drastically (0.23 ± 0.10-fold), and obestatin partially counteracted this decrease (0.66 ± 0.05-fold; Figure R34C).

On the other hand, MAG, a glycoprotein that is believed to play a key role in axonal recognition, axonal adhesion and membrane spacing (Garbay et al. 2000; Quarles 2007), expression was also decreased in the crushed nerves (0.50 ± 0.13 fold); however, although there was an upward trend (0.78 ± 0.06 fold), obestatin was not able to significantly increase MAG protein levels (Figure R34D).

The signals that promote myelination converge in a variety of transcription factors, which are responsible for directing the transition from immature/promyelinating to myelinating SC. One of the transcription factors that seems to play a key role in this process is EGR2 (Svaren and Meijer 2008), whose expression and activation is controlled mainly by Oct6 during myelination of SCs (Ghislain and Charnay 2006).

According to the data presented above, the addition of obestatin significantly counteracted the loss of expression of Oct6 (47.82 % increase; Figure R34F) as well as EGR2 (65.18 % increase; Figure R33G) caused by the injury.

GAP43 is a protein associated with neuronal plasticity and presynaptic neuronal outgrowth. Although GAP43 is absent in myelinated axons, during nerve regeneration its synthesis is upregulated, enhancing nerve sprouting (Benowitz and Routtenberg 1997; Holahan 2015). As seen in Figure R34E, the crush-injured nerves treated with saline showed a tendency to increase GAP43 protein levels (1.28 ±0.37 fold) with respect to

the sham group. The addition of obestatin produced a significant increment in GAP43 protein expression (2.49 ± 0.33-fold) when compared to the saline-treated group.

Obestatin attenuates muscle atrophy in a sciatic nerve crush injury model.

Based on the ability of obestatin to promote peripheral nerve myelination and improve sciatic nerve structure and function, we studied whether this improvement led to any benefit in the muscle atrophy associated with a nerve injury.

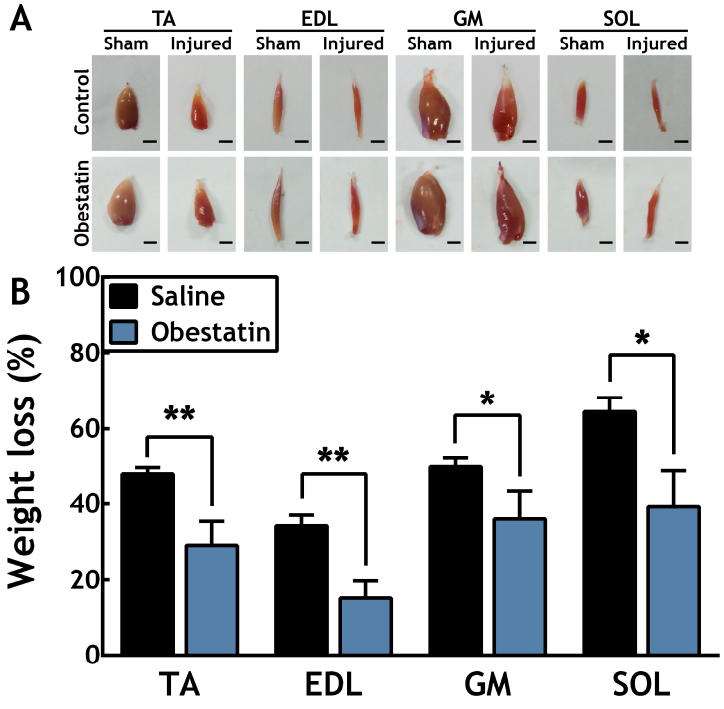

Figure R35. Muscle mass loss analysis in a crush-injured sciatic nerve model. *(A) Representative images of hind limb muscles 12 days after crush injury treated or not with obestatin. (B) Relative muscle mass loss of tibialis anterior (TA), extensor digitorum longus (EDL), gastrocnemius (GM) and soleus (SOL) after 12 days of recovery. The data were expressed as fold of control (mean ± SEM; n=4). The scale bars correspond to 5 mm (A,B) or 50 µm (C, D). The asterisks (*, **) denotes p<0.05 and p<0.01 (unpaired t test).*

After denervation, both the neuromuscular junction and the muscle itself undergo several changes. The instability of the neuromuscular junctions causes a gradual atrophy, clearly evidenced by a reduction of the muscle wet weight and a reduction of the muscle fibre diameter (Wu et al. 2014).

Once the sciatic nerve crush assay was completed, the hind leg muscles were significantly atrophied (Figure R35A). After 12 d of recovery in the presence or absence of obestatin, the hind leg muscles were extracted and weighed to detect any differences in wet muscle mass. The results showed that in the tibialis anterior (TA), gastrocnemius (GM), extensor digitorum longus (EDL) and soleus (SOL), the muscle mass was clearly decreased within 12 d after the sciatic nerve was crushed and treated with saline, compared with sham group (Figure R35A). It was also observed that obestatin treatment in the sciatic nerve was able to attenuate this loss of mass significantly in all the hind leg muscles (Figure R35B). The maximum differences in muscle wet weight recuperation were observed in muscles involved in dorsiflexion (40% and 55% for TA and EDL, respectively), while in the muscles involved in plantar flexion, the weight recuperation was lower and more variable (28% and 40% for GM and SOL, respectively).

Based on the data obtained in the wet muscle mass recovery, TA was selected, the main muscle implied in dorsiflexion, to analyse the cross-section area since it suffered a large muscle mass reduction and the lowest variability. Frozen cross-sections of the TA stained with HE was analysed, and the cross-section area (CSA) of each muscle fibre was quantified. According to the decrease in muscle mass described above, the crushing of the sciatic also produces an appreciable reduction in the area of the muscle fibres (Figure 36A) becoming a 20% of the sham muscle area, and as before, obestatin was able to significantly attenuate this decrease in the muscle fibres areas, assuming a 50% increase in the mean cross-section area of the fibre. (Figure R36A-B).

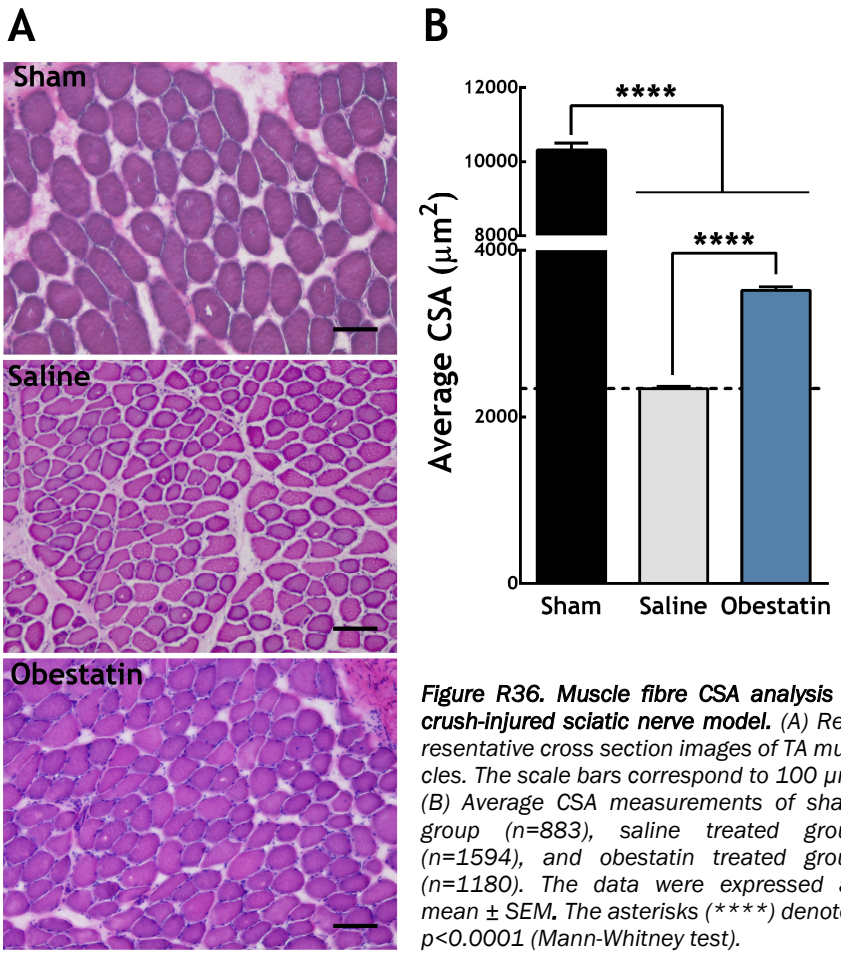

Figure R36. Muscle fibre CSA analysis in crush-injured sciatic nerve model. *(A) Representative cross section images of TA muscles. The scale bars correspond to 100 µm. (B) Average CSA measurements of sham group (n=883), saline treated group (n=1594), and obestatin treated group (n=1180). The data were expressed as mean ± SEM. The asterisks (****) denotes p<0.0001 (Mann-Whitney test).*

USC
UNIVERSIDADE
DE SANTIAGO
DE COMPOSTELA



DISCUSSION

USC
UNIVERSIDADE
DE SANTIAGO
DE COMPOSTELA

CHAPTER 1

The PNS is the part of the nervous system formed by the peripheral nerves and ganglia, whose function is the information exchange between the central nervous system and the peripheral tissues (Noback et al. 2012). Although the PNS has the intrinsic ability to regenerate itself and form functional connections again, various factors such as the age of the patient, the type of injury or the delay in the medical intervention will determine the final prognosis after injury is repaired.

There is currently a great deal of interest in potential therapies for the treatment of peripheral nerve injuries, as current treatments are often unable to fully counteract the damage inflicted. For this reason, the identification of endogenous systems involved in the regeneration of the nervous system would facilitate its applicability as potential therapeutic targets. In this scenario, the obestatin/GPR39 system has been recognized as an endogenous system with a demonstrated regenerative capacity on skeletal muscle (Gurriarán-Rodríguez et al. 2012, 2015). Besides, obestatin presents regenerative/protective properties on the pancreatic tissue after or before the induction of acute pancreatitis (Bukowczan et al. 2015, 2016), accelerates the healing of chronic gastric ulcers (Dembiński et al. 2011) and inhibits the development of induced colitis (Ceranowicz et al. 2009). These premises prompted us to study the expression of this system in the nervous system.

The main finding of this chapter is that the obestatin/GPR39 system is expressed in the nervous system, mainly in the SCs at the PNS level and in the motor and sensory neurons at the CNS. This fact makes the obestatin/GPR39 system a strong candidate to be a therapeutic target in the case of nerve injury, since the SCs are currently located at the coordination centre of the suitability of the cellular environment, the clearance of cellular and myelin debris, the enhancement of axonal growth and functional repair (Kim, Mindos, and Parkinson 2013). These highly specialized

cells play a key role in the regenerative process: they acquire a repairing/proliferating phenotype after an injury, and the dedifferentiation, proliferation and organization of the SCs are crucial events in the peripheral nerve repair process (Jessen, Mirsky, and Lloyd 2015). Therapeutic strategies targeting these processes are used for improving peripheral nerve regeneration and repair.

After peripheral nerve injury, a significant proportion of sensitive and motor neurons are at risk of cell death (Hart, Terenghi, and Wiberg 2008). Based on its action on increasing cell survival, obestatin may have a neuroprotective effect against cell damage in neurons caused by peripheral nerve injury. Reinforcing this hypothesis a new role for obestatin as a neuroprotector has been proposed as a new therapeutic approach for increased neurogenesis and neurodegenerative disorders (Gargantini et al. 2016).

The immunohistochemical analysis performed in a regenerated previously sectioned sciatic nerve, showed different expression pattern and intensity for the obestatin/GPR39 system depending on the zone analysed, the distal or the proximal site. GPR39 expression in the proximal area resembles that of the uninjured tissue; however, at the distal site, GPR39 is associated with tubular structures that could correspond to the Büngner bands. These structures are formed by SCs with a proliferative/repairing phenotype within the basal lamina, providing the essential substrate and guidance to the growing axon (Jessen, Mirsky, and Lloyd 2015). Regarding obestatin, its expression seems to be confined to the distal end of the sciatic nerve. This fact may involve obestatin signalling with the regulation of some of starting events promoting regeneration after an injury, such as proliferation and migration of SCs, secretion of growth factors or the recruitment of macrophages (Jessen, Mirsky, and Lloyd 2015).

We had detected obestatin and GPR39 expression in sensory neurons in adult rat DRGs and motor neurons in the adult rat anterior horn of the

spinal cord. These data reinforce the potential neuroprotective action of the obestatin/gpr39 system in both CNS and PNS.

In a sample of sciatic nerve sectioned from rat, we observed in the proximal area a basal expression of GPR39 associated with glial cells equivalent to what would be found in uninjured tissue. However, at the distal site from the injury, it was observed that the expression of GPR39 is associated with tubular structures that could correspond to the Büngner bands. These structures are formed by SCs with a proliferative/repairing phenotype within the basal lamina, providing essential substrate and guidance to the growing axon (Jessen, Mirsky, and Lloyd 2015).

On the other hand, expression of obestatin is barely detected in the proximal area, while in the distal area the expression of obestatin is clearly increased, expressed both in a diffuse manner. This increase in the expression of obestatin located in the regenerating area may involve its signalling in the regulation of some of the events that promote regeneration after nerve injuries such as the proliferation and migration of SCs, the secretion of growth factors or the recruitment of macrophages (Jessen, Mirsky, and Lloyd 2015).

As a first approximation for the study of the obestatin/GPR39 system in the PNS recovery, *in vitro* models must be used. Two models were proposed: the PC12 cell line, a cell model widely used in neurodegeneration, neuroprotection or neurosecretion studies (Greene and Tischler 1976; Westerink and Ewing 2008; Wang et al. 2015), and in IFRS1 cells, a cell line of spontaneously immortalized Schwann cells (Sango et al. 2011, 2012), obestatin and its receptor GPR39 are expressed. This makes these two cell lines a valid model for *in vitro* study of the effect of obestatin on the peripheral nervous system and its regeneration.

In summary, the obestatin/GPR39 system is expressed in the nervous system, which allows us to evaluate its properties as a target in peripheral nerve regeneration.

USC
UNIVERSIDADE
DE SANTIAGO
DE COMPOSTELA

CHAPTER 2

After an ischemic damage during surgery or post-traumatic injury in the nervous system, there is often a lack of nutrients and oxygen, associated with an interruption of blood flow (Smith et al. 2011). Nutrient deprivation triggers an induction of apoptosis, which can be mimicked *in vitro* by replacing the culture medium with a saline solution without nutrients, glucose and sera. For this purpose, differentiated or undifferentiated PC12 cells, a cell line from a rat pheochromocytoma, have been widely used in neuroprotection studies (Tabakman et al. 2005; Pera et al. 2013). In this work, we used undifferentiated PC12 cells as an *in vitro* model to explore the potential neuroprotective role of obestatin. The observed mitogenic capability of obestatin in these cells, might potentiate cell survival or delay the progression of the degenerative processes (Wu et al. 2018). Cell death is a final consequence of the stressful situations following traumatic damage, ischemia or a degenerative process, and its reduction has been one of the main treatment strategies in the past and present (Faden and Stoica 2007). Glucose/nutrient deprivation, as well as other stressful conditions such as hypoxia or oxidative stress, causes an increment of cell death. Obestatin is able to partially reverse the cell death induced by nutrient deprivation.

Nutrient deprivation triggers an induction of apoptosis, which can be mimicked *in vitro* by replacing the culture medium with a saline solution without nutrients, glucose and sera. The nutrient removal in undifferentiated PC12 cells causes a clear decrease in cell viability, while the addition of obestatin is able to mitigate this viability reduction.

The exogenous obestatin treatment of PC12 cells causes an increase in cell proliferation. This increase in proliferative capacity makes obestatin a promising peptide whose action could prolong cell survival or delay the progression of degenerative processes (Wu et al. 2018).

At the molecular level, deprivation of nutrients in PC12 cells decreases the expression of BCL2 and caspase 3 cleaves and becomes active, which is associated with an increase in apoptosis. Obestatin treatment is able to increase the expression of BCL2 and decrease the expression of active caspase 3, thus decreasing the apoptosis. GSK-3 has been proposed as a key point in the regulation of cellular apoptosis, representing a crossroads of different signalling pathways. Both the Ras-ERK and the PI3K-AKT routes inactivate GSK-3 (Mendoza, Er, and Blenis 2011; Maurer et al. 2014), which promotes the anti-apoptotic protein BCL2, triggering the inactivation of caspase 3 and the decrease of apoptosis. Nutrient deprivation causes a decrease in the phosphorylation of AKT and ERK1/2 in PC12 cells, which allows the activation of GSK3, which has been attributed to a pro-apoptotic activity. However, when incubated in the presence of obestatin, phosphorylation of both AKT and ERK increases, inactivating GSK3 and reducing apoptosis (Figure D1). These data are consistent with those presented above for proteins related to apoptosis BCL2 and caspase 3.

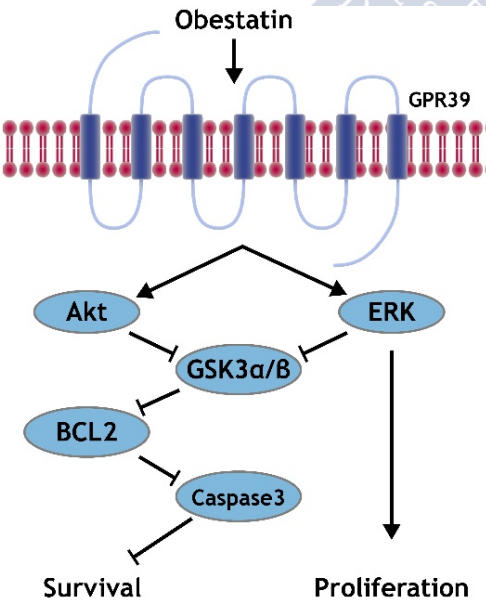

Figure D1. Model of obestatin mediated neuroprotection. *Proposed model of signalling pathway for GSK3α/β inactivation by Akt and ERK1/2 activation in response to obestatin. Source: author original.*

This leads us to propose a model of neuroprotection by obestatin (Figure D1) focused on the regulation of GSK3 based, partly, on obestatin signalling models previously proposed by Pazos's group (Álvarez et al. 2009).

In summary, based on the exposed data, obestatin might exert a neuroprotective effect on motor and sensory neurons.

USC UNIVERSIDADE DE SANTIAGO DE COMPOSTELA

USC
UNIVERSIDADE
DE SANTIAGO
DE COMPOSTELA

CHAPTER 3

After a nerve injury, the axons must grow to the distal end in a coordinated non-isolated way process, which needs that both microenvironments in the damaged and the distal area were suitable for the reception of new axons. SCs play a fundamental role in the processes that accommodate the injured area. After an injury, the SCs dedifferentiate, proliferate, and clean the injured area so the new axons can grow properly (Svennigsen and Dahlin 2013).

Obestatin promotes SCs proliferation and migration. Although the proliferation of SCs does not appear to be indispensable for peripheral nerve regeneration (Yang et al. 2008), it may play an important role in maintaining the SCs pool after damage (Svennigsen and Dahlin 2013). In the same line, migration is known to be a key process for peripheral nerve development and repair (Heermann and Schwab 2013). The pro-migratory capacity of obestatin has already been demonstrated in different systems such as gastric cell lines, skeletal muscle or activated human pancreatic stellate cells (Alén et al. 2016; Santos-Zas et al. 2017; Estévez-Perez et al. 2018). In addition, directed migration requires the existence and the exposure to a gradient of chemoattracting compounds and/or substrates that promote migration. This piece of information could be related with the augmented expression observed for obestatin in the distal site of the regenerated sciatic nerve (Chapter 1).

All these data suggest that the obestatin/GPR39 system could be a suitable therapeutic target that could be involved in the plasticity, proliferation and migration of SCs.

USC
UNIVERSIDADE
DE SANTIAGO
DE COMPOSTELA

CHAPTER 4

Different research groups have been using PC12 cell cocultures with SCs differentiated from stem cells or primary SC cultures. In 2012, Sango et al presented a coculture model with PC12 cells and an immortalized SC line, IFRS1 (Sango et al. 2012). This coculture system has several advantages as it is very versatile for researchers and allows them to adjust many conditions to the needs of the study; it eliminates the risk of cross-contamination with other cell types (i.e. endoneural, epineural and perineural fibroblast) as occurs in primary coculture systems; and meets the requirement of the three Rs (Replacement, Reduction, and Refinement) for limiting the use of experimental animals. This model allows the analyses of different aspects of the myelination process and the assessment of obestatin effect under highly controlled experimental myelinating conditions. However, due to the fact that both cell lines expressed GPR39, they were also analysed independently.

During the differentiation stage of PC12 cells, obestatin significantly decreases cell differentiation, including the decrease in the number of neurites per cell, and the mean length of neurite, which is consistent with the effect of obestatin on proliferation seen above. However, 7 d differentiated PC12 cells treated presented a quite different behaviour since, although the differentiation and number of neurites continue to decrease at high doses of obestatin, the mean length of neurites increases compared to the control, while the mean length of the principal neurite is not altered. Obestatin affects smaller neurites by revoking their differentiation while favouring the maintenance of a population of PC12 cells with a large neurite length. It might be that obestatin exerted different effects depending on the differentiation degree of the neurite, that is, it does not affect in the same way neurites that are beginning to differentiate as those that are already in advanced stages of differentiation. Indeed, although NGF-induced differentiation of PC12 is reversible (Greene and Tischler 1976), it is possible to block the re-entry into the cell cycle by cyclic adenosine

monophosphate (cAMP)-dependent mechanisms (Yamamoto et al. 2016). Obestatin may have some effect in decreasing the reversibility of differentiation, via the production of cAMP (Zhang et al. 2005), at least in cells that are in advanced stages of differentiation, which could explain the preservation of a cell population with a large neurite length.

On the other hand, during the differentiation of PC12 cells, two types of neurites are generated according to their terminal end, varicones and growth cones. The endings of the growth cones have a zone of lamellipods and filopods rich in actin, which is collapsed in the varicones, and the growth cones usually have a smaller size than the varicones (Mingorance-Le Meur, Mohebiany, and O'Connor 2009). Taking these data into account, obestatin may only affect growth cones, stopping neurite elongation and reducing their length, but may maintain the length of varicones or at least affecting them in a lesser degree. Whether the presence of varicones and the susceptibility to reversibility are related is still unknown, and no apparent relationship has yet been found.

Furthermore, the neuronal polarity is a crucial characteristic for the organization and assembly of neuronal networks and synaptic propagation. The research of cell polarity control has involved many efforts in the study of molecules, signals and substrates (Tahirovic and Bradke 2009). The increased polarity of PC12 cell neurites through obestatin signalling may turn this peptide into a valuable mechanism of promoting neuronal polarity; however, if the effect is intrinsic to the cell signalling promoted by obestatin or a consequence of the reduction in the neurite number must be clarified in the future.

In PC12-IFRS1 coculture, after differentiation of PC12 cells, IFRS1 cells were added under myelinating conditions. As a first approach, PC12-IFRS1 coculture system proliferation was evaluated, as the SCs proliferation is one of the main processes that promote PNS regeneration. Obestatin has a clear proliferating effect in the PC12-IFRS1 coculture system under myelinating conditions, as it was the case in IFRS1 and PC12

under growing conditions. By isolating each cell type we proved that this proliferating effect of obestatin mostly affects IFRS1 but not PC12 cells. This obestatin inability towards PC12 cells proliferation under myelinization conditions may be due to NGF signalling. NGF, which is present in the myelinating medium, promotes PC12 cell differentiation, characterized by halting proliferation and neurite outgrowth (Vaudry et al. 2002), and obestatin is not able to reverse the effects of NGF. This means that, under myelinating conditions, obestatin acts selectively on SCs proliferation. In addition, SCs are grouped into clusters with a high proliferative capability, with an uneven distribution along the culture. Obestatin increases the number, area and cell density of these clusters, mainly affecting those SCs with a superior proliferative predisposition. Thus, obestatin may exert different effects depending on whether the SCs phenotype is myelinating or repairing.

Obestatin increases the expression of MPZ and MBP myelin proteins in the PC12-IFRS1 coculture under myelinating condition. After WD and axonal outgrowth, it is necessary a remyelination of growing axons by the SCs (Menorca, Fussell, and Elfar 2013). MPZ and MBP are two of the main proteins present in the myelin sheath of the peripheral nervous system and are located in the interperiod line and the major dense line, respectively. These proteins are implicated in different stages of myelination, especially in myelin compaction. The augmentation of MPZ and MBP with obestatin treatment suggests that obestatin may exert a positive effect in myelin compaction *in vitro*. Obestatin also increases the expression of MAG. In the PNS, MAG is located in the periaxonal space, in the paranodal loops and in the Schmidt-Lanterman incisures. Although this protein has been suggested as an axonal growth inhibitor (Filbin 2003), it is an important protein for axon recognition and adhesion, intermembrane spacing and myelinization initiation and maintenance (Garbay et al. 2000; Schnaar and Lopez 2009). Thus, obestatin may not only have an effect on the formation, compaction and maintenance of myelin but may also have

a potential effect on the promotion of axon recognition by SCs and SCs-axon interactions.

In PC12-IFRS1 coculture under myelinating conditions, obestatin increases SCAP expression, which leads to an increase in the synthesis of fatty acids, mainly sterols. This is confirmed by an increase in lipid content in the coculture. During myelination, in addition to an increase in myelin-associated proteins, an increase in lipid synthesis, especially cholesterol/sterol synthesis, is necessary (Saher et al. 2005; Saher and Stumpf 2015). In this sense, sterol regulation mediated by SCAP, an activator of SREBP, is fundamental in SCs myelination (Verheijen et al. 2009).

In the PC12-IFRS1 coculture system, physiological and even morphological changes can be observed which are indicative of interactions between both cell types (Sango et al. 2012). By using double immunofluorescence, it is possible to confirm that the obestatin not only increases the expression of MBP, but also causes an agglutination of the MBP+ SCs around the neurites of PC12, which suggests a role for obestatin on the approach/mobility of SCs, axon-glia contact and the wrapping of the SCs over the axon, in addition to the increase of indispensable proteins for myelin formation, compaction and maintenance.

Taking all these data together, obestatin has an enhancer effect on SCs proliferation and migration and acts as a regeneration/remyelination promoting agent in the PNS.

CHAPTER 5

Regeneration of the PNS is a process commonly studied because of its impact on human disease and traumatic regenerative responses. Nerve crush injury (axonotmesis), which causes an interruption in the continuity of the axons but maintains main integrity in the basal lamina and SCs, is one of the most commonly used models in research works (Bauder and Ferguson 2012). This model can provide reliable data on the morphological, physiological and functional changes that occur after peripheral nervous system injury.

The recovery of nerve function is one of the main features studied in the regeneration of the peripheral nervous system, and one of the most used tests is the calculation of the sciatic functional index after retrieving data from the footprints after a walking track test (Oliveira et al. 2001). In the present work, we demonstrate that obestatin is able to significantly increase the sciatic functional index, which represents an enhancement in the peripheral nerve function after a crush injury.

The histological analyses reveal that the animals treated with obestatin present greater integrity of the axons, supported by increased expression of GAP43 and NF, as well as increased density of NF positive axons in the injured area. GAP43 is overexpressed during early development of the murine nervous system and downregulated after two weeks of development. However, GAP43 is re-expressed during regeneration after a nerve injury and is associated with nerve sprouting enhancement (Holahan 2015). Moreover, NF, together with intermediate filaments, is one of the main structural components in mature myelinated axons. The expression of NF drastically diminishes after nerve injury, during WD, while in the course of nerve regeneration its expression increases again, giving stability to the new axons that undergo myelinization (Wang et al. 2012).

Indeed, the histological analysis of MBP, one of the main markers of myelin compaction, shows that obestatin treatment increases its expression in the injured area of the sciatic nerve. In addition, this expression seems to be associated with some columnar structures that are longitudinally found in the nerve, which could be associated with Büngner bands. These structures, which provide a permissive growth environment and guide extending axons towards potential peripheral targets (Gaudet, Popovich, and Ramer 2011), are increased in density in the nerves treated with obestatin in comparison to the sham group.

According to the previous results in the PC12-IFRS1 coculture (Chapter 4), obestatin signalling increases the protein associated with myelin compaction such as MPZ and MBP. Myelinization in the PNS is regulated by several transcription factors, including POU-protein Oct6 and zinc-finger protein EGR2. Oct6 is expressed in SCs during the promyelinating stage (Jaegle et al. 2003) activating EGR2 transcription during the myelinating stage (Liu et al. 2015). EGR2 is a key transcription factor in myelination in PNS (Salzer 2015), which leads to the transcription of key myelin-associated structural proteins such as MPZ and MBP (Le et al. 2005). Obestatin significantly increases the expression of both Oct6 and EGR2 suggesting an increase in the promyelinating and myelinating stage SCs (Figure D2).

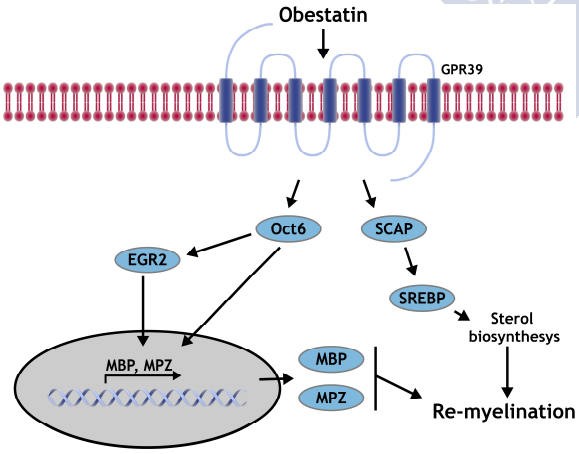

Figure D2. Proposed model of obestatin mediated myelination. *Proposed model of signalling pathway for myelin associated proteins and sterol biosynthesis leading remyelination. Source: author original.*

On the other hand, although there is an increasing trend, no significant increase in MAG expression has been detected after obestatin treatment. MAG is a glycoprotein present in myelin-producing cells (Quarles 2007), which is involved in the initiation of myelinization and the maintenance and stability of the myelin sheath (Schnaar and Lopez 2009). The fact that this protein is typically expressed in the early stages of myelination may explain why there are no significant differences between the two experimental groups since many of the SCs present in the injured area are in more advanced stages of myelinization.

Another major and key aspect is that obestatin is able to exert a positive effect on neuromuscular recovery. Obestatin treatment in the injured area of the sciatic nerve is able to increase the muscle mass of the hind leg and increase the cross section of the muscle fibres, supporting a partial restoration of the nerve to a level at which muscle atrophy in the target muscles is attenuated.

In summary, obestatin treatment after a sciatic nerve injury recovers not only the functionality of the damaged nerve but also diminishes the muscles atrophy caused by the injury. The data obtained so far support the use of obestatin in the treatment of peripheral nerve damages or injuries.

USC
UNIVERSIDADE
DE SANTIAGO
DE COMPOSTELA

CONCLUSIONS

USC
UNIVERSIDADE
DE SANTIAGO
DE COMPOSTELA

Our results lead us to the following conclusions:

CHAPTER 1

- The obestatin/GPR39 system is expressed in the nervous system, mainly in the SCs at the PNS level and in the motor and sensory neurons at the CNS.
- In a regenerated nerve, GPR39 expression in the proximal area resembles that of the uninjured tissue; however, at the distal site, GPR39 is associated with tubular structures that could correspond to the Büngner bands. However, obestatin expression seems to be confined to the distal end of the sciatic nerve.
- The obestatin/GPR39 system is expressed in the PC12 and IFRS1 cell models, which makes them suitable for exploring the effect of obestatin *in vitro*.

CHAPTER 2

- Obestatin increases cell proliferation of undifferentiated PC12 cells.
- Obestatin attenuates cell death and the fall of viability induced by nutrient deprivation in PC12 cells.
- In PC12 cells, obestatin activates the Akt and ERK1/2 pathways, inhibiting GSK3α/β activity leading to BCL2 overexpression and inhibition of caspase3

CHAPTER 3

- Obestatin treatment increases the proliferation of IFRS1 *in vitro*.

- Obestatin increases migration and exerts a chemoattracting effect on IFRS1 *in vitro*.

CHAPTER 4

- Obestatin decreases PC12 cell differentiation under differentiation conditions, as well as the mean length and number of neurites. However, in differentiated cells, this effect is reduced and the population of highly differentiated neurites is augmented.
- In the PC12-IFRS1 coculture, obestatin increases proliferation of SCs, the expression of myelin-associated structural proteins MPZ and MBP (myelin compaction) and MAG (myelination initialization and myelin maintenance). Besides, obestatin also raises the lipid content and SCAP expression.
- Obestatin increases PC12 neurite wrapping with MBP^+ IFRS1 cells.

CHAPTER 5

- Obestatin is able to accelerate the nerve recovery in a rat sciatic nerve crush model.
- Obestatin recovers the functionality of the damaged nerve as well as diminishes the atrophy caused in the innervated muscles.
- At the molecular level, obestatin increases GAP43 and NF expression, and NF^+ axons density. Furthermore, obestatin increases Oct6 and EGR2 expression and therefore increments the expression of the myelin-associated proteins MAG, MPZ and MBP.



RESUMEN

USC
UNIVERSIDADE
DE SANTIAGO
DE COMPOSTELA

El sistema nervioso es el mecanismo a través del cual la maquinaria interna de un organismo se mantiene en contacto y reacciona a cambios ambientales, transmitiendo, procesando y regulando señales desde las estructuras sensitivas a las efectoras (Keijzer, van Duijn, and Lyon 2013). El sistema nervioso central se conecta con los tejidos periférico a través de los nervios del sistema nervioso periférico. Las señales, bien sean sensitivas o motoras, confluyen en la espina dorsal, que conecta el sistema nervioso central y sistema nervioso periférico (Noback et al. 2012). El nervio periférico está compuesto principalmente por axones y células de Schwann, que componen la unidad mínima funcional de nervio periférico, la fibra nerviosa (Topp and Boyd 2012). Esta fibra nerviosa se encuentra recogida en fascículos y rodeada por tejido conectivo endoneural, perineural y epineural (Felten and Shetty 2009). Las fibras nerviosas pueden encontrarse mielinizadas o no mielinizadas, sin embargo, en los dos casos se encuentran rodeadas por las células de Schwann.

La mielina es una envoltura proteo-lipídica que forma un denso aislamiento alrededor del axón, lo que permite acelerar la señal nerviosa. La composición de la mielina en el sistema nervioso central y en el sistema nervioso periférico difieren sensiblemente, aunque algunas proteínas se conserven aun difiriendo en su proporción. Las principales proteínas que componen la mielina del sistema nervioso periférico son la proteína cero de mielina (MPZ), proteína básica de mielina (MBP) y glicoproteína asociada a la mielina (MAG). Las dos primeras se encuentran asociadas a la compactación de la mielina mientras que MAG se encuentra presente en las zonas más laxas de la vaina de mielina y se cree que tiene una gran importancia en las etapas iniciales de la mielinización, estando relacionada con la conexión y estabilización de la unión entre el axón y las células de Schwann (Martini et al. 1995; Garbay et al. 2000).

Los nervios periféricos pueden ser dañados por distintas causas, como presiones excesivas, estiramiento excesivo o cortes, y el daño puede ir desde una molestia leve hasta una disfunción permanente (Menorca,

Fussell, and Elfar 2013). Tras un daño, el nervio sufre cambios morfológicos y fisiológicos tanto en la zona dañada como en el extremo distal y proximal. La zona proximal comienza a producir prolongaciones de los axones que van a avanzar hacia la zona dañada, mientras que, en la zona dañada y zona distal, comienza un proceso degradativo que elimina la mielina y restos celulares para que el nuevo nervio pueda crecer (Geuna et al. 2009). Este proceso degradativo se denomina degeneración Walleriana y es realizado en parte por las células de Schwann, que se dediferencian, proliferan y adquieren un fenotipo reparador ayudando en la limpieza de la zona dañada, e incrementando el reclutamiento de macrófagos. Estas células de Schwann reparadoras quedan recluidas en la lámina basal apareciendo alineadas en estructuras denominadas bandas de Büngner (Griffin and Thompson 2008). Una vez se completa la degeneración Walleriana, el cono de crecimiento avanza hacia el extremo distal, en donde las células de Schwann juegan un papel fundamental, fomentando el crecimiento axonal y adecuando el microambiente para la recepción y mantenimiento de los axones.

La obestatina es un aminoácido derivado de la preproghrelina aislado del estómago de rata. Inicialmente fue descrito como un péptido circulante con secreción pulsátil, con una acción opuesta a la acción orexigénica de la grelina aunque su papel en la ingesta de comida es aún muy controvertida (Hassouna, Zizzari, and Tolle 2010). Tras la escisión de la preprogrelina además de la obestatina ha sido identificado un fragmento truncado de 13 aminoácidos: obestatina (11-23) que algunos autores sugieren que tiene una actividad biológica similar a la obestatina (Scrima et al. 2007; Alén et al. 2012). A pesar de que la mayoría de las células que expresan obestatina se encuentran en el tracto digestivo, ha sido encontrado en otros tejidos (Grönberg et al. 2008; Alén et al. 2016). El receptor acoplado a proteínas G 39 (GPR39) ha sido propuesto como receptor de la obestatina (Zhang et al. 2005), sin embargo, algunos autores cuestionan que la obestatina sea un ligando específico de GPR39 (Chartrel et al. 2007). Se ha demostrado la actividad de la obestatina en diversos tejidos

implicada en procesos que pueden ser útiles en la regeneración nerviosa periférica.

A pesar de que el nervio periférico es capaz de regenerarse y formar conexiones funcionales, diversos factores, tales como la edad del paciente, el retraso en la intervención y el tipo de lesión, determinan el pronóstico final después de la reparación. Para que ocurra la regeneración, los axones deben poseer la capacidad intrínseca de volver a crecer, el entorno distal debe apoyar ese crecimiento, y los tejidos diana deben aceptar esos nuevos axones. Aunque muchos de estos factores han sido estudiados en detalle, las únicas aplicaciones clínicas relevantes se han llevado a cabo en el campo de las técnicas quirúrgicas. Las células de Schwann juegan un papel fundamental en este proceso. Estas células altamente especializadas están normalmente en un estado quiescente. Tras una lesión, se dediferencian en masa a un estado progenitor/stem-like y la proliferación y la organización de estas células se sabe que es crítica para el proceso reparador. En este contexto, nuestro equipo posee datos preliminares sobre la implicación del sistema obestatina/GPR39 en diferentes etapas en las SC, implicadas en el proceso regenerativo del nervio periférico (migración, proliferación y activación de dianas intracelulares).

En la actualidad, existe un gran interés en las terapias celulares dirigidas al tratamiento de las lesiones del sistema nervioso periférico. Sin embargo, muchas de estas terapias no son capaces de conseguir contrarrestar el daño ocurrido, por lo que existe una gran demanda de tratamientos más efectivos que deben partir del conocimiento de los sistemas moleculares reguladores del proceso regenerativo.

Nuestro objetivo es el de estudiar el posible establecimiento y validación de la capacidad regenerativa nerviosa del sistema obestatina/GPR39 para el uso del péptido a estudio como agente terapéutico para el tratamiento de lesiones o patologías asociadas a la regeneración del sistema nervioso periférico. Esto será acometido mediante los siguientes puntos: (I) determinando la expresión de obestatina y GPR39 en tejido del nervio

periférico y modelos celulares, (II) analizando un posible efecto neuroprotector de la obestatina y sus posibles mecanismos de acción, (III) estudiando los efectos de la obestatina sobre las células de Schwann y procesos implicados en la regeneración, (IV) analizando los efectos mitogénicos, morfológicos y fisiológicos de la obestatina en un modelo de mielinización *in vitro* y (V) determinando el efecto de la administración local de obestatina en un nervio dañado mediante axonotmesis sobre la estructura, funcionalidad y fisiología del nervio y sobre la fisionomía de los músculos diana.

Para el estudio del efecto del sistema obestatina/GPR39 recurrimos a modelos *in vitro* e *in vivo* con los que se analizó el efecto de la obestatina sobre procesos implicados en la protección, mielinización y regeneración del sistema nervioso periférico. Como modelos *in vitro* se escogieron las células PC12, una línea celular derivada de un feocromocitoma de rata que adquiere un fenotipo neuronal en respuesta a factor de crecimiento nervioso (NGF), por lo que es ampliamente utilizado en estudios neurológicos, y las células IFRS1, células de Schwann de rata inmortalizadas de manera espontánea. A mayores se utilizó un sistema de cocultivo de las células PC12 y las IFRS1, como modelo de mielinización *in vitro*, para comprobar cómo afecta la obestatina a este proceso. Por último, se utilizó un modelo *in vivo* de aplastamiento del nervio periférico, para evaluar el efecto de la obestatina en la regeneración del nervio periférico.

En el presente trabajo se demuestra que tanto la obestatina como el receptor GPR39 se expresan tanto en neuronas sensitivas como en motoneuronas, además de en las células gliales del sistema nervioso periférico, principalmente células de Schwann. Esto es una característica deseable en aquellas moléculas candidatas a tener un potencial como agente terapéutico, aunque por sí sólo no tenga ninguna implicación. El hecho de estar presente en células de origen neuronal abre la puerta a que este sistema ejerza un efecto protector sobre células con este origen. Además, también se ha analizado la expresión del sistema obestatina/GPR39 en

los dos modelos escogidos para los estudios *in vitro*, PC12 e IFRS1, comprobando que el GPR39 se expresa en ambas líneas celulares de manera clara con un nivel más intenso de expresión en la membrana plasmática y en la zona ectoplásmica, mientras que la obestatina se expresa con una expresión débil y difusa. Esto hace de estos sistemas celulares idóneos para el estudio del sistema obestatina/GPR39 *in vitro*.

Tras un daño en el sistema nervioso periférico, un porcentaje de neuronas sensitivas y motoras se encuentran en grave riesgo de sufrir daños que podrían conducir a la muerte celular (Hart, Terenghi, and Wiberg 2008). Las estrategias terapéuticas sobre la neuroprotección y la disminución de la muerte celular han sido ampliamente estudiadas tanto en el sistema nervioso periférico como sistema nervioso central. Considerando las funciones descritas para la obestatina (Gurriarán-Rodríguez et al. 2012, 2015; Santos-Zas et al. 2017), parece una molécula prometedora para ejercer un efecto sobre los procesos que favorecen la neuroprotección en células de origen neuronal. Las células PC12, bien sean diferenciadas o no, son una línea celular habitualmente utilizada para explorar los distintos procesos implicados en la neuroprotección, y uno de los modelos más usados para comprobar el efecto de los daños y evaluar posibles candidatos con potencial neuroprotector es la restricción de nutrientes.

En una primera aproximación, verificamos que la obestatina aumenta la proliferación de las células PC12 de un modo dosis dependiente. Por otro lado, cuando se retiran los nutrientes al medio en el que se cultivan las células PC12 el número de células se ven claramente disminuidos, mientras que si en ese medio se añade obestatina esta reducción en la cantidad de células viables se ve atenuada de un modo dosis dependiente hasta llegar a niveles similares a los del control. Adicionalmente la restricción de nutrientes aumenta la muerte celular en células PC12, evidenciado por el aumento en la incorporación de ioduro de propidio en el núcleo de la célula, mientras que la adición de obestatina reduce la incorporación de ioduro de propidio lo que se traduce en una disminución de la

muerte celular, lo que correlaciona perfectamente con el aumento de la viabilidad visto con anterioridad. Para confirmar estos datos se realizaron análisis mediante inmunoblot, a través de los cuales se confirmó que la deprivación de nutrientes disminuye la expresión de la proteína antiapoptótica BCL2 mientras que la proteína proapoptótica caspasa 3 activa se ve aumentada. La adición de la obestatina en el medio recupera parcialmente la expresión de BCL2, mientras que vuelve a disminuir la expresión de la caspasa 3 activa. Los cambios en la expresión de caspasa 3 activa se ve inversamente correlacionada con la expresión de la pro-caspasa 3 (forma no activa). Estos datos confirman no solo el efecto antiapoptótico de la obestatina, si no la principal vía por la que actúa. Una de las principales rutas de señalización que afectan a BCL2/Caspasa3 son las rutas PI3K/Akt y ERK1/2, rutas que son dianas del sistema obestatina/GPR39 (Camiña et al. 2007; Álvarez et al. 2009; Alén et al. 2012; Gurriarán-Rodríguez et al. 2012). Tanto en el caso de Akt como en el de ERK1/2 la eliminación de nutrientes hace disminuir drásticamente la activación de estas proteínas mientras que la adición de obestatina recupera la activación de estas proteínas casi al nivel del control. Consecuentemente a la desactivación de Akt y ERK1/2, se produce una desactivación de GSK3, que ha sido descrito como uno de los principales promotores de supervivencia neuronal, mientras que la adición de obestatina es capaz de incrementar parcialmente la activación de GSK3.

Tras un daño la respuesta inicial conlleva la transformación de las células de Schwann de un fenotipo mielinizante a uno reparador (Kim, Mindos, and Parkinson 2013) el cual prolifera y migra, formando guías de regeneración denominadas bandas de Büngner. Tras la regeneración las células de Schwann se vuelven a asociar con los axones comenzando a remielinizar los axones (Jessen and Mirsky 2016).

La incorporación de obestatina es capaz de aumentar la proliferación, uno de los principales y más importantes procesos que ocurren durante la regeneración nerviosa tras un daño, de una manera dosis dependiente.

La migración de las células de Schwann es otro de los principales procesos que tienen lugar tras un daño permitiendo que las células de Schwann con fenotipo reparador puedan moverse y formar las bandas de Büngner. La obestatina es capaz de aumentar la migración de células IFRS1 *in vitro*, teniendo además un efecto quimioatrayente sobre dichas células.

Para estudiar el efecto sobre la mielinización y la regeneración *in vitro* escogimos un modelo de cocultivo de PC12 junto con IFRS1 (Sango et al. 2011). Como primer paso se caracterizó dicho cocultivo, para lo cual es necesario identificar claramente cada tipo celular presente en él. Por ello, se seleccionaron anticuerpos contra distintas proteínas disponibles (neurofilamentos, tirosina hidroxilasa y enolasa especifica de neuronas para las PC12 y S100 para IFRS1) y los analizamos mediante inmunofluorescencia para su elección. Descartamos como marcadores aquellos que no fueran específicos de un tipo celular o bien aquellos con una intensidad insuficiente. Teniendo todos los datos obtenidos en cuenta, seleccionamos S100 como marcador de IFRS1, mientras que escogimos tirosina hidroxilasa como marcador de células PC12. Estos marcadores fueron evaluados también en un cocultivo, comprobando que no existe reacción cruzada entre ambos anticuerpos. Además, caracterizamos también la expresión de MBP, una de las principales proteínas implicadas en la compactación de la mielina. MBP se expresa de forma poco intensa y difusa en todo el cocultivo, sin embargo, la expresión aumenta en las zonas adyacentes al cuerpo y neuritas de las células PC12 presentes en el cocultivo.

En una primera aproximación, quisimos averiguar cómo la obestatina afecta a las células PC12 durante la diferenciación y tras la diferenciación. Para ello realizamos un análisis de la diferenciación de las células PC12 y un análisis morfológico de las neuritas. Durante la diferenciación, la obestatina disminuye el porcentaje de diferenciación de células PC12, así como la longitud media de la neurita principal y el número medio de neuritas, sin embargo, no parece afectar a la longitud media de neurita. Tras la diferenciación, la disminución del porcentaje de diferenciación y el número medio de neuritas causada por la obestatina parece verse atenuada,

mientras que la longitud media de neurita aumenta y la longitud media de la neurita principal no varía. En ambos casos la polaridad de las neuritas aumenta. El análisis de la población de neuritas nos muestra que la obestatina reduce la diferenciación en las etapas iniciales, mientras que es capaz de mantener una población de neuritas largas, cuando la población incluye células con una alta diferenciación.

Por otra parte, la obestatina aumenta la proliferación de células en el cocultivo de PC12 e IFRS1, aumento que afecta únicamente a las células IFRS1. En muchos casos la proliferación parece asociada a clusters de células que muestran una gran positividad para el marcador proliferativo Ki67. El análisis morfológico de estos clusters nos permitió observar que la obestatina es capaz de aumentar el número, tamaño y densidad de estos clusters.

La obestatina es capaz además de aumentar proteínas relacionadas tanto con el comienzo de la mielinización como la compactación de la mielina como MAG, MBP o MPZ lo cual sugiere un incremento potencial de la mielinización. El análisis mediante inmunofluorescencia de MBP, nos muestra un aumento del solapamiento de las neuritas y cuerpos de las células PC12 por células IFRS1 positivas para MBP, lo cual, sumado con el aumento de las proteínas relacionadas con la mielina sugiere un aumento de la mielinización en el sistema. Además del aumento de las proteínas componentes de la mielina, otro aspecto importante es el aumento de la síntesis de lípidos (Saher and Stumpf 2015). La obestatina es capaz de aumentar el contenido lipídico del sistema de cocultivo y la expresión de SCAP, una proteína clave en la síntesis lipídica, especialmente esteroles (Verheijen et al. 2009).

Una de las principales metas del tratamiento de nervios periféricos dañados es la recuperación de la función motora y sensitiva. Uno de los modelos más usados para evaluar agentes terapéuticos en este aspecto es el aplastamiento de ciático en ratas (axonotmesis), que permite un estudio preciso del crecimiento axonal y la interacción con las células gliales

y lamina basal. La administración local de obestatina en nervios ciáticos, incrementa la funcionalidad motora asociada con el nervio ciático, medido mediante el índice funcional del ciático, un parámetro morfométrico ampliamente usado en la cuantificación de la regeneración nerviosa. Las muestras de nervios tratados con obestatina presentan un aumento en la expresión de GAP43, una proteína relacionada con el crecimiento axonal, en la zona dañada y en el distal, lo que sugiere un aumento en el crecimiento de los axones. Esto se ve respaldado por el aumento de la expresión de neurofilamentos y el aumento de la densidad de axones en los nervios tratados con obestatina. Además, el aumento de la expresión de MBP y la disminución de la presencia de cámaras de degeneración en la zona distal sugiere un estado más avanzado de regeneración en aquellos nervios tratados con obestatin. La expresión de las principales proteínas constituyentes de la mielina (MAG, MPZ y MBP), se ven aumentados en los nervios tratados con obestatina, así como Oct6 y EGR2, dos factores transcripción en los cuales convergen muchas de las señales que promueven la mielinización. GAP43, una proteína relacionada con la plasticidad axonal cuya expresión aumenta durante la regeneración del nervio periférico, también se ve favorecida con el tratamiento con obestatina.

Por último, consecuentemente con el poder de la obestatina en la promoción de la mielinización y la recuperación de la estructura y función del nervio periférico, el tratamiento con obestatina, es capaz de atenuar la pérdida de masa muscular en el tren inferior provocada por el daño en el nervio ciáticos. El daño en el ciático provoca una disminución del área de fibra en el tibial que se muestra atenuada en las muestras tratadas con obestatina.

Teniendo en cuenta todos estos datos, podemos concluir que la obestatina se postula como un firme candidato como agente terapéutico tras un daño en el sistema nervioso periférico, dado su efecto sobre la neuroprotección, proliferación y migración de células de Schwann, y como promotor de la mielinización y regeneración del sistema nervioso periférico.

USC
UNIVERSIDADE
DE SANTIAGO
DE COMPOSTELA

ACKNOWLEDGEMENTS

USC
UNIVERSIDADE
DE SANTIAGO
DE COMPOSTELA

En primer lugar, me gustaría agradecer a mis tres directores por darme la oportunidad de realizar esta tesis, a la Dra. Yolanda Pazos Randulfe, el Dr. Jesús Pérez Camiña y el Dr. José Luis Relova Quinteiro. A Yola le agradezco la confianza depositada en mí, por la dedicación y por guiarme durante todos estos años en esta larga y complicada empresa, y sobre todo gracias por valorar mi trabajo, esfuerzo y capacidades. Agradezco a Jesús todo el tiempo que me ha dedicado (mucho de él identificando bandas de blots), y por su estimada guía y orientación en este trabajo. Gracias a los dos por vuestra dedicación, en lo profesional, y vuestro apoyo y comprensión, en lo personal. A José Luís me gustaría agradecerle su accesibilidad, consejo y ayuda siempre que lo he necesitado.

A la Dra. Rosalía Gallego por su asesoramiento, ayuda y amabilidad, y por todas las dudas que me ha resuelto y trucos que me ha enseñado. Al servicio de anatomía patológica del CHUS, en concreto al Dr. Tomás García Caballero y a María Otero por su ayuda, asesoramiento y disposición para echarme una mano con la cantidad ingente de muestras histológicas. Me gustaría agradecer a la Deputación da Coruña por su apoyo en esta investigación. Me gustaría agradecérselo también al Dr. Kazunori Sango por su generosa y desinteresada donación de la línea celular IFRS1 y su inestimable ayuda.

A mis compañeros del laboratorio 4, Boli, Carlos, Saúl y Tania. De todos vosotros me llevo recuerdos, me he reído con vosotros, hemos vivido crisis juntos y he aprendido mucho de vosotros. En especial me gustaría agradecérselo a Larita, eres una persona increíblemente fuerte, trabajadora, solidaria y afectuosa. Si pudiese escoger un equipo, siempre estarías en él y no creo que exista cosa que no puedas conseguir. Por último, a Bego, mi antecesora y mi mentora, que siempre me ha apoyado, ayudado y guiado en esta andadura. Creo que eres una de las personas más valiosas con las que puede contar un laboratorio, a todos los niveles.

A todas las personas del IDIS que me han acompañado y ayudado durante mi tesis, especialmente al laboratorio 3 en el que residí un

tiempo, en especial a la Dra. María Pardo por acogerme en el laboratorio como si fuese el mío y a Tamara, por transmitir cariño a todo aquel que está a tu lado. Prometo no pegarte más sustos.

Este trabajo es duro y muchas veces requiere sacrificios. En mi caso, uno de mis mayores sacrificios es el no poder ver a mis amigos todo lo que querría, mis amigos de siempre. Alberto, Brigos Cris, Diego, Emma, Ferrín, Godo, Guille, Ian, Varis, Noa, Adri gracias por hacerme sentir que no ha pasado más de un día cada vez que quedamos cada varios meses. Os valoro mucho.....y habrá churrasco.

A Anita, Brais, Anselmo y Matilde, me alegráis la vida cada vez que os veo y estáis cuando lo he necesitado. Lo siento, pero seguiré cultivando la cultura friki en vuestros retoños. A Marta y Pepe, por ser como sois y todos los paseos que nos damos y nos daremos, y espero que el que está por llegar se parezca un poco a vosotros. Marta, eres la persona más fuerte que conozco y toda una inspiración para mí.

Quiero agradecérselo especialmente a mis padres, sin ellos no podría haberlo hecho. Sois los padres que todos desearían, cariñosos, atentos y desinteresados. Sois una brújula por la que guiarme y un espejo en el que mirarme, y sin vosotros no habría llegado hasta aquí. Os quiero. A mi hermana y a Leo, admiro mucho vuestra actitud valiente en la vida, y seguid haciendo lo que queráis hacer siempre.

Por último, quiero agradecérselo a Jess, la persona más importante en mi vida. Me has alegras el día cuando sonríes y me encanta hacerte sonreír. Eres la persona más integra, buena, inteligente y trabajadora que conozco y te mereces absolutamente todo por lo que has luchado, y en verdad deseo que lo obtengas. Una cosa que tengo clara es que, de no ser por ti, dudo que tuviese la fuerza suficiente para acabar la tesis. Eres la persona que más me ha apoyado y ayudado, y parte de esta tesis es tuya. Gracias por ser como eres. Te quiero y quiero acabar esta etapa como empezó.....mola, mola mola mola.

USC
UNIVERSIDADE DE SANTIAGO DE COMPOSTELA

BIBLIOGRAPHY

USC
UNIVERSIDADE
DE SANTIAGO
DE COMPOSTELA

Ahn, Jee-Yin. 2014. “Neuroprotection Signaling of Nuclear Akt in Neuronal Cells.” *Experimental Neurobiology* 23 (3): 200–206.

Alén, Begoña O., Lidia Nieto, Uxía Gurriarán-Rodríguez, Carlos S. Mosteiro, Juan C. Álvarez-Pérez, María Otero-Alén, Jesús P. Camiña, et al. 2012. “The NMR Structure of Human Obestatin in Membrane-Like Environments: Insights into the Structure-Bioactivity Relationship of Obestatin.” *PLoS ONE* 7 (10): e45434.

Alén, Begoña Otero, Saúl Leal-López, María Otero Alén, Patricia Viaño, Victoria García-Castro, Carlos S Mosteiro, Andrés Beiras, et al. 2016. “The Role of the Obestatin/GPR39 System in Human Gastric Adenocarcinomas.” *Oncotarget* 7 (5): 5957–71.

Allegra Mascaro, Anna Letizia, Paolo Cesare, Leonardo Sacconi, Giorgio Grasselli, Georgia Mandolesi, Bohumil Maco, Graham W Knott, et al. 2013. “In Vivo Single Branch Axotomy Induces GAP-43-Dependent Sprouting and Synaptic Remodeling in Cerebellar Cortex.” *Proceedings of the National Academy of Sciences of the United States of America* 110 (26): 10824–29.

Álvarez, Carlos J. P., María Lodeiro, Marily Theodoropoulou, Jesús P. Camiña, Felipe F. Casanueva, and Yolanda Pazos. 2009. “Obestatin Stimulates Akt Signalling in Gastric Cancer Cells through β-Arrestin-Mediated Epidermal Growth Factor Receptor Transactivation.” *Endocrine-Related Cancer* 16 (2): 599–611.

Bain, J. R., S. E. Mackinnon, and D. A. Hunter. 1989. “Functional Evaluation of Complete Sciatic, Peroneal, and Posterior Tibial Nerve Lesions in the Rat.” *Plastic and Reconstructive Surgery* 83 (1): 129–36.

Bakhti, Mostafa, Shweta Aggarwal, and Mikael Simons. 2014. "Myelin Architecture: Zippering Membranes Tightly Together." *Cellular and Molecular Life Sciences* 71 (7): 1265–77.

Bauder, Andrew R., and Toby A. Ferguson. 2012. "Reproducible Mouse Sciatic Nerve Crush and Subsequent Assessment of Regeneration by Whole Mount Muscle Analysis." *Journal of Visualized Experiments : JoVE*, no. 60 (February): 1–7.

Benowitz, Larry I., and Aryeh Routtenberg. 1997. "GAP-43: An Intrinsic Determinant of Neuronal Development and Plasticity." *Trends in Neurosciences* 20 (2): 84–91.

Besser, Limor, Ehud Chorin, Israel Sekler, William F. Silverman, Stan Atkin, James T. Russell, and Michal Hershfinkel. 2009. "Synaptically Released Zinc Triggers Metabotropic Signaling via a Zinc-Sensing Receptor in the Hippocampus." *The Journal of Neuroscience* 29 (9): 2890–2901.

Boggs, J. M. 2006. "Myelin Basic Protein: A Multifunctional Protein." *Cellular and Molecular Life Sciences* 63 (17): 1945–61.

Bresciani, Elena, D. Rapetti, F. Donà, I. Bulgarelli, L. Tamiazzo, V. Locatelli, and A. Torsello. 2006. "Obestatin Inhibits Feeding but Does Not Modulate GH and Corticosterone Secretion in the Rat." *Journal of Endocrinological Investigation* 29 (8): RC16-RC18.

Bukowczan, Jakub, Jakub Cieszkowski, Zygmunt Warzecha, Piotr Ceranowicz, Beata Kusnierz-Cabala, Romana Tomaszewska, and Artur Dembinski. 2016. "Therapeutic Effect of Obestatin in the Course of Cerulein-Induced Acute Pancreatitis." *Pancreas* 45 (5): 700–706.

Bukowczan, Jakub, Zygmunt Warzecha, Piotr Ceranowicz, Beata Kuśnierz-Cabala, and Romana Tomaszewska. 2015. “Obestatin Accelerates the Recovery in the Course of Ischemia/Reperfusion-Induced Acute Pancreatitis in Rats.” Edited by Zoltán Rakonczay. *PloS One* 10 (7): e0134380.

Camiña, Jesus P., Jacobo F. Campos, J. Eduardo Caminos, Carlos Dieguez, and Felipe F. Casanueva. 2007. “Obestatin-Mediated Proliferation of Human Retinal Pigment Epithelial Cells: Regulatory Mechanisms.” *Journal of Cellular Physiology* 211 (1): 1–9.

Carlini, Valeria P., Helgi B. Schiöth, and Susana R. DeBarioglio. 2007. “Obestatin Improves Memory Performance and Causes Anxiolytic Effects in Rats.” *Biochemical and Biophysical Research Communications* 352 (4): 907–12.

Catalán, V., J. Gómez-Ambrosi, F. Rotellar, C. Silva, M. J. Gil, A. Rodríguez, J. A. Cienfuegos, J. Salvador, and G. Frühbeck. 2007. “The Obestatin Receptor (GPR39) Is Expressed in Human Adipose Tissue and Is down-Regulated in Obesity-Associated Type 2 Diabetes Mellitus.” *Clinical Endocrinology* 66 (4): 598–601.

Ceranowicz, P., Z. Warzecha, A Dembinski, J. Cieszkowski, M. Dembinski, R. Sendur, B. Kusnierz-Cabala, R. Tomaszewska, A. Kuwahara, and I. Kato. 2009. “Pretreatment with Obestatin Inhibits the Development of Cerulein-Induced Pancreatitis.” *Journal of Physiology and Pharmacology : An Official Journal of the Polish Physiological Society* 60 (3): 95–101.

Charles, Perrine, Richard Reynolds, Danielle Seilhean, Geneviève Rougon, Marie S Aigrot, Adam Niezgoda, Bernard Zalc, and Catherine Lubetzki. 2002. "Re-Expression of PSA-NCAM by Demyelinated Axons: An Inhibitor of Remyelination in Multiple Sclerosis?" *Brain* 125 (Pt 9): 1972–79.

Chartrel, N., R. Alvear-Perez, J. Leprince, X. Iturrioz, A. R.-L. Goazigo, V. Audinot, P. Chomarat, et al. 2007. "Comment on 'Obestatin, a Peptide Encoded by the Ghrelin Gene, Opposes Ghrelin's Effects on Food Intake.'" *Science* 315 (5813): 766c–766c.

Chen, Yuan Yuan, David McDonald, Chu Cheng, Brooks Magnowski, Jeff Durand, and Douglas W. Zochodne. 2005. "Axon and Schwann Cell Partnership during Nerve Regrowth." *Journal of Neuropathology and Experimental Neurology* 64 (7): 613–22.

Chernousov, Michael A., Wei-Ming Yu, Zu-Lin Chen, David J. Carey, and Sidney Strickland. 2008. "Regulation of Schwann Cell Function by the Extracellular Matrix." *Glia* 56 (14): 1498–1507.

Chung, Hyunju, Sanghee Seo, Minho Moon, and Seungjoon Park. 2008. "Phosphatidylinositol-3-Kinase/Akt/Glycogen Synthase Kinase-3 Beta and ERK1/2 Pathways Mediate Protective Effects of Acylated and Unacylated Ghrelin against Oxygen-Glucose Deprivation-Induced Apoptosis in Primary Rat Cortical Neuronal Cells." *The Journal of Endocrinology* 198 (3): 511–21.

Dembiński, Artur, Zygmunt Warzecha, Piotr Ceranowicz, Jakub Cieszkowski, Marcin Dembiński, Agata Ptak-Belowska, Atsukasu Kuwahara, and Ikuo Kato. 2011. "Administration of Obestatin Accelerates the Healing of Chronic Gastric Ulcers in Rats." *Medical Science Monitor : International Medical Journal of Experimental and Clinical Research* 17 (8): BR196-200.

Depoortere, Inge. 2012. "GI Functions of GPR39: Novel Biology." *Current Opinion in Pharmacology* 12 (6): 647–52.

Dittmer, Sonja, Mert Sahin, Anna Pantlen, Ambrish Saxena, Diamandis Toutzaris, Ana-Luisa Pina, Andreas Geerts, Stefan Golz, and Axel Methner. 2008. "The Constitutively Active Orphan G-Protein-Coupled Receptor GPR39 Protects from Cell Death by Increasing Secretion of Pigment Epithelium-Derived Growth Factor." *The Journal of Biological Chemistry* 283 (11): 7074–81.

Dombrowski, Mary A., Masanori Sasaki, Karen L. Lankford, Jeffery D. Kocsis, and Christine Radtke. 2006. "Myelination and Nodal Formation of Regenerated Peripheral Nerve Fibers Following Transplantation of Acutely Prepared Olfactory Ensheathing Cells." *Brain Research* 1125 (1): 1–8.

Dun, Siok L., G. Cristina Brailoiu, Eugen Brailoiu, Jun Yang, Jaw Kang Chang, and Nae J. Dun. 2006. "Distribution and Biological Activity of Obestatin in the Rat." *The Journal of Endocrinology* 191 (2): 481–89.

Estévez-Perez, Lara, Saul Leal-lopez, Agustin Sanchez-Temprano, Begoña Otero-Alen, Carlos Seoane-Mosteiro, Rosalia Gallego- Gomez, Matthias Löhr, J Enrique Dominguez-Muñoz, Jesus Perez-Camiña, and Yolanda Pazos-Randulfe. 2018. "Role of the Endogenous Obestatin/G-Protein Coupled Receptor 39 (GPR39) System in the Regulation of Proliferation and Migration of Activated Human Pancreatic Stellate Cells." *Pancreatology* 18 (4): S118.

Faden, Alan I., and Bogdan Stoica. 2007. "Neuroprotection." *Archives of Neurology* 64 (6): 794–800.

Faroni, Alessandro, S. Atefeh Mobasseri, Paul J. Kingham, and Adam J. Reid. 2015. "Peripheral Nerve Regeneration: Experimental Strategies and Future Perspectives." *Advanced Drug Delivery Reviews* 82–83 (March): 160–67.

Felten, David L., and Anil N. Shetty. 2009. "Peripheral Nervous System." In *Netter's Atlas of Neuroscience*, 2nd Editio, 153–231. Elsevier.

Filbin, Marie T. 2003. "Myelin-Associated Inhibitors of Axonal Regeneration in the Adult Mammalian CNS." *Nature Reviews. Neuroscience* 4 (9): 703–13.

Frostick, S. P., Q. Yin, and G. J. Kemp. 1998. "Schwann Cells, Neurotrophic Factors, and Peripheral Nerve Regeneration." *Microsurgery* 18 (7): 397–405.

Garbay, B., A. M. Heape, F. Sargueil, and C. Cassagne. 2000. "Myelin Synthesis in the Peripheral Nervous System." *Progress in Neurobiology* 61 (3): 267–304.

Gardner, Ernest D., and Richard P. Bunge. 2005. “Gross Anatomy of the Peripheral Nervous System.” In *Peripheral Neuropathy*, 1:11–33. Elsevier.

Garg, Abhimanyu. 2007. “The Ongoing Saga of Obestatin: Is It a Hormone?” *The Journal of Clinical Endocrinology and Metabolism* 92 (9): 3396–98.

Gargantini, Eleonora, Laura Lazzari, Fabio Settanni, Marina Taliano, Letizia Trovato, Iacopo Gesmundo, Ezio Ghigo, and Riccarda Granata. 2016. “Obestatin Promotes Proliferation and Survival of Adult Hippocampal Progenitors and Reduces Amyloid-β-Induced Toxicity.” *Molecular and Cellular Endocrinology* 422 (February): 18–30.

Gaudet, Andrew D., Phillip G. Popovich, and Matt S. Ramer. 2011. “Wallerian Degeneration: Gaining Perspective on Inflammatory Events after Peripheral Nerve Injury.” *Journal of Neuroinflammation* 8 (August): 110.

Geuna, Stefano, Stefania Raimondo, Giulia Ronchi, Federica Di Scipio, Pierluigi Tos, Krzysztof Czaja, and Michele Fornaro. 2009. “Histology of the Peripheral Nerve and Changes Occurring During Nerve Regeneration.” In *International Review of Neurobiology*, 1st ed., 87:27–46. Elsevier Inc.

Ghislain, Julien, and Patrick Charnay. 2006. “Control of Myelination in Schwann Cells: A Krox20 Cis-Regulatory Element Integrates Oct6, Brn2 and Sox10 Activities.” *EMBO Reports* 7 (1): 52–58.

Granata, Riccarda, Fabio Settanni, Davide Gallo, Letizia Trovato, Luigi Biancone, Vincenzo Cantaluppi, Rita Nano, et al. 2008. "Obestatin Promotes Survival of Pancreatic Beta-Cells and Human Islets and Induces Expression of Genes Involved in the Regulation of Beta-Cell Mass and Function." *Diabetes* 57 (4): 967–79.

Green, B. D., N. Irwin, and P. R. Flatt. 2007. "Direct and Indirect Effects of Obestatin Peptides on Food Intake and the Regulation of Glucose Homeostasis and Insulin Secretion in Mice." *Peptides* 28 (5): 981–87.

Greene, L. A., and A. S. Tischler. 1976. "Establishment of a Noradrenergic Clonal Line of Rat Adrenal Pheochromocytoma Cells Which Respond to Nerve Growth Factor." *Proceedings of the National Academy of Sciences of the United States of America* 73 (7): 2424–28.

Griffin, John W., and Wesley J. Thompson. 2008. "Biology and Pathology of Nonmyelinating Schwann Cells." *Glia* 56 (14): 1518–31.

Grönberg, Malin, Apostolos V. Tsolakis, Linda Magnusson, Eva T. Janson, and Jan Saras. 2008. "Distribution of Obestatin and Ghrelin in Human Tissues: Immunoreactive Cells in the Gastrointestinal Tract, Pancreas, and Mammary Glands." *The Journal of Histochemistry and Cytochemistry : Official Journal of the Histochemistry Society* 56 (9): 793–801.

Gualillo, Oreste, Francisca Lago, Felipe F. Casanueva, and Carlos Dieguez. 2006. "One Ancestor, Several Peptides Post-Translational Modifications of Preproghrelin Generate Several Peptides with Antithetical Effects." *Molecular and Cellular Endocrinology* 256 (1–2): 1–8.

Gurriarán-Rodríguez, Uxía, Omar Al-Massadi, Arturo Roca-Rivada, Ana Belén Crujeiras, Rosalía Gallego, Maria Pardo, Luisa Maria Seoane, Yolanda Pazos, Felipe F. Casanueva, and Jesús P. Camiña. 2011. "Obestatin as a Regulator of Adipocyte Metabolism and Adipogenesis." *Journal of Cellular and Molecular Medicine* 15 (9): 1927–40.

Gurriarán-Rodríguez, Uxía, Icía Santos-Zas, Omar Al-Massadi, Carlos S. Mosteiro, Daniel Beiroa, Rubén Nogueiras, Ana B. Crujeiras, et al. 2012. "The Obestatin/GPR39 System Is up-Regulated by Muscle Injury and Functions as an Autocrine Regenerative System." *The Journal of Biological Chemistry* 287 (45): 38379–89.

Gurriarán-Rodríguez, Uxía, Icía Santos-Zas, Jessica González-Sánchez, Daniel Beiroa, Viviana Moresi, Carlos S. Mosteiro, Wei Lin, et al. 2015. "Action of Obestatin in Skeletal Muscle Repair: Stem Cell Expansion, Muscle Growth, and Microenvironment Remodeling." *Molecular Therapy* 23 (6): 1003–21.

Han, Huijong, Matti Myllykoski, Salla Ruskamo, Chaozhan Wang, and Petri Kursula. 2013. "Myelin-Specific Proteins: A Structurally Diverse Group of Membrane-Interacting Molecules." *BioFactors* 39 (3): 233–41.

Haney, C. A., Z. Sahenk, C. Li, V. P. Lemmon, J. Roder, and B. D. Trapp. 1999. "Heterophilic Binding of L1 on Unmyelinated Sensory Axons Mediates Schwann Cell Adhesion and Is Required for Axonal Survival." *Journal of Cell Biology* 146 (5): 1173–83.

Hart, Andrew M., Giorgio Terenghi, and Mikael Wiberg. 2008. "Neuronal Death after Peripheral Nerve Injury and Experimental Strategies for Neuroprotection." *Neurological Research* 30 (10): 999–1011.

Hartline, D. K., and D. R. Colman. 2007. "Rapid Conduction and the Evolution of Giant Axons and Myelinated Fibers." *Current Biology* 17 (1): R29-35.

Hassouna, Rim, Philippe Zizzari, and Virginie Tolle. 2010. "The Ghrelin/Obestatin Balance in the Physiological and Pathological Control of GH Secretion, Body Composition and Food Intake." *Journal of Neuroendocrinology* 22 (7): no-no.

Heermann, Stephan, and Markus H. Schwab. 2013. "Molecular Control of Schwann Cell Migration along Peripheral Axons: Keep Moving!" *Cell Adhesion & Migration* 7 (1): 18–22.

Heusinkveld, Harm J., and Remco H.S. Westerink. 2017. "Comparison of Different in Vitro Cell Models for the Assessment of Pesticide-Induced Dopaminergic Neurotoxicity." *Toxicology in Vitro* 45 (Pt 1): 81–88.

Holahan, Matthew. 2015. "GAP-43 in Synaptic Plasticity: Molecular Perspectives." *Research and Reports in Biochemistry* 5 (June): 137.

Holahan, Matthew R. 2017. "A Shift from a Pivotal to Supporting Role for the Growth-Associated Protein (GAP-43) in the Coordination of Axonal Structural and Functional Plasticity." *Frontiers in Cellular Neuroscience* 11 (August): 266.

Holst, Birgitte, Kristoffer L. Egerod, Enrico Schild, Steve P. Vickers, Sharon Cheetham, Lars-Ole Gerlach, Laura Storjohann, et al. 2007. "GPR39 Signaling Is Stimulated by Zinc Ions But Not by Obestatin." *Endocrinology* 148 (1): 13–20.

Jackson, Valerie R., Hans-Peter Nothacker, and Olivier Civelli. 2006. "GPR39 Receptor Expression in the Mouse Brain." *Neuroreport* 17 (8): 813–16.

Jaegle, Martine, Mehrnaz Ghazvini, Wim Mandemakers, Marko Piirsoo, Siska Driegen, Françoise Levavasseur, Smiriti Raghoenath, Frank Grosveld, and Dies Meijer. 2003. "The POU Proteins Brn-2 and Oct-6 Share Important Functions in Schwann Cell Development." *Genes and Development* 17 (11): 1380–91.

Jahn, Olaf, Stefan Tenzer, and Hauke B. Werner. 2009. "Myelin Proteomics: Molecular Anatomy of an Insulating Sheath." *Molecular Neurobiology* 40 (1): 55–72.

Jeffery, P. L., R. P. Duncan, A. H. Yeh, R. A. Jaskolski, D. S. Hammond, A. C. Herington, and L. K. Chopin. 2005. "Expression of the Ghrelin Axis in the Mouse: An Exon 4-Deleted Mouse Proghrelin Variant Encodes a Novel C Terminal Peptide." *Endocrinology* 146 (1): 432–40.

Jessen, K. R., and R. Mirsky. 2016. "The Repair Schwann Cell and Its Function in Regenerating Nerves." *Journal of Physiology* 594 (13): 3521–31.

Jessen, Kristján R., Rhona Mirsky, and Alison C Lloyd. 2015. "Schwann Cells: Development and Role in Nerve Repair." *Cold Spring Harbor Perspectives in Biology* 7 (7): a020487.

Jin, Li-Qing, Guixin Zhang, Curtis Jamison, Hajime Takano, Philip G. Haydon, and Michael E. Selzer. 2009. "Axon Regeneration in the Absence of Growth Cones: Acceleration by Cyclic AMP." *The Journal of Comparative Neurology* 515 (3): 295–312.

Kalbermatten, D. F., P. Erba, D. Mahay, M. Wiberg, G. Pierer, and G. Terenghi. 2008. "Schwann Cell Strip for Peripheral Nerve Repair." *Journal of Hand Surgery* 33 (5): 587–94.

Keijzer, Fred, Marc van Duijn, and Pamela Lyon. 2013. "What Nervous Systems Do: Early Evolution, Input–output, and the Skin Brain Thesis." *Adaptive Behavior* 21 (2): 67–85.

Kim, Haesun A., Thomas Mindos, and David B. Parkinson. 2013. "Plastic Fantastic: Schwann Cells and Repair of the Peripheral Nervous System." *Stem Cells Translational Medicine* 2 (8): 553–57.

Le, N., R. Nagarajan, J. Y. T. Wang, T. Araki, R. E. Schmidt, and J. Milbrandt. 2005. "Analysis of Congenital Hypomyelinating Egr2Lo/Lo Nerves Identifies Sox2 as an Inhibitor of Schwann Cell Differentiation and Myelination." *Proceedings of the National Academy of Sciences* 102 (7): 2596–2601.

Liu, Zhangyin, Yu-Qing Jin, Lulu Chen, Yang Wang, Xiaonan Yang, Jia Cheng, Wei Wu, Zuoliang Qi, and Zunli Shen. 2015. "Specific Marker Expression and Cell State of Schwann Cells during Culture In Vitro." Edited by Maria Cristina Vinci. *PLOS ONE* 10 (4): e0123278.

Manders, E. M. M., F. J. Verbeek, and J. A. Aten. 1993. "Measurement of Co-Localization of Objects in Dual-Colour Confocal Images." *Journal of Microscopy* 169 (3): 375–82.

Martini, Rudolf, Jürgen Zielasek, Klaus V. Toyka, K. Peter Giese, and Melitta Schachner. 1995. "Protein Zero (P0)–deficient Mice Show Myelin Degeneration in Peripheral Nerves Characteristic of Inherited Human Neuropathies." *Nature Genetics* 11 (3): 281–86.

Maurer, U., F. Preiss, P. Brauns-Schubert, L. Schlicher, and C. Charvet. 2014. “GSK-3 - at the Crossroads of Cell Death and Survival.” *Journal of Cell Science* 127 (7): 1369–78.

McKee, Karen Kulju, Carina P Tan, Oksana C Palyha, Jim Liu, Scott D Feighner, Donna L Hreniuk, Roy G Smith, Andrew D Howard, and Lex H.T. Van der Ploeg. 1997. “Cloning and Characterization of Two Human G Protein-Coupled Receptor Genes (GPR38 and GPR39) Related to the Growth Hormone Secretagogue and Neurotensin Receptors.” *Genomics* 46 (3): 426–34.

Mendoza, Michelle C., E. Emrah Er, and John Blenis. 2011. “The Ras-ERK and PI3K-MTOR Pathways: Cross-Talk and Compensation.” *Trends in Biochemical Sciences* 36 (6): 320–28.

Menorca, Ron M. G., Theron S. Fussell, and John C. Elfar. 2013. “Nerve Physiology: Mechanisms of Injury and Recovery.” *Hand Clinics* 29 (3): 317–30.

Mingorance-Le Meur, Ana, Alma N. Mohebiany, and Timothy P. O’Connor. 2009. “Varicones and Growth Cones: Two Neurite Terminals in PC12 Cells.” *PloS One* 4 (2): e4334.

Moechars, Dieder, Inge Depoortere, Benoit Moreaux, Betty de Smet, Ilse Goris, Luc Hoskens, Guy Daneels, et al. 2006. “Altered Gastrointestinal and Metabolic Function in the GPR39-Obestatin Receptor-Knockout Mouse.” *Gastroenterology* 131 (4): 1131–41.

Mueller, Marcus, Christine Leonhard, Karin Wacker, E. Bernd Ringelstein, Masaru Okabe, William F. Hickey, and Reinhard Kiefer. 2003. "Macrophage Response to Peripheral Nerve Injury: The Quantitative Contribution of Resident and Hematogenous Macrophages." *Laboratory Investigation* 83 (2): 175–85.

Muinelo-Romay, Laura, Eva Colas, Jorge Barbazan, Lorena Alonso-Alconada, Marta Alonso-Nocelo, Marta Bouso, Teresa Curiel, et al. 2011. "High-Risk Endometrial Carcinoma Profiling Identifies TGF-B1 as a Key Factor in the Initiation of Tumor Invasion." *Molecular Cancer Therapeutics* 10 (8): 1357–66.

Murinson, Beth B., David R Archer, Yongbo Li, and John W Griffin. 2005. "Degeneration of Myelinated Efferent Fibers Prompts Mitosis in Remak Schwann Cells of Uninjured C-Fiber Afferents." *The Journal of Neuroscience : The Official Journal of the Society for Neuroscience* 25 (5): 1179–87.

Nave, Klaus-Armin, and Hauke B. Werner. 2014. "Myelination of the Nervous System: Mechanisms and Functions." *Annual Review of Cell and Developmental Biology* 30 (1): 503–33.

Noback, Charles R. , Norman L. Strominger, Robert J. Demarest, and David A. Ruggiero. 2012. *The Human Nervous System*. *The Human Nervous System, Structure and Function*. Seventh ed. Totowa, NJ: Humana Press.

Nogueiras, Rubén, Paul Pfluger, Sulay Tovar, Myrtha Arnold, Sharon Mitchell, Amanda Morris, Diego Perez-Tilve, et al. 2007. "Effects of Obestatin on Energy Balance and Growth Hormone Secretion in Rodents." *Endocrinology* 148 (1): 21–26.

Ogata, Toru, Shin-ichi Yamamoto, Kozo Nakamura, and Sakae Tanaka. 2006. “Signaling Axis in Schwann Cell Proliferation and Differentiation.” *Molecular Neurobiology* 33 (1): 51–62.

Oliveira, E. F., N. Mazzer, C. H. Barbieri, and M. Selli. 2001. “Correlation between Functional Index and Morphometry to Evaluate Recovery of the Rat Sciatic Nerve Following Crush Injury: Experimental Study.” *Journal of Reconstructive Microsurgery* 17 (1): 69–75.

Pang, Tao, Li-Xin Sun, Tao Wang, Zhen-Zhou Jiang, Hong Liao, and Lu-Yong Zhang. 2014. “Telmisartan Protects Central Neurons against Nutrient Deprivation-Induced Apoptosis in Vitro through Activation of PPARγ and the Akt/GSK-3β Pathway.” *Acta Pharmacologica Sinica* 35 (6): 727–37.

Pera, Marta, Pelayo Camps, Diego Muñoz-Torrero, Belen Perez, Albert Badia, and M. Victoria Clos Guillen. 2013. “Undifferentiated and Differentiated PC12 Cells Protected by Huprines against Injury Induced by Hydrogen Peroxide.” Edited by Stefan Strack. *PloS One* 8 (9): e74344.

Perrone-Bizzozero, N. I., and D. C. Tanner. 2007. “GAP-43 in Neuronal Development and Plasticity.” In *Handbook of Neurochemistry and Molecular Neurobiology*, edited by Abel Lajtha, 3th Editio. Boston, MA: Springer US.

Popovics, Petra, and Alan J. Stewart. 2011. “GPR39: A Zn(2+)-Activated G Protein-Coupled Receptor That Regulates Pancreatic, Gastrointestinal and Neuronal Functions.” *Cellular and Molecular Life Sciences : CMLS* 68 (1): 85–95.

Quarles, Richard H. 2007. “Myelin-Associated Glycoprotein (MAG): Past, Present and Beyond.” *Journal of Neurochemistry* 100 (6): 1431–48.

Quarles, Richard H., Wendy B. Macklin, and Pierre Morell. 2006. “Myelin Formation, Structure and Biochemistry.” In *Basic Neurochemistry: Molecular, Cellular and Medical Aspects*, 7:51–71. Elsevier/North Holland Amsterdam.

Rosenbluth, Jack, Amanda Mierzwa, and Seema Shroff. 2013. “Molecular Architecture of Myelinated Nerve Fibers: Leaky Paranodal Junctions and Paranodal Dysmyelination.” *The Neuroscientist* 19 (6): 629–41.

Saher, Gesine, Britta Brügger, Corinna Lappe-Siefke, Wiebke Möbius, Ryu-ichi Tozawa, Michael C. Wehr, Felix Wieland, Shun Ishibashi, and Klaus-Armin Nave. 2005. “High Cholesterol Level Is Essential for Myelin Membrane Growth.” *Nature Neuroscience* 8 (4): 468–75.

Saher, Gesine, and Sina Kristin Stumpf. 2015. “Cholesterol in Myelin Biogenesis and Hypomyelinating Disorders.” *Biochimica et Biophysica Acta* 1851 (8): 1083–94.

Salzer, James L. 2015. “Schwann Cell Myelination.” *Cold Spring Harbor Perspectives in Biology* 7 (8): a020529.

Samson, Willis K., Meghan M. White, Christopher Price, and Alastair V. Ferguson. 2007. “Obestatin Acts in Brain to Inhibit Thirst.” *American Journal of Physiology-Regulatory, Integrative and Comparative Physiology* 292 (1): R637–43.

Sango, Kazunori, Emiko Kawakami, Hiroko Yanagisawa, Shizuka Takaku, Masami Tsukamoto, Kazunori Utsunomiya, and Kazuhiko Watabe. 2012. “Myelination in Coculture of Established Neuronal and Schwann Cell Lines.” *Histochemistry and Cell Biology* 137 (6): 829–39.

Sango, Kazunori, Hiroko Yanagisawa, Shizuka Takaku, Emiko Kawakami, and Kazuhiko Watabe. 2011. “Immortalized Adult Rodent Schwann Cells as In Vitro Models to Study Diabetic Neuropathy.” *Experimental Diabetes Research* 2011: 1–9.

Santos-Zas, Icía, Tania Cid-Díaz, Jessica González-Sánchez, Uxía Gurriarán-Rodriguez, Carlos Seoane-Mosteiro, Begoña Porteiro, Rubén Nogueiras, et al. 2017. “Obestatin Controls Skeletal Muscle Fiber-Type Determination.” *Scientific Reports* 7 (1): 1–14.

Santos-Zas, Icía, Uxía Gurriarán-Rodríguez, Tania Cid-Díaz, Gabriela Figueroa, Jessica González-Sánchez, Mónica Bouzo-Lorenzo, Carlos S. Mosteiro, et al. 2016. “β-Arrestin Scaffolds and Signaling Elements Essential for the Obestatin/GPR39 System That Determine the Myogenic Program in Human Myoblast Cells.” *Cellular and Molecular Life Sciences* 73 (3): 617–35.

Santos-Zas, Icia, Elisa Negroni, Kamel Mamchaoui, Carlos S. Mosteiro, Rosalia Gallego, Gillian S. Butler-Browne, Yolanda Pazos, Vincent Mouly, and Jesus P. Camiña. 2017. “Obestatin Increases the Regenerative Capacity of Human Myoblasts Transplanted Intramuscularly in an Immunodeficient Mouse Model.” *Molecular Therapy* 25 (10): 2345–59.

Sazdova, Iliyana, Bilyana Ilieva, Ignat Minkov, Rudolf Schubert, and Hristo Gagov. 2009. "Obestatin as Contractile Mediator of Excised Frog Heart." *Open Life Sciences* 4 (3): 327–34.

Schindelin, Johannes, Ignacio Arganda-Carreras, Erwin Frise, Verena Kaynig, Mark Longair, Tobias Pietzsch, Stephan Preibisch, et al. 2012. "Fiji: An Open-Source Platform for Biological-Image Analysis." *Nature Methods* 9 (7): 676–82.

Schnaar, Ronald L., and Pablo H. H. Lopez. 2009. "Myelin-Associated Glycoprotein and Its Axonal Receptors." *Journal of Neuroscience Research* 87 (15): 3267–76.

Scrima, Mario, Pietro Campiglia, Cinzia Esposito, Isabel Gomez-Monterrey, Ettore Novellino, and Anna Maria D'Ursi. 2007. "Obestatin Conformational Features: A Strategy to Unveil Obestatin's Biological Role?" *Biochemical and Biophysical Research Communications* 363 (3): 500–505.

Seddon, H. J. 1943. "Three Types of Nerve Injury." *Brain* 66 (4): 237–88.

Seidl, A. H. 2014. "Regulation of Conduction Time along Axons." *Neuroscience* 276 (September): 126–34.

Seoane, L. M., O Al-Massadi, Y. Pazos, U. Pagotto, and F. F. Casanueva. 2006. "Central Obestatin Administration Does Not Modify Either Spontaneous or Ghrelin-Induced Food Intake in Rats." *Journal of Endocrinological Investigation* 29 (8): RC13-5.

Sherman, Diane L., and Peter J. Brophy. 2005. "Mechanisms of Axon Ensheathment and Myelin Growth." *Nature Reviews. Neuroscience* 6 (9): 683–90.

Smith, Craig M., Yaming Chen, Mara L. Sullivan, Patrick M. Kochanek, and Robert S.B. Clark. 2011. “Autophagy in Acute Brain Injury: Feast, Famine, or Folly?” *Neurobiology of Disease* 43 (1): 52–59.

Spiegeleer, Bart De, Sylvia Van Dorpe, Valentijn Vergote, Evelien Wynendaele, Ewald Pauwels, Christophe Van De Wiele, Pablo Garcia-Solis, and Juan Carlos Solis-Sainz. 2012. “In Vitro Metabolic Stability of Iodinated Obestatin Peptides.” *Peptides* 33 (2): 272–78.

Spiegeleer, Bart De, Valentijn Vergote, Adel Pezeshki, Kathelijne Peremans, and Christian Burvenich. 2008. “Impurity Profiling Quality Control Testing of Synthetic Peptides Using Liquid Chromatography-Photodiode Array-Fluorescence and Liquid Chromatography-Electrospray Ionization-Mass Spectrometry: The Obestatin Case.” *Analytical Biochemistry* 376 (2): 229–34.

Stirling, David P., and Peter K. Stys. 2010. “Mechanisms of Axonal Injury: Internodal Nanocomplexes and Calcium Deregulation.” *Trends in Molecular Medicine* 16 (4): 160–70.

Sunderland, Sydney. 1951. “A Classification of Peripheral Nerve Injuries Producing Loss of Function.” *Brain* 74 (4): 491–516.

Svaren, John, and Dies Meijer. 2008. “The Molecular Machinery of Myelin Gene Transcription in Schwann Cells.” *Glia* 56 (14): 1541–51.

Svennigsen, Åsa Fex, and Lars B. Dahlin. 2013. “Repair of the Peripheral Nerve-Remyelination That Works.” *Brain Sciences* 3 (3): 1182–97.

Szentirmai, Eva, and James M. Krueger. 2006. “Obestatin Alters Sleep in Rats.” *Neuroscience Letters* 404 (1–2): 222–26.

Tabakman, Rinat, Hao Jiang, Iris Shahar, Hadar Arien-Zakay, Robert A. Levine, and Philip Lazarovici. 2005. "Neuroprotection by NGF in the PC12 in Vitro OGD Model: Involvement of Mitogen-Activated Protein Kinases and Gene Expression." *Annals of the New York Academy of Sciences* 1053 (August): 84–96.

Tahirovic, Sabina, and Frank Bradke. 2009. "Neuronal Polarity." *Cold Spring Harbor Perspectives in Biology* 1 (3): a001644.

Topp, Kimberly S., and Benjamin S. Boyd. 2012. "Peripheral Nerve: From the Microscopic Functional Unit of the Axon to the Biomechanically Loaded Macroscopic Structure." *Journal of Hand Therapy : Official Journal of the American Society of Hand Therapists* 25 (2): 142–51; quiz 152.

Tremblay, Frédéric, Mylène Perreault, Lori D. Klaman, James F. Tobin, Erica Smith, and Ruth E. Gimeno. 2007. "Normal Food Intake and Body Weight in Mice Lacking the G Protein-Coupled Receptor GPR39." *Endocrinology* 148 (2): 501–6.

Tricaud, Nicolas, and Hwan Tae Park. 2017. "Wallerian Demyelination: Chronicle of a Cellular Cataclysm." *Cellular and Molecular Life Sciences* 74 (22): 4049–57.

Trovato, Letizia, Davide Gallo, Fabio Settanni, Iacopo Gesmundo, Ezio Ghigo, and Riccarda Granata. 2014. "Obestatin: Is It Really Doing Something?" *Frontiers of Hormone Research* 42: 175–85.

Unniappan, Suraj, Madeleine Speck, and Timothy J. Kieffer. 2008. "Metabolic Effects of Chronic Obestatin Infusion in Rats." *Peptides* 29 (8): 1354–61.

Vassall, Kenrick A., Vladimir V. Bamm, and George Harauz. 2015. "MyelStones: The Executive Roles of Myelin Basic Protein in Myelin Assembly and Destabilization in Multiple Sclerosis." *The Biochemical Journal* 472 (1): 17–32.

Vaudry, D., P. J. S. Stork, P. Lazarovici, and L. E. Eiden. 2002. "Signaling Pathways for PC12 Cell Differentiation: Making the Right Connections." *Science* 296 (5573): 1648–49.

Verheijen, Mark H. G., Nutabi Camargo, Valerie Verdier, Karim Nadra, Anne-Sophie de Preux Charles, Jean-Jacques Médard, Adrienne Luoma, et al. 2009. "SCAP Is Required for Timely and Proper Myelin Membrane Synthesis." *Proceedings of the National Academy of Sciences of the United States of America* 106 (50): 21383–88.

Verhulst, P. J., A. Lintermans, S. Janssen, D. Loeckx, U. Himmelreich, J. Buyse, J. Tack, and I. Depoortere. 2011. "GPR39, a Receptor of the Ghrelin Receptor Family, Plays a Role in the Regulation of Glucose Homeostasis in a Mouse Model of Early Onset Diet-Induced Obesity." *Journal of Neuroendocrinology* 23 (6): 490–500.

Wang, Haitao, Minfei Wu, Chuanjun Zhan, Enyuan Ma, Maoguang Yang, Xiaoyu Yang, and Yingpu Li. 2012. "Neurofilament Proteins in Axonal Regeneration and Neurodegenerative Diseases." *Neural Regeneration Research* 7 (8): 620–26.

Wang, W-L., Rong Dai, Han-wen Yan, Chun-ni Han, and Li-song Liu. 2015. "Current Situation of PC12 Cell Use in Neuronal Injury Study." *International Journal of Biotechnology of Wellness Industries* 4: 61–66.

Wang, Ying, Hong-Lin Teng, and Zhi-hui Huang. 2012. "Intrinsic Migratory Properties of Cultured Schwann Cells Based on Single-Cell Migration Assay." Edited by Rafael Linden. *PLoS ONE* 7 (12): e51824.

Westerink, R. H. S., and A. G. Ewing. 2008. "The PC12 Cell as Model for Neurosecretion." *Acta Physiologica* 192 (2): 273–85.

Woolf, C. J., M. L. Reynolds, C. Molander, C. O'Brien, R. M. Lindsay, and L. I. Benowitz. 1990. "The Growth-Associated Protein GAP-43 Appears in Dorsal Root Ganglion Cells and in the Dorsal Horn of the Rat Spinal Cord Following Peripheral Nerve Injury." *Neuroscience* 34 (2): 465–78.

Wu, Peng, Aditya Chawla, Robert J. Spinner, Cong Yu, Michael J. Yaszemski, Anthony J Windebank, and Huan Wang. 2014. "Key Changes in Denervated Muscles and Their Impact on Regeneration and Reinnervation." *Neural Regeneration Research* 9 (20): 1796–1809.

Wu, Yanqing, Zhouguang Wang, Pingtao Cai, Ting Jiang, Yiyang Li, Yuan Yuan, Rui Li, et al. 2018. "Dual Delivery of BFGF- and NGF-Binding Coacervate Confers Neuroprotection by Promoting Neuronal Proliferation." *Cellular Physiology and Biochemistry* 47: 948–56.

Yamamoto, Naoki, Kiyokazu Agata, Kinichi Nakashima, and Takuya Imamura. 2016. "Bidirectional Promoters Link CAMP Signaling with Irreversible Differentiation through Promoter-Associated Non-Coding RNA (PancRNA) Expression in PC12 Cells." *Nucleic Acids Research*, gkw113.

Yang, David P., Dan P. Zhang, Kimberley S. Mak, Daniel E. Bonder, Scott L. Pomeroy, and Haesun A. Kim. 2008. “Schwann Cell Proliferation during Wallerian Degeneration Is Not Necessary for Regeneration and Remyelination of the Peripheral Nerves: Axon-Dependent Removal of Newly Generated Schwann Cells by Apoptosis.” *Molecular and Cellular Neuroscience* 38 (1): 80–88.

Yuan, Junying, and Bruce A. Yankner. 2000. “Apoptosis in the Nervous System.” *Nature* 407 (6805): 802–9.

Zhai, Qiwei, Jing Wang, Anna Kim, Qing Liu, Ryan Watts, Eric Hoopfer, Timothy Mitchison, Liqun Luo, and Zhigang He. 2003. “Involvement of the Ubiquitin-Proteasome System in the Early Stages of Wallerian Degeneration.” *Neuron* 39 (2): 217–25.

Zhang, Jian V., Holger Jahr, Chin-Wei Luo, Cynthia Klein, Kristof Van Kolen, Luc Ver Donck, Ananya De, et al. 2008. “Obestatin Induction of Early-Response Gene Expression in Gastrointestinal and Adipose Tissues and the Mediatory Role of G Protein-Coupled Receptor, GPR39.” *Molecular Endocrinology* 22 (6): 1464–75.

Zhang, Jian V., Cynthia Klein, Pei-Gen Ren, Stefan Kass, Luc Ver Donck, Dieder Moechars, and Aaron J. W. Hsueh. 2007. “Response to Comment on ‘Obestatin, a Peptide Encoded by the Ghrelin Gene, Opposes Ghrelin’s Effects on Food Intake.’” *Science* 315 (5813): 766d–766d.

Zhang, Jian V., Lei Li, Qingsheng Huang, and Pei Gen Ren. 2013. “Obestatin Receptor in Energy Homeostasis and Obesity Pathogenesis.” In *Progress in Molecular Biology and Translational Science*, 1st ed., 114:89–107. Elsevier Inc.

Zhang, Jian V., Pei-Gen Ren, Orna Avsian-Kretchmer, Ching-Wei Luo, Rami Rauch, Cynthia Klein, and Aaron J W Hsueh. 2005. "Obestatin, a Peptide Encoded by the Ghrelin Gene, Opposes Ghrelin's Effects on Food Intake." *Science* 310 (5750): 996–99.

Zhu, Xiaorong, Yun Cao, Keith Voodg, and Donald F. Steiner. 2006. "On the Processing of Proghrelin to Ghrelin." *Journal of Biological Chemistry* 281 (50): 38867–70.

Zizzari, Philippe, Romaine Longchamps, Jacques Epelbaum, and Marie Thérèse Bluet-Pajot. 2007. "Obestatin Partially Affects Ghrelin Stimulation of Food Intake and Growth Hormone Secretion in Rodents." *Endocrinology* 148 (4): 1648–53.

Zochodne, Douglas W. 2012. "The Challenges and Beauty of Peripheral Nerve Regrowth." *Journal of the Peripheral Nervous System* 17 (1): 1–18.

Zoupi, Lida, Maria Savvaki, and Domna Karagogeos. 2011. "Axons and Myelinating Glia: An Intimate Contact." *IUBMB Life* 63 (9): 730–35.



ATTACHED DOCUMENTS

USC
UNIVERSIDADE
DE SANTIAGO
DE COMPOSTELA

XUNTA DE GALICIA
CONSELLERÍA DO MEDIO RURAL

Departamento Territorial
Edificio Administrativo de Servizos Múltiples
Vicente Ferrer, 2
15071 – A Coruña

REXISTRO XERAL DA XUNTA DE GALICIA
REXISTRO DO EDIFICIO ADMINISTRATIVO DE A CORUÑA
A CORUÑA
Data 20/04/2018 14:15:06
SAÍDA 41589 / RX 586278

José Manuel Cifuentes
Departamento de Anatomía
Facultade de Veterinaria
Campus Universitario
27002 Lugo

RESOLUCIÓN DE AUTORIZACIÓN DE PROXECTOS DE EXPERIMENTACIÓN ANIMAL

Expediente núm.: 15010/17/005
Persoa interesada: Jesús Pérez Camiña
Procedemento: resolución de autorización

Data de inicio: 19.04.2018
Forma de inicio: solicitude do interesado

ANTECEDENTES

A persoa interesada, como representante do centro CIMUS (Universidade de Santiago de Compostela), presentou con data 1.12.2017 e rexistro de entrada 124566/RX 2968513, unha solicitude para a realización do proxecto de experimentación animal, cuxos datos se detallan a continuación:

Denominación do proxecto: Potencial rexenerativo do sistema obestatin/GPR39 para o tratamento de patoloxías caracterizadas pola atrofia muscular
Nome do centro usuario: Animalario do CIMUS
Persoa responsable do proxecto: Jesús Pérez Camiña
Establecemento onde se realizarán os procedementos do proxecto (ou lugar xeográfico no caso de traballos de campo): Animalario do CIMUS
Clasificación do proxecto : Tipo I ☐ Tipo II ☐ Tipo III ☒

CONSIDERACIÓNS LEGAIS E TÉCNICAS

1. O Real decreto 53/2013, de 1 de febreiro (BOE 34, do 8 de febreiro), polo que se establecen as normas básicas aplicables para a protección dos animais utilizados en experimentación e outros fins científicos, incluíndo a docencia, establece no seu artigo 33 as condicións de autorizacións dos proxectos con animais de experimentación.

2. O artigo 88 da Lei 39/2015, de 1 de outubro, do procedemento administrativo común das administracións públicas (BOE 236, do 2 de outubro de 2015) establece que a resolución que poña fin o procedemento decidirá todas as cuestións expostas polos interesados e aquelas outras derivadas deste.

CVE: x2zcc5b14
Verificación: https://sede.xunta.gal/cve

XUNTA DE GALICIA
CONSELLERÍA DO MEDIO RURAL

Departamento Territorial
Edifício Administrativo de Servizos Múltiples
Vicente Ferrer, 2
15071 – A Coruña

3. O Servizo de Gandaría da Coruña revisou a documentación achegada na solicitude e o resultado favorable da avaliación do proxecto, realizada polo órgano habilitado da Sección de Experimentación Animal do Comité de Bioética da Universidade de Santiago de Compostela.

Esta xefatura territorial é competente para ditar unha resolución, de conformidade co artigo 11 do Decreto 245/2009 de 30 de abril, polo que se regulan as delegacións territoriais da Xunta de Galicia (DOG 84, do 1 de maio de 2009) e o Decreto 166/2015, de 13 de novembro, polo que se aproba a estrutura orgánica da Consellería do Medio Rural (DOG 220, do 18 de novembro de 2015).

De acordo con todo o indicado, RESOLVO:

1 Autorizar o proxecto solicitado.
2 O mencionado proxecto precisa someterse a unha avaliación retrospectiva aos dous anos.
3 A autorización deste proxecto terá unha duración de cinco anos e unha vez transcorrido este tempo deberá ser renovada.

A citada autorización é unicamente válida nas condicións que figuran no expediente. Ante calquera cambio significativo no proxecto que poida ter efectos negativos sobre o benestar dos animais, deberá solicitar a confirmación da autorización ao Servizo Provincial de Gandaría.

Esta autorización poderá ser suspendida, no caso de que o proxecto non se leve a cabo de acordo coas condicións de autorización e retirala, previo expediente tramitado ao que se lle dará audiencia.

Contra a presente resolución, que non lle pon fin á vía administrativa, poderá interpoñer un recurso de alzada ante a conselleira de Medio Rural. O prazo comezará a contar dende o día seguinte ao da recepción desta resolución. Todo isto, segundo o disposto nos artigos 121 e 122 da citada Lei 39/2015.

Mediante este escrito notifícaselle ao CIMUS da USC esta resolución segundo o esixido no artigo 40.1 da antedita Lei 39/2015.

A Coruña, 19 de abril de 2018
O xefe territorial

Manuel Rodríguez Vázquez

Asinado por: RODRIGUEZ VAZQUEZ, MANUEL
Cargo: XEFE TERRITORIAL
Data e hora: 20/04/2018 09:25:05

CVE: x5ZzCBd4
Verificación: https://sede.xunta.gal/cve

XUNTA DE GALICIA
CONSELLERÍA DO MEDIO RURAL
Dirección Xeral de Ordenación Forestal

San Lázaro, s/n
15781 Santiago de Compostela
Teléfono: 981 546 108 Fax: 981 546 101
mediorural.montesgalicia@xunta.es

galicia

Certificado de capacitación en materia de protección de animais utilizados, criados ou subministrados con fins de experimentación e otros fins científicos, incluíndo a docencia conforme coa Orde ECC/566/2015 de 20 de marzo.

Certificado de capacitación en materia de protección de animales utilizados, criados o suministrados con fines de experimentación y otros fines científicos, incluyendo la docencia conforme con la Orden ECC/566/2015 de 20 de marzo.

1. IDENTIFICACIÓN

1.1. Apelidos / *Apellidos / Surname:*
SÁNCHEZ TEMPRANO

1.2. Nome / *Nombre / First names:*	DNI / *DNI / Identity card number:*
AGUSTÍN	**44848268Q**

1.3. Categoría/*Categoría/Category:*	1.4. Especies/*Especies/Species:*	1.5. Válido ata/ *válido hasta/expires:*
"b"	*Todas*	***2.04.2023***

2. Nº DO CERTIFICADO / *Nº DEL CERTIFICADO / CERTIFICATE NUMBER*

b322

3.ORGANISMO QUE EXPIDE O CERTIFICADO / *ORGANISMO QUE EXPIDE EL CERTIFICADO / BODY ISSUING THE CERTIFICATE:*

3.1. Nome e enderezo do organismo que expide o certificado / *Nombre y dirección del organismo que expide el certificado / Name and address of the body issuing the certificate:*

Dirección Xeral de Ordenación Forestal
CONSELLERÍA DO MEDIO RURAL – XUNTA DE GALICIA
San Lázaro, s/n
15781 Santiago de Compostela
A Coruña (España)

3.2. Teléfono / *Teléfono / Telephone:*	3.3. Fax / *Fax / Fax:*	3.4. Correo electrónico / *Correo electrónico / Email:*
981 546 654	981 546 651	formacion.cmrm@xunta.es

3.5. Data / *Fecha / Date:*	3.6. Lugar / *Lugar / Place:*
30/04/2018	**Santiago de Compostela**

3.7. Nome e sinatura / *Nombre y firma / Name and signature*	3.8. Selo / Sello / Stamp
Asdo.: **Tomás Fernández-Couto Juanas** **Director Xeral de Ordenación Forestal**	

galicia

MÓDULOS FUNDAMENTAIS OU TRONCAIS E ESPECÍFICOS CORRESPONDENTES Á CATEGORÍA "B" EUTANASIA DOS ANIMAIS – ORDE ECC/566/2015, DE 20 DE MARZO

MÓDULOS FUNDAMENTAIS OU TRONCAIS

1.- Lexislación nacional (1 hora).

2.- Ética, benestar animal e as "tres erres", nivel 1 (2 horas).

3.- Bioloxía básica e adecuada, nivel 1 (3 horas).

4.- Coidado, saúde e manexo dos animais, nivel 1 (5 horas).

5.- Recoñecemento do dolor, o sufrimento e a angustia (3 horas).

6.- Métodos incruentos de sacrificio, nivel 1 (2 horas)

MÓDULOS ESPECÍFICOS DA CATEGORÍA "B"

1.-Bioloxía básica e adecuada, nivel 2 (3 horas)

2.- Métodos incruentos de sacrificio, nivel 2 (3 horas)

.....

MÓDULOS FUNDAMENTALES O TRONCALES

1.- Legislación nacional (1 hora).

2.- Ética, bienestar animal y las "tres erres", nivel 1 (2 horas).

3.- Biología básica y adecuada, nivel 1 (3 horas).

4.- Cuidado, salud y manejo de los animales, nivel 1 (5 horas).

5.- Reconocimiento del dolor, el sufrimiento y la angustia (3 horas).

6.- Métodos incruentos de sacrificio, nivel 1 (2 horas)

MÓDULOS ESPECÍFICOS DE LA CATEGORÍA "B"

1.-Biología básica y adecuada, nivel 2 (3 horas)

2.- Métodos incruentos de sacrificio, nivel 2 (3 horas)

XUNTA DE GALICIA
CONSELLERÍA DO MEDIO RURAL
Dirección Xeral de Ordenación Forestal

San Lázaro, s/n
15781 Santiago de Compostela
Teléfono: 981 546 108 Fax: 981 546 101
mediorural.montesgalicia@xunta.es

galicia

Certificado de capacitación en materia de protección de animais utilizados, criados ou subministrados con fins de experimentación e otros fins científicos, incluíndo a docencia conforme coa Orde ECC/566/2015 de 20 de marzo.

Certificado de capacitación en materia de protección de animales utilizados, criados o suministrados con fines de experimentación y otros fines científicos, incluyendo la docencia conforme con la Orden ECC/566/2015 de 20 de marzo.

1. IDENTIFICACIÓN			
1.1. Apelidos / *Apellidos / Surname:* **SÁNCHEZ TEMPRANO**			
1.2. Nome / *Nombre / First names:* **AGUSTÍN**			DNI /*DNI / Identity card number:* **44848268Q**
1.3. Categoría/*Categoría/Category:* **"c"**	1.4. Especies/*Especies/Species:* *Todas*	1.5. Válido ata/ *válido hasta/expires:* ***2.04.2023***	

2. Nº DO CERTIFICADO / *Nº DEL CERTIFICADO / CERTIFICATE NUMBER*

c357

3.ORGANISMO QUE EXPIDE O CERTIFICADO / *ORGANISMO QUE EXPIDE EL CERTIFICADO / BODY ISSUING THE CERTIFICATE:*

3.1. Nome e enderezo do organismo que expide o certificado / *Nombre y dirección del organismo que expide el certificado / Name and address of the body issuing the certificate:*

Dirección Xeral de Ordenación Forestal
CONSELLERÍA DO MEDIO RURAL – XUNTA DE GALICIA
San Lázaro, s/n
15781 Santiago de Compostela
A Coruña (España)

3.2. Teléfono / *Teléfono / Telephone:*	3.3. Fax / *Fax / Fax:*	3.4. Correo electrónico / *Correo electrónico / Email:*
981 546 654	981 546 651	formacion.cmrm@xunta.es
3.5. Data / *Fecha / Date:* 30/04/2018	3.6. Lugar / *Lugar / Place:* **Santiago de Compostela**	
3.7. Nome e sinatura / *Nombre y firma / Name and signature*		3.8. Selo / Sello / Stamp

Asdo.: **Tomás Fernández-Couto Juanas**
Director Xeral de Ordenación Forestal

galicia

MÓDULOS FUNDAMENTAIS OU TRONCAIS E ESPECÍFICOS CORRESPONDENTES Á CATEGORÍA "C" REALIZACIÓN DOS PROCEDEMENTOS – ORDE ECC/566/2015, DE 20 DE MARZO

MÓDULOS FUNDAMENTAIS OU TRONCAIS

1.- Lexislación nacional (1 hora).

2.- Ética, benestar animal e as "tres erres", nivel 1 (2 horas).

3.- Bioloxía básica e adecuada, nivel 1 (3 horas).

4.- Coidado, saúde e manexo dos animais, nivel 1 (5 horas).

5.- Recoñecemento do dolor, o sufrimento e a angustia (3 horas).

6.- Métodos incruentos de sacrificio, nivel 1 (2 horas)

MÓDULOS ESPECÍFICOS DA CATEGORÍA "C"

1.- Bioloxía básica e adecuada, nivel 2 (3 horas)

2.- Procedementos minimamente invasores sen anestesia, nivel 1 (5 horas)

3.- Procedementos minimamente invasores sen anestesia, nivel 2 (10 horas)

4.- Anestesia para procedementos menores (5 horas)

5.- Anestesia avanzada para intervencións cirúrxicas ou procedementos prolongados (8 horas)

6.- Principios de cirurxía (5 horas)

.....

MÓDULOS FUNDAMENTALES O TRONCALES

1.- Legislación nacional (1 hora).

2.- Ética, bienestar animal y las "tres erres", nivel 1 (2 horas).

3.- Biología básica y adecuada, nivel 1 (3 horas).

4.- Cuidado, salud y manejo de los animales, nivel 1 (5 horas).

5.- Reconocimiento del dolor, el sufrimiento y la angustia (3 horas).

6.- Métodos incruentos de sacrificio, nivel 1 (2 horas)

MÓDULOS ESPECÍFICOS DE LA CATEGORÍA "C"

1.- Biología básica y adecuada, nivel 2 (3 horas)

2.- Procedimientos mínimamente invasivos sin anestesia, nivel 1 (5 horas)

3.- Procedimientos mínimamente invasivos sin anestesia, nivel 2 (10 horas)

4.- Anestesia para procedementos menores (5 horas)

5.- Anestesia avanzada para intervenciones quirúrgicas o procedimientos prolongados (8 horas)

6.- Principios de cirugía (5 horas)

Plagiarism Checker X Originality Report

Similarity Found: 10%

Date: domingo, octubre 14, 2018
Statistics: 1955 words Plagiarized / 20035 Total words
Remarks: Low Plagiarism Detected - Your Document needs Optional Improvement.



USC
UNIVERSIDADE
DE SANTIAGO
DE COMPOSTELA



“You can’t always get what you want.

But if you try sometimes, you might find, you get what you need”

-M Jagger and K. Richards-

1969

USC
UNIVERSIDADE
DE SANTIAGO
DE COMPOSTELA